

CONSTRUCTION AND CHARACTERIZATION OF NON-TOXIC BACTERIAL
ENTEROTOXINS AS VACCINE ADJUVANTS

by

Lavanya Vempati

A thesis

submitted in partial fulfillment
of the requirements for the degree of
Master of Science in Biology
Boise State University

August 2014

© 2014

Lavanya Vempati

ALL RIGHTS RESERVED

BOISE STATE UNIVERSITY GRADUATE COLLEGE

DEFENSE COMMITTEE AND FINAL READING APPROVALS

of the thesis submitted by

Lavanya Vempati

Thesis Title: Construction and Characterization of Non-Toxic Bacterial Enterotoxins
as Vaccine Adjuvants

Date of Final Oral Examination: 24 June 2014

The following individuals read and discussed the thesis submitted by student Lavanya Vempati, and they evaluated her presentation and response to questions during the final oral examination. They found that the student passed the final oral examination.

Juliette Tinker, Ph.D. Chair, Supervisory Committee

Kristen Mitchell, Ph.D. Member, Supervisory Committee

Troy Rohn, Ph.D. Member, Supervisory Committee

The final reading approval of the thesis was granted by Juliette Tinker, Ph.D., Chair of the Supervisory Committee. The thesis was approved for the Graduate College by John R. Pelton, Ph.D., Dean of the Graduate College.

DEDICATION

To my family, Prameela Vempati, Madhava Naidu Vempati, Murali Mohan Gurajala, and Pragnya Gurajala for their continuous support and encouragement throughout the course of my studies.

ACKNOWLEDGEMENTS

I would like to first extend my thanks and acknowledgements to my advisor, Dr. Juliette Tinker, for her guidance over the course of my study at Boise State University. I would also like to thank my committee members, Dr. Kristen Mitchell and Dr. Troy Rohn, for their expert advice, support, and generosity. I would also like to thank the following members of the Biology and Chemistry Department: Dr. Jeff Habig, Dr. Shin Pu, Dr. Laura Bond, Dr. Rychert, Dr. Wingett, Dr. John Rasmussen, Ezequiel Martinez, Raquel Brown, Beth Gee, Barb Jibben, Diane Smith, and Sindia Padilla.

From Dr. Tinker's lab, I would like to thank Sara Wilson, Dr. Jenny Yan, Britni Arlian, Brad Morris, Nathan Levitt, and Casey Denton who have helped me. Finally, I would like to express my deep gratitude to my family and close friends for all of their encouragement, kindness, and love, especially my husband, Murali.

This work was supported by a 2009 Department of Defense grant (#W81XWH-09-1-0588) West Nile Vaccine P.I. K. Cornell, Co-PI Tinker and an NSF Major Research Instrumentation grant (#0619793) Confocal microscope P.I. Oxford., Co-PI Tinker.

ABSTRACT

The development of adjuvants that can promote the delivery of purified subunit vaccines by mucosal routes, such as the nose or the mouth, is recognized as a top priority for vaccine research. The bacterial enterotoxins cholera toxin (CT) and *E.coli* heat-labile toxin (LTI) have long been recognized as powerful adjuvants with the ability to stimulate specific immune responses to co-administered antigens when delivered to mucosal surfaces. Shiga toxin 1 (ST1) and pertussis toxin (PT) are structurally homologous bacterial toxins secreted by *Escherichia coli* 0157:H7 and *Bordetella pertussis*, respectively. ST1 and PT also have reported adjuvant activity but it is less well characterized. The receptor-binding affinity and protein stability of these AB₅-type toxins appear to be the basis for their unique immunomodulatory properties. However, the toxicity of these molecules is a limiting factor for use as adjuvants in human vaccines. The non-toxic B subunit of CT, as well as chimeric CTA₂B molecules, have shown recent promise as novel mucosal vaccines. A₂B chimeras of CT retain the capacity to introduce antigens into host cells and modulate the immune response, but toxic domains are replaced with a vaccine antigen of interest. This work reveals the construction of a number of plasmids for the expression of ST1A₂B chimeras containing the *Yersinia pestis* bacterial antigen, LcrV and the West Nile virus domain III (DIII) antigen. Plasmids were also constructed for expression of the ST1 B subunit and this pentamer was purified from the *E.coli* periplasm. The ability of the ST1 A₂/B chimeras and STB to stimulate antigen uptake and immune stimulation *in vitro* was assayed by fluorescence microscopy,

metabolic dye assay, T-cell proliferation assay, and cytokine ELISA using both macrophage and dendritic cells. Findings suggest that STB can induce antigen uptake and may stimulate more of a Th-2 type and anti-inflammatory response, similar to CTB. These studies will contribute to the development of these toxins as novel mucosal adjuvants.

TABLE OF CONTENTS

DEDICATION	iv
ACKNOWLEDGEMENTS	v
ABSTRACT	vi
LIST OF TABLES	x
LIST OF FIGURES	xi
LIST OF ABBREVIATIONS	xvi
CHAPTER I. INTRODUCTION.....	1
Bacterial AB5 Toxins	1
<i>Vibrio cholerae</i> Cholera Toxin	5
<i>E.coli</i> Heat-Labile Toxin	9
<i>Shigella dysenteriae</i> Shiga Toxin	10
<i>Bordetella pertussis</i> Pertussis Toxin.....	14
Vaccine Adjuvants	15
Cholera Toxin and <i>E.coli</i> LTI Toxin as Vaccine Adjuvants	16
Pertussis Toxin as a Vaccine Adjuvant.....	19
Shiga Toxin as a Vaccine Adjuvant.....	20
Vaccines of Interest and Potential Vaccine Antigens	21
<i>Yersinia pestis</i> and LcrV	21
West Nile Virus and Domain III of the Envelope Protein	24

CHAPTER II. MATERIALS AND METHODS.....	27
2.1. Bacterial Strains, Vectors, and Construction of Plasmids	27
2.1.1. Bacterial Strains.....	27
2.2 Protein Expression and Purification.....	30
2.3. Electrophoresis and Blotting.....	31
2.3.1. Agarose Gel Electrophoresis.....	31
2.3.2. SDS-PAGE	31
2.3.3. Western Blot Analysis	32
2.4. Cell Culture Methods and Assays.....	32
2.4.1. Internalization of Toxins and Toxin Subunits in Cell Culture.....	32
2.4.2. Cellular Proliferation Assay.....	33
2.4.3. Cytokine Assays.....	34
2.4.4. B3Z Antigen Presentation Assay	34
2.4.5. Antigen Uptake Assay	35
CHAPTER III. RESULTS.....	37
Construction of Plasmids for A ₂ /B Chimeric Protein Expression	37
Construction of Plasmids and Purification of Shiga Toxin A ₂ /B or STB.....	50
<i>In vitro</i> Adjuvant Characterization Assays.....	54
CHAPTER IV. DISCUSSION AND CONCLUSIONS.....	66
REFERENCES	76

LIST OF TABLES

Table 1.1.	Summary of AB5 toxins structure and function. Reprinted with permission.	5
Table 2.1.	Primers, enzymes, and plasmids for shiga toxin A ₂ B expression.....	29
Table 2.2.	Primers, enzymes, and plasmids for shiga toxin B protein expression.....	29
Table 3.1	Plasmids for A ₂ /B chimeric proteins.....	39
Table 3.2	Plasmids for Shiga toxin A ₂ /B or STB expression	50

LIST OF FIGURES

- Figure 1.1. Specific glycan binding and cellular internalization. Toxin's A-subunits are represented as a pentagon and their subunit activities are illustrated with different colors (blue, protease activity; green, ADP- ribosyl transferase activity; magenta, N-glycosidase activity). Illustrates the route of internalization of the toxins through the endosomes, Golgi, and endoplasmic reticulum. Figure reprinted with permission 3
- Figure 1.2. Structures of the four main AB5 toxin families. The binding or B subunit is indicated as a molecular surface. The A subunits of Sub AB, Ctx, LT, Stx and Ptx are colored according to the respective catalytic activity (light blue for subtilase activity, light green for ADP-ribosylase activity and purple for RNA N-glycosidase activity). The common structural element (helix A2) is represented by red, and the level of sequence identity of the A-subunit inside a family is indicated. Figure reprinted with permission . 4
- Figure 1.3. Cholera toxin structure. A subunit (blue) of Ctx is contains CTA1 (22 kDa) and CTA2 (5 kDa), connected by a single disulfide bond. The enzymatically active CTA1 peptide is the (toxic) mono-ADP-ribosyltransferase subunit, and CTA2 helical peptide links the CTA1 subunit to the pentameric CTB subunits. The cholera toxin B subunit (10.6 kDa) is made up of five identical polypeptide subunits (yellow, purple, red, orange, and turquoise), each with membrane receptor GM1ganglioside binding capacity. Figure reprinted with permission..... 7
- Figure 1.4. Ctx pathogenesis and mechanism of action: *V. cholerae* secretes Ctx after bacterial ingestion and B subunits binds to oligosaccharide of GM1 ganglioside receptors in the apical membrane. Figure illustrates the toxin endocytosis and its travel to the ER via a retrograde pathway dependent on cell type. Ctx traffics through Golgi to ER where the A subunit dissociates to bind to ADP-ribosylates Gs, stimulating the Adenylate Cyclase complex to produce increased cellular levels of cAMP, leading to activation of PKA, phosphorylation of the major chloride channel, CFTR, and secretion of chloride (Cl⁻) and water. Figure reprinted with permission 8
- Figure 1.5. The structure of Shiga toxin: the crystallographic structure has been obtained from the PDB protein data bank (1DM0). Shiga toxin consists of an A subunit (moiety) (~32 kDa) that is non-covalently attached to a B subunit (moiety) composed of five identical subunits (~7.7 kDa each). The

A-moiety is cleaved by the protease furin into an enzymatically active A1-fragment (~27 kDa) and a carboxyl terminal A2-fragment (~5 kDa), which remain linked by a disulfide bond. Figure reprinted with permission. 12

- Figure 1.6. Mechanism of action of Stx on sensitive cells. Stx binds to Gb3 receptor and gets transported into the ER from endosomes to Golgi to ER. In the ER the A subunit gets cleaved by the enzyme furin and enters the cytosol and inhibits proteins synthesis. Figure reprinted with permission..... 13
- Figure 1.7. Pertussis toxin (Ptx) structure. The Ptx subunits are in hexameric composition with a combined molecular weight of 105 kDa. Subunits are represented in different colors as S1 (blue), S2 (green), S3 (pink), S4 (yellow and purple), and S5 (turquoise). S1 is the enzymatically active subunit with a molecular weight of 28 kDa .The binding subunit is composed of S2 (23 kDa), S3 (22 kDa), two S4's (11.7 kDa each), and an S5 (9.3 kDa) oligomer forming an asymmetrical hetero pentameric ring structure. Figure reprinted with permission. 15
- Figure 1.8. Structure of *Y. pestis* LcrV. A) Ribbon diagram of of LcrV, with helices and strands colored red and blue. B) LcrV amino acid sequence in single letter code. Figure reprinted with permission. 23
- Figure 1.9. A) Schematic representation model of a flavivirus particle. Illustrating different components of the West Nile Virus B) Ribbon diagram Envelope protein E composed of three distinct domains (DI, DII, and DIII). C) Organization of E protein dimers at the surface of mature virions. Figure reprinted with permission 26
- Figure 3.1. A) Schematic representation of pSW006. B) SDS gel of the *E.coli* periplasm showing LcrV –Stx A₂ at approximately 40 kDa and STB below 11 kDa. C. Western blot showing LcrV-StxA₂ using primary LcrV antibodies. 40
- Figure 3.2. A) Schematic representation of pSW004. B and C) Schematic representation of pLGV002 and the multiple cloning site, to express HIS-LcrV-StxA₂/B. D) Colony PCR of pLGV002. Insert was found at the expected size of 854 bps. 42
- Figure 3.3. A) pLGV002 (*Yersinia pestis*) SDS-PAGE of *E. coli* periplasm. Protein band at approximately 39.7 kDa in protein preparations of periplasm and pellets. 1. protein ladder; 2. Cell pellet; 3. Culture PPE; 4. Column flow through; 5. wash 1; 6. wash 2; 7. wash 3; 8. Elution 1; 9. elution 2; 10. elution 3; B) pLGV002 (*Yersinia enterocolitica*) SDS gel of *E. coli* periplasm. Protein band showing approximately at 39.7 kDa in protein preparations of periplasm and pellets 1. Protein ladder; 2. Cell pellet; 3.

	culture supernatant; 4. Column flow through; 5. wash 1; 6. wash 2; 7. wash 3; 8. Elution 1; 9. Elution 2; 10. elution 3.	43
Figure 3.4.	A and B) Schematic representation of pLGV003, the expression vector for LcrV-STX-His chimera. C) Colony PCR of pLGV003 Insert found at the expected size: 834bps. D) pLGV003 SDS gel of <i>E. coli</i> periplasm band showing approximately at 39kDa and 13kDa in protein preparations of periplasm and pellets 1-Ladder; 2. FT-PPE; 3. Wash 1 –PPE.....	44
Figure 3.5.	A and B) Schematic representation of pLGV004, the expression vector for WNVDIII-StxA ₂ /B-HIS chimera. C) Colony PCR of pLGV004. Insert found at expected size: 370bps. Lanes: 1 kB ladder; 1. Colony 1; 2. Colony 2; 3. Colony 3; 4. Colony 4; 5. Colony 5; 6. Colony 6; and 7. negative control.....	45
Figure 3.6.	A and B) Schematic representation of pLGV005, the expression vector for WNVDIII-StxA ₂ /B chimera . C. Colony PCR of pLGV005 showing insert at expected size of 370bps. Lanes 1.1 kB DNA ladder; 2. Positive control; 3. Colony1; 4. Colony 2; 5. Colony 3; 6. Colony 4; 7. Colony 5; 8. Colony 6; 9. Colony 7; 10. Colony 8; 11.Colony 9; 12. Colony 10; 13. Colony 11; 14. negative control.....	47
Figure 3.7.	A and B) Schematic representation of pLGV006, the expression vector for HIS-DIII-StxA ₂ /B chimera. C) Colony PCR of pLGV006 showing insert at expected size of 388bps. Lanes: 1. 1 kB DNA ladder; 2. positive control; 3. colony 1; 4. colony 2; 5. colony 3; 6. colony 4; 7. colony 5; 8. colony 6; 9.colony 7; 10. negative control. D) SDS-PAGEof periplasmic and supernatant proteins from <i>E.coli</i> TE1 + pLGV006 purified on Ni column. Lanes: 1. flow through of periplasmic extracts (PPE); 2. Flow through of supernatant; 3.first wash of PPE (protein band visible at 20 kD for His-DIII-StxA ₂ and at 9.7kDa for STB); 4. first wash of supernatant; E) SDS-PAGE of <i>E.coli</i> TE1 + pLGV006 elutions and pellet fraction; Lanes: 1. elution 1 of supernatant; 2. elute 2 of supernatant; 3. insoluble pellet fraction (protein band of HIS-LcrV-StxA ₂ shown at 20kDa); F) Western blot of <i>E.coli</i> TE1 + pLGV006 protein preparations using anti-HIS antibodies; Lanes: 1. flow through of periplasmic extracts (PPE); 2. first wash of PPE; 3. blank; 4. insoluble pellet fraction.....	48
Figure 3.8.	A and B) Schematic representation of pLGV0010, the expression plasmid for DIII-StxA ₂ /B chimera with TorA as the leader sequence for toxin secretion. C) Colony PCR of pLGV010 showing insert at the expected size of 649bps. Lanes: 1. colony 14; 2. colony 15; 3. colony 16; 4. colony 17.	49
Figure 3.9.	A and B) Schematic representation of pLGV001, the expression vector for DIII-StxA ₂ /B-HIS chimera construct and plasmid for the purification of	

StxA₂/B-HIS alone. C) Colony PCR of pLGV001 showing insert at expected size of 493bps. Lanes: 1. colony 1; 2. colony 2; 3. colony 3; D) SDS PAGE of protein preparations Lanes: 1. blank; 2. PPE of colony 2; 3. flowthrough of PPE of colony 2; 4. PPE of colony 3; 5. flow through of PPE of colony 3; 6. wash 1 of PPE of colony 2..... 51

- Figure 3.10. A and B) Schematic representation of pLGV007, the expression vector for STB-HIS C) Colony PCR of pLGV007 showing insert at the expected size of 570bps. Lanes: 1.1kB DNA ladder; 2. colony 1; 3. colony 2; 4. colony 3; 5. colony 4; 6. colony 5; 7. colony 6; 8. colony 7; 9. colony 8; 10. colony 9. D) SDS-PAGE of protein preparations from *E. coli* TE1 purified on Ni column. Lanes: 1.Flowthrough of PPE; 2. Wash 1; 3. Wash 2; 3. Wash 3; 4. wash 4 of PPE. E) Western blot of *E.coli* TE1 + pLGV007 protein preparations using anti-HIS antibodies with PPE..... 52
- Figure 3.11. A and B) Schematic representation of pLGV009, the expression vector for STB C) Colony PCR of pLGV009 showing insert at the expected size of 349 bps. Lanes: 1.1 kB DNA ladder;2. colony 13; 3.colony 14; 4. colony 15; 5. colony 16; 6.colony 17; 7. colony 18; 8. colony 19; 9.colony 20; 10. negative control; D) SDS-PAGE of periplasmic protein preparations from *E.coli* TE1 + pLGV009 after concentration with 30K filter..... 55
- Figure 3.12. LC-MS of purified STB and SDS–PAGE of purified toxin B subunit proteins. A) LC-MS results from STB purification showing 60.92 % of coverage; B) SDS–PAGE of STB from pLGV009; C) SDS–PAGE of CTB subunit from pARLDR19; D) SDS–PAGE of PTB; E) SDS-PAGE of Heat labile toxin B subunit from pJKT68..... 56
- Figure 3.13. Binding and internalization of the A) RFP-CTA₂/B. B) RFP-StxA₂/B chimera on Vero cells at 4°C and at 37°C showing internalization. DAPI is labelling the nucleus of the cells as blue and red color indicates the Rhodamine fluorescence. Movement of Red fluorescence towards perinuclear space indicates the internalization. 57
- Figure 3.14. Confocal microscopy of CTB and PTB after incubation on dendritic cells (DC2.4) at 37°C for 1 hour using anti-CTB and anti-PTB primary antibodies and FITC labeled secondary antibodies. Results have indicated that antibody staining is showing good Internalization of B subunits of CT and PT. Movement of Green fluorescence towards perinuclear space indicates internalization (indicated by arrow). Blue color center indicated the Nucleus of the cells stained by DAPI. 58
- Figure 3.15. Confocal microscopy of FITC-OVA mixed with toxin B subunit proteins or mock extract and incubated on DC2.4 cells for 1 hour at 37°C. Blue-nucleus of the cells labelled by DAPI staining. Movement of green fluorescence towards perinuclear space indicates internalization. 59

- Figure 3.16. Metabolic activity as shown by Alamar blue on J774 macrophage cells with different adjuvants at different concentrations. Cholera toxin (CT) at 5 $\mu\text{g/ml}$, CT at 10 $\mu\text{g/ml}$, cholera toxin B subunit (CTB) at 5 $\mu\text{g/ml}$, CTB at 10 $\mu\text{g/ml}$, Pertussis toxin B subunit (PTB) at 5 $\mu\text{g/ml}$, PTB at 10 $\mu\text{g/ml}$, Envelope Domain III of West Nile Virus (DIII) at 5 $\mu\text{g/ml}$, and DIII at 10 $\mu\text{g/ml}$. Mock is the periplasmic extracts without testing protein. Error bars indicate STD error of assay performed in triplicate..... 60
- Figure 3.17. Schematic representation of the *in vitro* antigen presentation assay using the B3Z cell line. Adjuvant proteins and antigens are applied and incubated on DC2.4 cells followed by co-incubation of cells with B3Z cells and measurement of B3Z T cell stimulation through β -galactosidase activity..... 62
- Figure 3.18. A) *In vitro* B3Z stimulation assay. Measurement of beta-galactosidase activity using adjuvants Cholera toxin (CT) and Heat labile toxin B subunit (LTB); CT1 (1 $\mu\text{g/ml}$); CT2 (2 $\mu\text{g/ml}$); CT3 (3 $\mu\text{g/ml}$); and LTB1 (1 $\mu\text{g/ml}$) and LTB2 (2 $\mu\text{g/ml}$). B) Comparative study of adjuvant activity between CT and PTB; CT (0.01 $\mu\text{g/ml}$); PTB1 (1 $\mu\text{g/ml}$) and PTB2 (2 $\mu\text{g/ml}$). Analyzed using student's t-test compared with the control value and based on two independent samples ($P < 0.05$). 63
- Figure 3.19. Cytokine production on C57Bl/6 murine dendritic cells line (DC2.4) stimulated with different purified adjuvant proteins. DC2.4 cells were incubated for 24 hours with media containing the indicated concentrations of proteins. A) Comparison between CT, CTB, PTB, and STB at different concentrations for the stimulation of TNF- α . CT (5 $\mu\text{g/ml}$) CTB (5 $\mu\text{g/ml}$), PTB (5 $\mu\text{g/ml}$), STB (5 $\mu\text{g/ml}$). B) Comparison of IL-12 stimulation by CT, CTB, PTB, and STB a different concentrations. CT (5 $\mu\text{g/ml}$), CTB (5 $\mu\text{g/ml}$), PTB (5 $\mu\text{g/ml}$), STB (5 $\mu\text{g/ml}$). The values were determined by ELISA and the data shown are determinations from two independent experiments. 64
- Figure 3.20. Multi-analyte cytokine analysis on C57Bl/6 murine dendritic cells line (DC2.4) stimulated with adjuvant proteins CTB and STB at 2 $\mu\text{g/ml}$ concentration. DC2.4 cells were incubated with media containing the indicated concentrations of proteins for 24 hours prior to collection of supernatant. Standard error is based on results of two independent samples..... 65

LIST OF ABBREVIATIONS

CT, Ctx	Cholera Toxin
ST, Stx	Shiga toxin
ST1, Stx1	Shigatoxin1
PT, Ptx	Pertussis toxin
LT, LT1	Heat labile toxin
CTA, Ctx A	Cholera toxin A (active) subunit
CTB, Ctx B	Cholera toxin B (Binding) subunit
STA, StxA	Shiga toxin A (active) subunit
STB, StxB	Shiga toxin B (Binding) subunit
PTA, Ptx A	Pertussis toxin A (active subunit)
PTB, Ptx B	Pertussis toxin B (Binding) subunit
LTA	Heat labile toxin A (active)subunit
LTB	Heat labile toxin B (Binding) subunit
A2/B	toxin A2 domain and B subunit chimeric molecule
LcrV	Low calcium response virulence protein
DIII	Domain III

WNV	West Nile Virus
Gb3	Globotriaosylceramide
GM1	monosialotetrahexosylganglioside
<i>E. coli</i>	<i>Escherichia coli</i>
EHEC	Enterohemorrhagic <i>E. coli</i>
HUS	Hemolytic Uremic syndrome
ER	Endoplasmic reticulum
NAD	Nicotinamide adenine dinucleotide
TGN	trans-Golgi network
DC	Dendritic cells
TNF- α	Tumor necrosis factor alpha
IL	Interleukin
INF- γ	Interferon gamma
ERAD	ER-associated degradation
E	Envelope protein of West Nile Virus
O/N	overnight
IPTG	Isopropyl-beta-D-thiogalactopyranoside
6Xhis	Histidine tag for affinity purification
TAE buffer	Tris-acetate buffer

PBS	Phosphate buffered saline
PPE	Periplasmic exctacts
EtBr	Ethidium bromide
SDS-PAGE	sodium dodecyl sulfate – Poly acrylamide gel eletro phoresis
DMEM	Dulbecco's Modified Eagle Medium
ELISA	Enzyme linked immuno Sorbent assay
FITC-OVA	fluorescein isothiocyanate-ovalbumin

CHAPTER I. INTRODUCTION

Bacterial AB5 Toxins

Bacterial AB5 type toxins are large secreted multimeric proteins that bind to and trigger reactivity in host cells. AB5 toxins are highly significant proteins because of their pivotal role in virulence for pathogenic bacteria specifically *Escherichia coli*, *Shigella dysenteriae* and *Vibrio cholerae*. These three pathogens can cause severe gastroenteritis and diarrhea and are responsible for significant human mortality and morbidity globally [1, 2]. AB5 toxins are composed of two subunits including a catalytic domain, or A subunit, linked to a pentameric binding domain or B subunit. Two stages are involved in the process of AB5 toxin mechanism of action: 1) binding of the pentameric B subunit to distinctive receptors on the host cell surface that triggers the uptake and internalization of the holotoxin, and 2) translocation of the A subunit to the host cytosol leading to the suspension or dysfunction of imperative host cell activities and often leading to cell death (Figure 1.1). These toxins are often the main virulence factor produced by pathogenic Gram negative bacteria and many are well studied. There are four recognized AB5 toxin families that include the cholera toxin (Ctx) and *E.coli* heat-labile toxin (LT) family, the shiga toxin (Stx) family, the pertussis toxin (Ptx) family, and the subtilase cytotoxin (SubAB) family (Figure 1.2 and Table 1.1) [3].

The most well studied bacterial AB5 toxin is Ctx, produced by *Vibrio cholerae*. The Ctx family contains the highly homologous *E. coli* heat labile toxin LTI and the

closely related LTIIa and b toxins. The Stx family is composed of Stx from *Shigella dysenteriae*, and the Shiga-like toxins or Vero toxins produced by *E.coli* [4]. In addition to extensive characterization of the structure and function of these toxins, over the last two decades, AB5 toxins have emerged as highly effective mucosal adjuvants for strengthening immune responses to co-administered antigens. The adjuvanticity of these molecules can be attributed to their unique ability to bind to specific host cells and to constructively engineer signaling pathways in these cells [5]. Research shows that Ctx and the cholera toxin B subunit (CtxB) are gold standard mucosal vaccine adjuvants, but can also be used to promote diverse outcomes, such as the suppression of auto-immune responses in Type 1 diabetes and reduction of the salient features of asthma like eosinophilia in mice [6, 7]. Less is known about the immunostimulatory activity of other AB5 toxins; however, Stx has been shown to be a promising approach for the development of vaccines that target pancreatic and colon cancer, as these cells express more Gb3, which is a receptor for Shiga toxin B (StxB) [8-10]. Research shows that ST1 may possess adjuvant activity for inducing mucosal immunity [30]. We hypothesized that ST1 non-toxic derivatives can act as mucosal adjuvants for vaccines directed against infectious agents. We tested this hypothesis by constructing non-toxin ST1 fusions and characterizing these fusions *in vitro*.

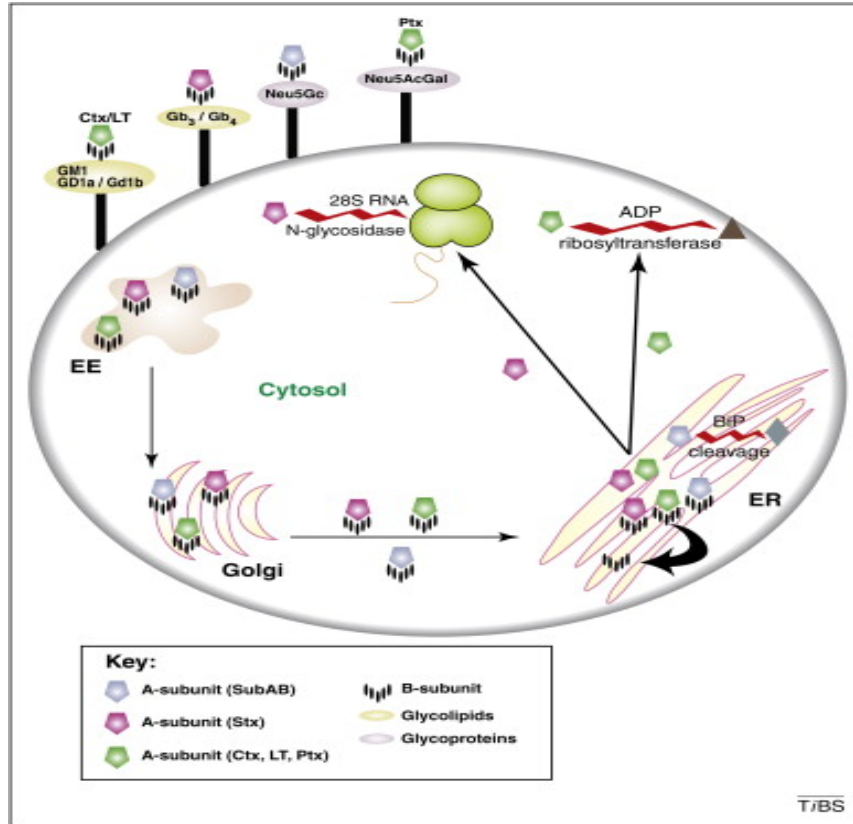


Figure 1.1. Specific glycan binding and cellular internalization. Toxin's A-subunits are represented as a pentagon and their subunit activities are illustrated with different colors (blue, protease activity; green, ADP- ribosyl transferase activity; magenta, N-glycosidase activity). Illustrates the route of internalization of the toxins through the endosomes, Golgi, and endoplasmic reticulum. Figure reprinted with permission [3].

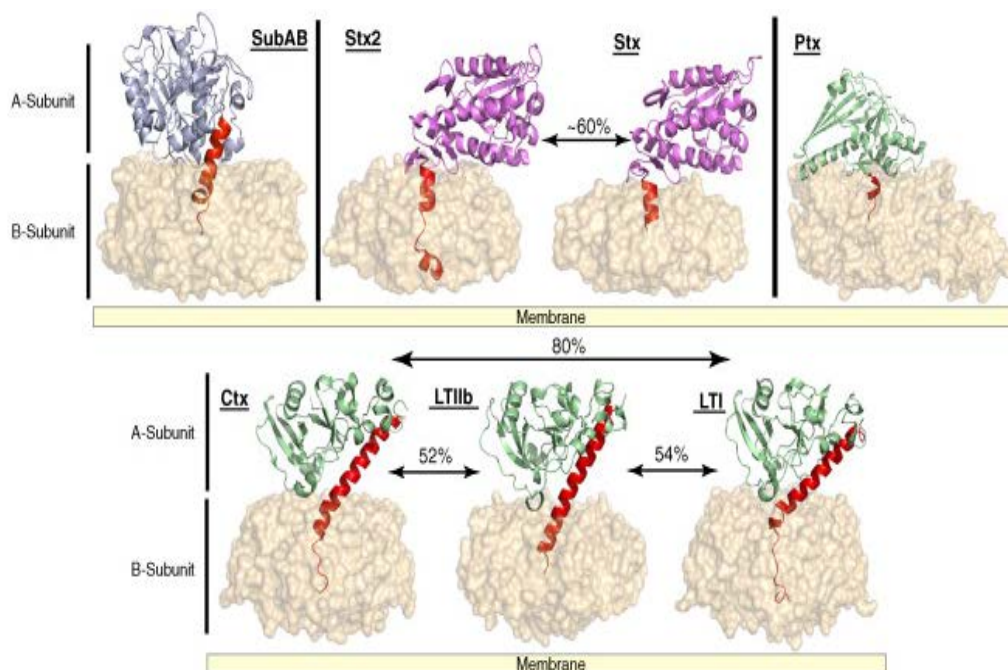


Figure 1.2. Structures of the four main AB5 toxin families. The binding or B subunit is indicated as a molecular surface. The A subunits of Sub AB, Ctx, LT, Stx and Ptx are colored according to the respective catalytic activity (light blue for subtilase activity, light green for ADP-ribosylase activity and purple for RNA N-glycosidase activity). The common structural element (helix A2) is represented by red, and the level of sequence identity of the A-subunit inside a family is indicated. Figure reprinted with permission [3].

Table 1.1. Summary of AB5 toxins structure and function. Reprinted with permission [5].

	A Subunit(s)	B Subunit(s)	Enzymatic Activity	Target	Receptor(s)
Cholera toxin	A1: 22 kDa A2: 5 kDa	(×5) 10.6 kDa	ADP-ribosyl transferase	Adenylate cyclase G-protein (G _{sa})	GM1 ganglioside
<i>E. coli</i> (LT)	A1: 22 kDa A2: 5 kDa	(×5) 11.6 kDa	ADP-ribosyl transferase	G-protein (G _{sa})	GM1 ganglioside Asialoganglioside
Shiga toxin	A1: 28 kDa A2: 4 kDa	(×5) 7.7 kDa	N-glycosylase (Cleaves adenine 4324)	rRNA (28S)	Gb3 glycolipid
Pertussis toxin	S1: 28 kDa	S2: 23 kDa S3: 22 kDa S4: (×2) 11.7 kDa S5: 9.3 kDa	ADP-ribosyl transferase	G-protein (G _{sa})	GD1a ganglioside
Anthrax	(LF): 90 kDa (EF): 89 kDa	(PA): (×7) 83 kDa	Zn metalloprotease Adenylate cyclase	MAPKK Protein kinases	ANTXR 1 ANTXR 2
Ricin	30 kDa	29 kDa	N-glycosylase (Cleaves adenine 4324)	rRNA (28S)	Glycoprotein Glycolipid

Vibrio cholerae Cholera Toxin

Cholera toxin (Ctx) is produced by the bacterium *Vibrio cholerae* and is responsible for the human diarrheal disease cholera. Ctx consists of an active A subunit (CtxA, or CTA) that is a single polypeptide chain with two domains (A1 and A2) that total approximately 27 kD, and a receptor binding pentameric B subunit (CtxB, or CTB), of approximately 10.6 kD per monomer (Table 1.1). CTA and CTB are folded after secretion within the bacterial periplasm to form a large, multimeric holotoxin that is greater than 80 kD. Ctx is the main virulence factor contributing to the pathogenesis of *V. cholerae* infection. Pathogenicity of *V. cholerae* is characterized by its ability to resist acidic environments of the stomach followed by colonizing the small intestine and secretion of Ctx [11, 12]. In the small intestine, the CTB subunit adheres to ganglioside

GM1 receptors on the surface of host intestinal epithelial cells, which triggers the uptake of Ctx by retrograde endocytosis through the Trans Golgi network (TGN) to the endoplasmic reticulum (ER). CTA is tethered to CTB via non-covalent interactions within the C-terminal, called the CTA2 domain (Figure 1.3). After internalization of the toxin, the active domain (CTA1) is translocated to the host cytoplasm via the ER-associated degradation pathway (ERAD). In the cytosol, CTA binds to and constitutively activates the regulatory protein Gs α by ADP-ribosylation (Figure 1.4) [13, 14]. This enzymatic activity in the host cytosol results in the activation of adenylate cyclase followed by the secretion of electrolytes and fluids into the lumen of the small intestine. While Ctx intoxication does not trigger apoptosis nor necessarily lead to host cell death, the massive fluid secretion stimulates cell sloughing, transmission of the bacterium, and fluid losses of up to 20 liters a day. Dehydration and shock can cause death within 24 hours especially in vulnerable populations. Despite the efficacy of prompt therapy, cholera still causes an estimated 3-5 million infections and over 100,000 deaths per year, largely in developing countries with inadequate access to clean water (WHO).

Immunomodulation by Ctx has been studied extensively over the past two decades; however, it is yet to be fully understood. Factors that contribute to immunomodulation include: antigen-presenting cell activation, B-cell isotype switching, and up regulation of co-stimulatory and MHC class II expression. As described in more detail below, the majority of these responses are the consequences of interactions between CTB and its receptor ganglioside GM1 on the surface of the effector cells, such as dendritic cells, which play major roles in antigen uptake, presentation, and cellular activation [15].

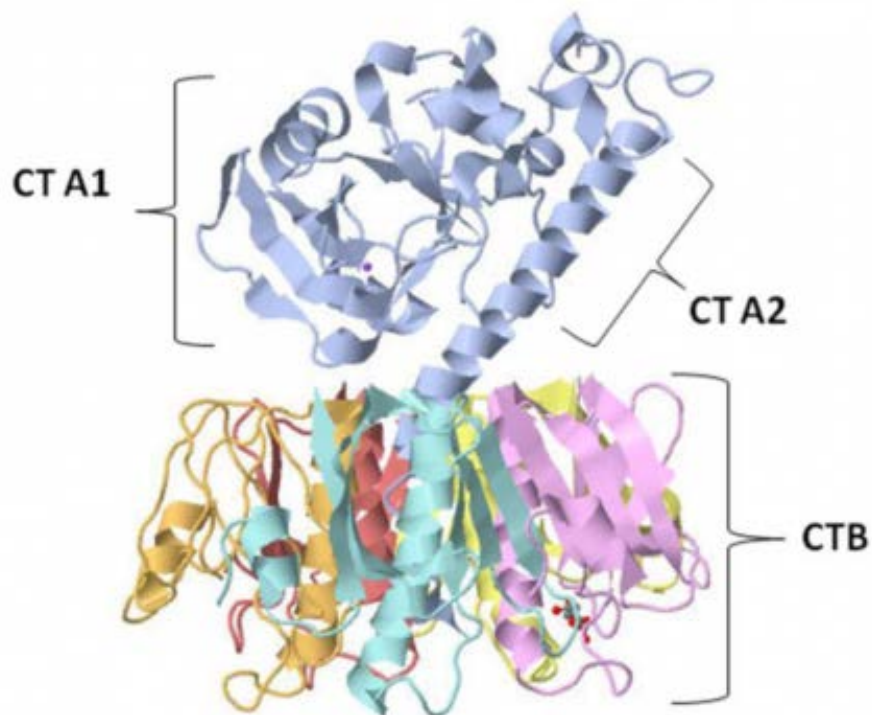


Figure 1.3. Cholera toxin structure. A subunit (blue) of Ctx is contains CTA1 (22 kDa) and CTA2 (5 kDa), connected by a single disulfide bond. The enzymatically active CTA1 peptide is the (toxic) mono-ADP-ribosyltransferase subunit, and CTA2 helical peptide links the CTA1 subunit to the pentameric CTB subunits. The cholera toxin B subunit (10.6 kDa) is made up of five identical polypeptide subunits (yellow, purple, red, orange, and turquoise), each with membrane receptor GM1ganglioside binding capacity. Figure reprinted with permission [5].

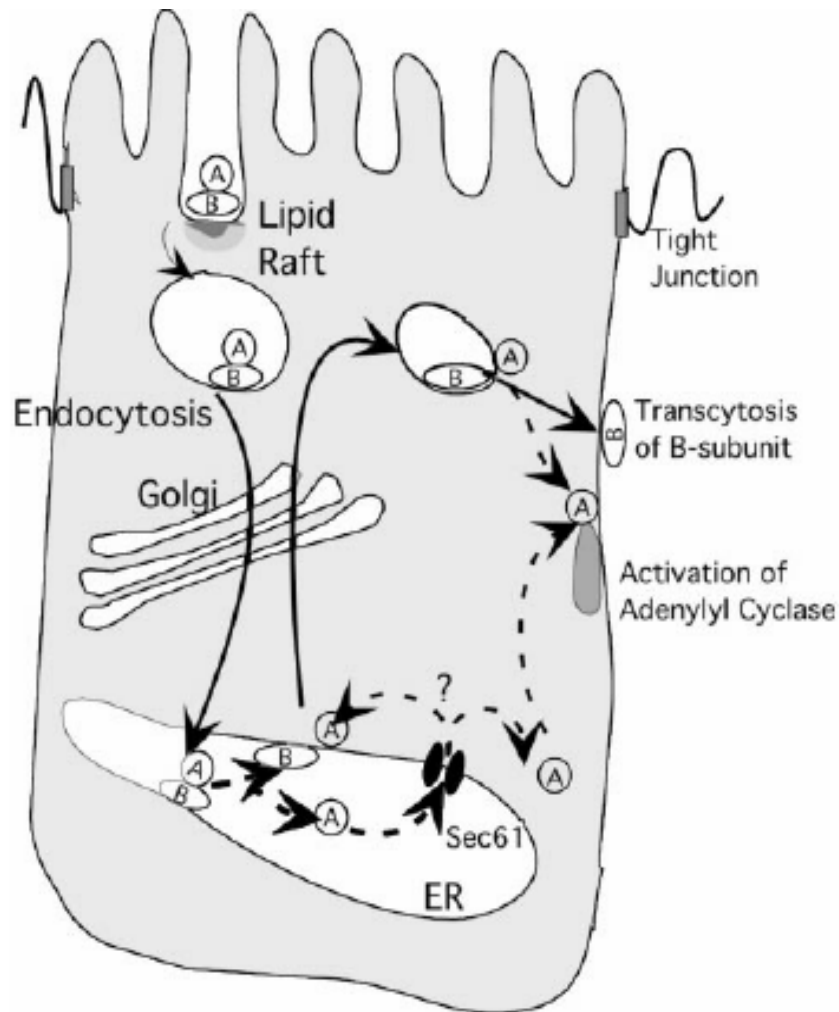


Figure 1.4. Ctx pathogenesis and mechanism of action: *V. cholerae* secretes Ctx after bacterial ingestion and B subunits binds to oligosaccharide of GM1 ganglioside receptors in the apical membrane. Figure illustrates the toxin endocytosis and its travel to the ER via a retrograde pathway dependent on cell type. Ctx traffics through Golgi to ER where the A subunit dissociates to bind to ADP-ribosylates Gs, stimulating the Adenylate Cyclase complex to produce increased cellular levels of cAMP, leading to activation of PKA, phosphorylation of the major chloride channel, CFTR, and secretion of chloride (Cl^-) and water. Figure reprinted with permission [16].

***E.coli* Heat-Labile Toxin**

Heat-labile enterotoxin (LT) is produced by enterotoxigenic *Escherichia coli* (ETEC). LT holotoxin has an enzymatically active A subunit (LtxA or LTA, 27 kDa) that, similar to CTA, is made of two subunits connected by a single disulfide bridge. LTA1 is the active catalytic portion and LTA2 is a linker peptide that joins the LTA1 subunit to the LTB pentamer via disulfide bond. The LTB subunit has five identical binding B subunits and binds strongly to ganglioside GM1, but also binds asialo-GM1, GD1b, and GM2 [5, 17-19]. LT is the major virulence factor of ETEC, and is highly similar to Ctx in sequence, structure, and function along with antigenicity [20]. CTA is identical to LTA, and CTB is 80% identical to LTB at the amino acid level [21]. These subtle differences in sequence contribute to distinct cellular binding and toxicity between Ctx and LT. LT endocytosis and LTA translocation also results in ADP-ribosylation and constitutive activation of adenylate cyclase, followed by increases in intracellular cAMP, declines in Na⁺ absorption by the epithelial cells, and increased chloride ion secretion through CFTR (cystic fibrosis transmembrane conductance regulator), leading to diarrhea [22]. ETEC infection results in what is known as Traveler's Diarrhea and it was initially identified as the cause of human diarrheal illness in the 1960s [23-25]. ETEC infections in humans are associated with contaminated food and water consumption. Infection occurs as a sudden onset of self-limiting diarrhea but can cause dehydration as a result of the fluid and electrolytes loss [26]. ETEC is estimated to cause 200 million diarrheal cases and approximately 380,000 deaths annually worldwide [27]. Additionally, it causes a significant problem for military personnel visiting countries where ETEC is endemic [26]. It also has significant financial ramifications in the farming industry as it is a primary pathogen of cattle, and neonatal and post weaning piglets [28].

***Shigella dysenteriae* Shiga Toxin**

Shiga toxin (Stx) produced by *Shigella dysenteriae* also belongs to the AB₅ family of secreted bacterial toxins that includes Ptx, Ctx, and LT [29]. Shiga toxins are named after the Japanese bacteriologist, Kiyoshi Shiga, who first described the bacterial origin of dysentery caused by *Shigella dysenteriae* in 1897 [30]. There are two main types of shiga toxins, shiga toxin 1 (Stx1 or ST1), and shiga toxin 2 (Stx2 or ST2). ST1 is produced by both *S. dysenteriae* and shiga-toxin producing strains of *E.coli* (STEC) and is virtually identical amino acid homology between these species [29]. ST2 is produced by *E. coli* and is not cross neutralized by poly clonal antisera against ST1 or vice versa [31, 32]. ST2 is often expressed by the 0157:H7 *E. coli* serotype, or enterohemorrhagic *E.coli* (EHEC) and epidemiological, experimental studies suggest that it is more often associated with clinical disease than ST1 [32].

E.coli and *Shigella* strains harboring ST1 and ST2 are transmitted via food, person to person, or hand to mouth and can also spread through cattle. Infection of the human small intestine with ST1 or ST2 expressing bacteria can lead to a range of clinical outcomes including shigellosis, bloody dysentery, hemolytic colitis, or hemolytic uremic syndrome (HUS). HUS is the most severe form of disease that can lead to kidney failure especially in young children. Symptoms of gastroenteritis usually appear within few hours of ingestion of toxin-expressing bacteria. Infections are highly communicable, and as low as 50-100 cells can result in significant disease [33, 34].

Like Ctx, shiga toxins are complex holotoxins with an AB₅ – type composition. ST1 includes a 32 kDa enzymatically active (ST1A) subunit that is non-covalently associated with a pentameric binding domain (ST1B) composed of five identical B

proteins (38.5 kDa) (Figure 1.5). The mature A and B subunits of ST1 and ST2 have 55 and 61% amino acid identity and 68 and 73 % similarity, respectively. Despite these sequence differences, the crystal structures of the ST1 and ST2 holotoxins are highly similar and the toxins have the same mode of action [31, 32]. Upon ingestion of bacteria and colonization of the host small intestine, Stx is secreted from the bacterium and the A subunit is asymmetrically cleaved by trypsin or furin into the A1 (~ 27kDa) and A2 (~ 5kDa) peptides. The A2 domain is non-toxic, but traverses the B subunit to bind the holotoxin together non-covalently before reduction. Similar to Ctx, the B pentamer confers toxin receptor-specificity and binds to eukaryotic receptors, however unlike Ctx, Stx binds to the unique receptor, globotriaosyl ceramide (Gb3) [3, 35]. Gb3 is found on many cells within the body, including intestinal epithelial cells, neuronal cells, dendritic cells, and germinal center B lymphocytes [36]. Gb3 is also found abundantly in the microvasculature of kidney [37].

Following toxin secretion and Gb3 binding, the holotoxin enters the cell by triggering endocytosis, and escapes the lysosomal pathway by passing from early endosomes to the TGN and then to the ER. The A1 and A2 domains of Stx remain associated through a disulfide bond while the toxin is internalized by this retrograde transport. Reduction and separation of A1 and A2 occurs within ER. The enzymatically active A1 domain is then translocated to the cytosol and once there acts as an N-glycosidase that removes an adenosine residue from the 28S rRNA on the 60S ribosome (the bond between the base and ribose is lysed). This alteration halts host cell protein synthesis and triggers apoptosis in the intoxicated cell [38]. The result is a sloughing of intestinal cells and bloody diarrhea associated with dysentery. More severe infections can

release toxin that binds to and targets cells of the kidneys, resulting in HUS that can have a mortality rate up to 10% [39].

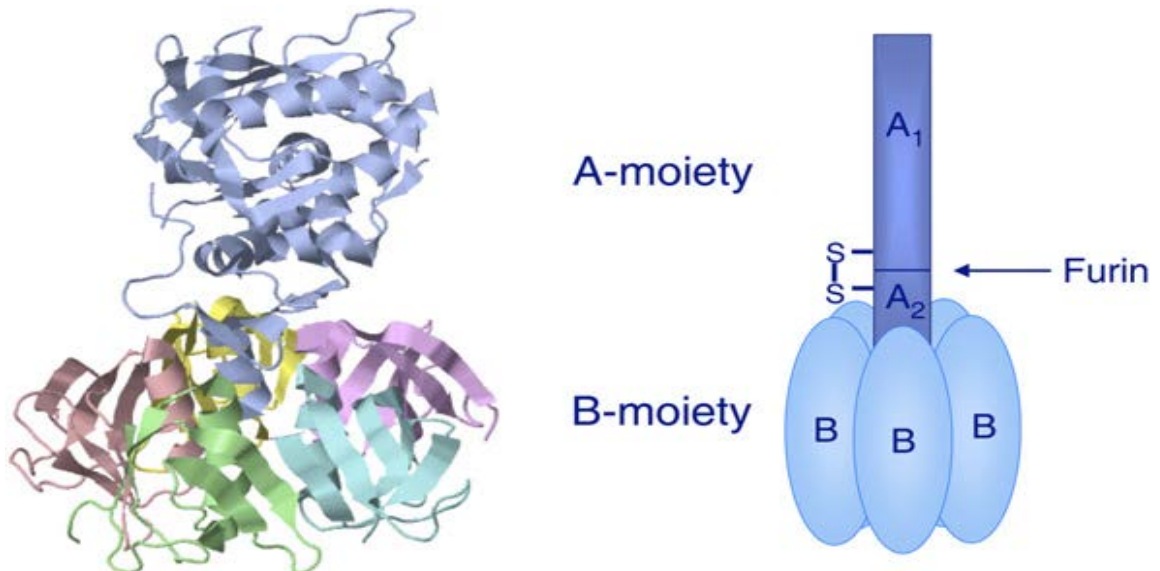


Figure 1.5. The structure of Shiga toxin: the crystallographic structure has been obtained from the PDB protein data bank (1DM0). Shiga toxin consists of an A subunit (moiety) (~32 kDa) that is non-covalently attached to a B subunit (moiety) composed of five identical subunits (~7.7 kDa each). The A-moiety is cleaved by the protease furin into an enzymatically active A1-fragment (~27 kDa) and a carboxyl terminal A2-fragment (~5 kDa), which remain linked by a disulfide bond. Figure reprinted with permission [32].

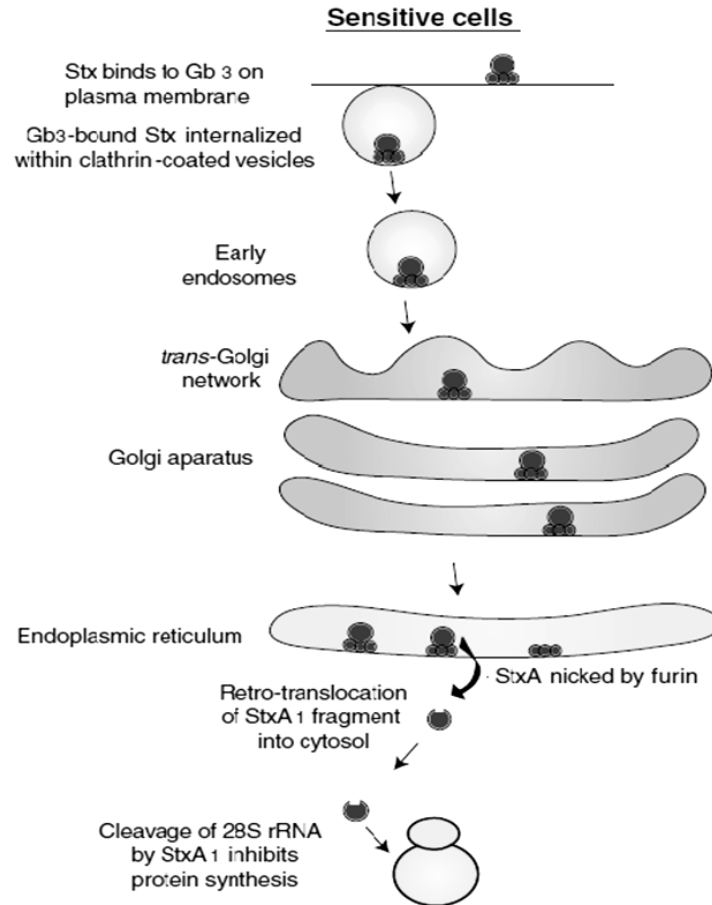


Figure 1.6. Mechanism of action of Stx on sensitive cells. Stx binds to Gb3 receptor and gets transported into the ER from endosomes to Golgi to ER. In the ER the A subunit gets cleaved by the enzyme furin and enters the cytosol and inhibits proteins synthesis. Figure reprinted with permission [1].

***Bordetella pertussis* Pertussis Toxin**

Pertussis toxin (Ptx) is secreted by the gram negative pathogen, *Bordetella pertussis*, that causes the respiratory infection commonly known as whooping cough. Ptx was first identified by the Belgian scientist, Jules Bordet, in 1906 [5]. While Ptx is an AB5-type toxin with an enzymatically active and binding subunit, unlike Ctx and Stx, it is a large hexamer that contains five different subunits (S1, S2, S3, two copies of S4 and S5) with a total molecular weight of 105kDa [40, 41]. The Ptx S1 subunit is the catalytic domain possessing enzymatic activity. S1 transfers an ADP-ribose from nicotinamide adenine dinucleotide (NAD) to the cysteine residue of trimetric guanine nucleotide-binding proteins (Sialo glyco proteins), leading to a decoupling of the G-protein α -subunit from its receptor. The decoupling event blocks the inhibition of adenylate cyclase activity, leading to an increase in accumulation of intracellular cAMP concentration and subsequent increase in respiratory secretions and mucus production [5]. This activity triggers a number of downstream cellular events including cytokine secretion, inflammation and cell death, that are the main mechanisms of pathogenesis associated with disease [42]. There is a 20% sequence identity between the S1 subunit of Ptx and the A subunit of Ctx, indicative of distinct functions within the cell [43]. The Ptx S2, S3, S4, and S5 fold to form a binding subunit or B oligomer that facilitates the binding of Ptx to target host cell receptors and the delivery of active S1 subunit into the cytosol by retrograde transport [44, 45]. The B subunit of Ptx binds to ganglioside GD1a available within lipid rafts buried in the plasma membrane of upper respiratory epithelial host cells. The S1 subunit undergoes tyrosine sulfation as it travels through the TGN along with *N*-glycosylation in the Golgi apparatus followed by ER to build its ADP-ribosylating

ability [46, 47]. As described below, Ptx also has significant immunomodulatory activities and studies show that Ptx is capable of augmenting antigen-specific immunoglobulin-IgG and IgE responses [48].

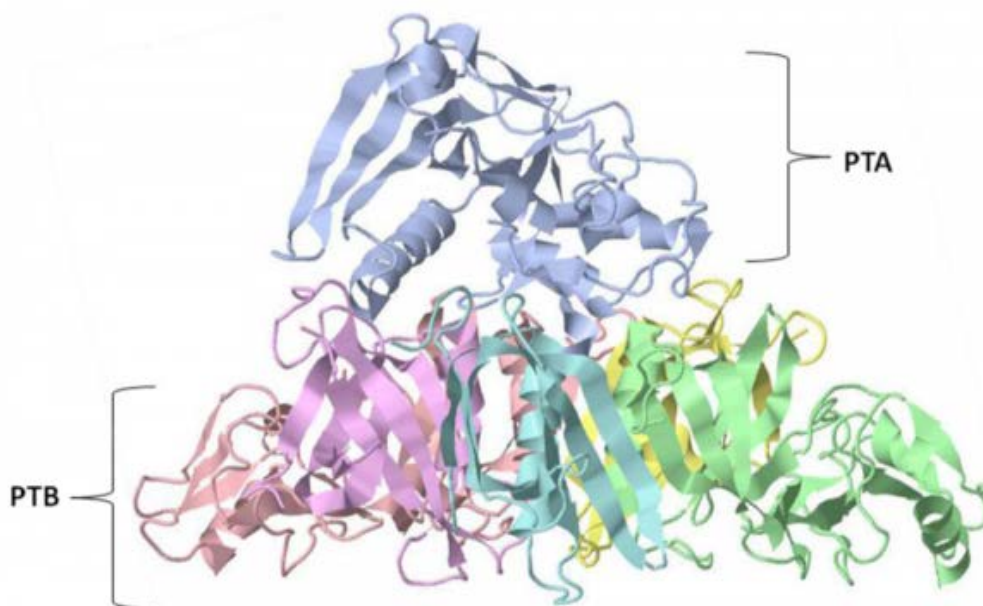


Figure 1.7. Pertussis toxin (Ptx) structure. The Ptx subunits are in hexameric composition with a combined molecular weight of 105 kDa. Subunits are represented in different colors as S1 (blue), S2 (green), S3 (pink), S4 (yellow and purple), and S5 (turquoise). S1 is the enzymatically active subunit with a molecular weight of 28 kDa. The binding subunit is composed of S2 (23 kDa), S3 (22 kDa), two S4's (11.7 kDa each), and an S5 (9.3 kDa) oligomer forming an asymmetrical heteropentameric ring structure. Figure reprinted with permission [5].

Vaccine Adjuvants

Successful vaccines are more effective than therapeutic drugs in establishing overall public health. For a vaccine to be successful, it must have the ability to stimulate specific immune responses, and recent vaccine development has focused on the use of highly purified antigens that can be delivered by non-traditional routes. Purified proteins are often not good immunogens, and delivery via the oral or nasal route requires the ability to overcome immune tolerance. These obstacles can be overcome with the use of a

vaccine adjuvant. Adjuvants are substances that, when co-administered with an antigen, increase the immune response to the antigen without having any specific effect itself. Development of potent adjuvants that are effective from mucosal surfaces is crucial as the delivery of vaccines through the oral or nasal route is very practical, non-invasive, and efficacious for the induction of immune responses against mucosal pathogens [49]. A number of important pathogens initiate infection by interacting with host mucosal surfaces of the respiratory, urogenital, and gastrointestinal tracts. The production of protective mucosal IgA antibodies at these surfaces is important for controlling infection. In addition, there is an increased need to induce immunity to a specific purified protein subunit or DNA vaccines that are safer and less toxic than traditional live attenuated vaccines. Using adjuvants in combination with these antigens can greatly enhance their immunogenicity. Despite intense research, there is currently only one vaccine adjuvant licensed for use in the U.S: alum, or aluminum salts. Alum is only effective with some vaccines and is not capable of inducing immune responses from mucosal surfaces [50, 51]. Currently there is only two more squalene-based oil-water emulsion MF59 and AS03 adjuvants licensed in Europe. MF59 has been mainly used to increase flu immunogenicity in the elderly and young children [52]. Adjuvant AS03 have been licensed for pandemic flu vaccines [53]. Thus, there is an important need to identify and characterize novel vaccine adjuvants.

Cholera Toxin and *E.coli* LTI Toxin as Vaccine Adjuvants

Ctx has long been known as an excellent immunostimulatory agent, however, wild-type Ctx is too toxic for use as a human vaccine adjuvant. Research has shown that detoxifying Ctx can reduce toxicity and retain immunogenicity [49, 54]. In addition, the

nontoxic B subunit by itself has good adjuvant activity [55-57]. Studies have revealed that Ctx is a potent vaccine adjuvant as it can induce antigen-specific mucosal IgA immunity, stimulate systemic IgG Th2 type immune responses, and inhibit innate inflammatory responses induced by pathogen-derived molecules like lipopolysaccharides (LPS) [54, 58]. Chemical or genetic conjugation of antigen with CTB enhances antigen presentation [59]. However, constructing A₂B chimeric molecules with Ctx is able to induce antigen specific immune responses without inducing immunological tolerance, which is a limitation of chemical conjugation [60]. Dendritic cells (DC) are very important for efficient priming of cellular and humoral immune responses, as they are professional antigen presenting cells (APC) specialized in the antigen uptake, processing and presentation to T cells. Ctx has been shown to bind efficiently to these cells [61, 62]. A number of studies have used native Ctx to stimulate protective responses to co-administered antigens [63-65]. Fewer studies have looked at the use of CTB alone as an adjuvant, but these studies have indicated that at higher concentrations, CTB can also act to induce antigen-specific protective responses that are largely Th2-type [65]. CTB has been found to trigger largely anti-inflammatory responses from monocytes, macrophages, and dendritic cells [66]. Cytokines IL-10 and TGF- β produced by B cells are essential in the regulation process of T cells to form T effector cells [67]. When B cells treated with CTB/Ag were isolated from a mice deficient of IL-10 , they still showed greater proliferation of T_{reg} (T regulator) cells compared to wild type B cells. It has been shown that CTB /Ag treated B cells were able to accomplish the regulatory function of T_{eff} cells in a TGF- β dependent manner and provide protection against experimental auto immune encephalomyelitis independent of IL-10 [68]. TNF- α is an important factor for

recruitment of antigen presenting cells like dendritic cells and lymphocytes to regional lymphnodes. Ctx has been shown to inhibit pro inflammatory cytokine TNF- α primarily through A subunit whereas CTB has stimulatory effect [69, 70] .

Lack of IgA is associated with increased rates of sensitization to inhaled and ingested allergens [71]. Chemical conjugation of antigens to CTB has been shown in a number of studies to stimulate tolerance when delivered at high concentrations to mucosal surfaces. This effect of CTB has promoted much research into the therapeutic use of this molecule to reduce allergies and treat autoimmune disease like Type 1 diabetes [72]. CTB-insulin conjugate has been shown to delay the onset of insulin dependent diabetes mellitus [5].

LT as a holotoxin has varied dimensions of interactions with the immune system and also possesses potent immunomodulatory activities [17, 73]. Binding to distinct host cell receptors and triggering unique responses, LT has been shown to induce more of a balanced Th1/Th2 type of immune response than Ctx [74, 75]. LT has been shown to trigger the migration of dendritic cells localization to the follicle associated epithelium of the Peyer's patches [76]. Dendritic cells are of major interest in studying the adjuvant capacity of subunit toxin proteins [76]. Research has also shown that the B subunit of LT has the capacity to increase the TNF- α induction by murine macrophages. Induction of TNF- α is important as it plays an important role in immunity against infections [69]. Use of LT mutants as vaccine adjuvants in intranasal influenza vaccines has shown an association with Bell's palsy; a sudden, but self-limiting, weakness or paralysis in facial muscles that may be neuro-toxic result of LT trafficking on neuronal cells of the central nervous system (CNS) [77, 78]. These studies indicate safety concerns for the use of Ctx,

LT, or mutants of these holotoxins, after intranasal delivery. However, LTB and CTB do not trigger inflammation in the CNS of mice and can be delivered via a number of alternative routes, including sublingual, intravaginal, subdermal, and transdermal, that do not result in trafficking to the CNS [79-81]. Thus, the non-toxic B subunits of Ctx and LT are still under intense study as potent adjuvants for vaccine applications [77]. Many studies have shown that CT and LT1 are powerful mucosal adjuvants when co-administered with soluble antigens [65, 73, 82].

Pertussis Toxin as a Vaccine Adjuvant

Ptx has also has potent immune-enhancing adjuvant activity. Studies have demonstrated that Ptx can activate CD4⁺ T cells via co-stimulatory molecules expressed by toxin-activated antigen presenting cells [83]. In addition, a non-toxic S1 mutant devoid of enzymatic activity is capable of receptor binding and maintained its adjuvanticity by augmenting the activation of both Th1 and Th2 subpopulations of T cells, antigen-specific T cell proliferation and the secretion of IFN- γ (Th1), IL-2(Th1), IL-4 (Th2) and IL-5(Th2) upon injection with foreign antigens [84]. Formalin or genetically detoxified Ptx is a major component of the current pertussis vaccine (DTaP or TDap) and is a protective antigen in its own right [85]. When used as an adjuvant, toxigenic Ptx is able to promote Th17 differentiation through IL-6 induction [86]. More recently, Ptx has been shown to induce the polyclonal activation and effector functions of CD8⁺ T cells with up-regulation of CD28 and CD69 and the production of IFN- γ and IL-17 [87]. Dendritic cells (DCs) are considered to be most potent antigen presenting cells. Ptx and the Ptx B subunit (PTB) were compared for the capacity to induce the maturation of both human and mouse DCs. These results suggested that both PT and PTB induced

the maturation of DCs and that was dependent on TLR4, a receptor for bacterial lipopolysaccharide (LPS) [88]. When used as an adjuvant for experimental autoimmune encephalomyelitis, Ptx was shown to reduce the number and function of regulatory CD4+ T cells [89].

Shiga Toxin as a Vaccine Adjuvant

DCs are known to be Gb3 positive and Stx also binds and targets these cells [62]. Toxicogenic Stx1 induces more of a Th1 type directed cellular immune response, which is an advantage of the use of Stx1 over Ctx as a vaccine adjuvant for effective defense against intracellular bacteria and viruses [90, 91]. Because of this unique pathway, Stx1 has been investigated for its ability to induce MHC class 1 – restricted presentation of antigen peptides to CD8+T lymphocytes *in vitro* [92] and *in vivo* [92, 93]. Recent studies have also shown that ST1 may possess adjuvant activity for inducing mucosal immunity [30]. Research suggests that the non-toxic B subunit of Stx1 (ST1B) interacts with Gb3, which is expressed preferentially on DC and B cells and induces a robust and long lasting CD 8+ T cell response *in vivo* [61]. In addition, ST1B, coupled to tumor antigens, showed tumor protection in both prophylactic and therapeutic settings [61]. These studies suggest that native Stx1 and ST1B may be potent vectors for the induction of cellular immunity and the development of novel immuno-therapeutic approaches [92, 93].

The binding and trafficking properties of the shiga toxins has also led to the use of Stx1, or the ST1B subunit alone, for investigating retrograde transport in eukaryotic cells [50]. B-subunits have been engineered as fusions to peptides that are specifically recognized and modified in different cell compartments. This has allowed the detailed characterization of toxin retrograde transport to the ER [29]. Additional studies have

determined that the active ST1 A1 domain is translocated from the ER into the cytosol through the ERAD pathway and the Sec 61 channel [3]. The distinct host-receptor interaction, pattern of cellular activation, and trafficking of Stx on host cells indicates that this toxin and its non-toxic B subunit possess unique and novel adjuvant properties worthy of further exploration.

Vaccines of Interest and Potential Vaccine Antigens

Yersinia pestis and LcrV

Yersinia. pestis was discovered by Alexandre Yersin, a Swiss/French physician and bacteriologist from the Pasteur Institute, during an epidemic of plague in Hong Kong in 1894 [94]. It is a Gram-negative rod-shaped bacterium, a member of the enterobacteriaceae family, and a facultatively anaerobic bacterium that can infect humans and other animals [95]. The genus *Yersinia* is comprised of Gram-negative coccobacilli and contains three well-recognized human pathogens including: *Y. pestis*, *Y. pseudotuberculosis*, and *Y. enterocolitica* [96]. *Y. pestis* is the causative agent of the black plague or black death, and the other species cause significant food-borne diarrheal diseases [97]. There are three recognized forms of plague caused by *Y. pestis* in humans: bubonic, pneumonic, and septicemic. Bubonic plague is an infection of the lymph system acquired through the bite of infected fleas or rodents causing painful and inflamed lymph nodes called buboes. The pneumonic form is inhaled, restricted to the lungs, and is extremely contagious via aerosolized droplets spread by infected individuals. Finally, the septicemic infection occurs when bacteria invade the blood stream from the lymph or the lungs [98, 99]. Symptoms and complications of a *Y. pestis* infection include adult

respiratory distress syndrome, disseminated intravascular coagulation, shock, and multiple organ failure [100].

The black plague has a lengthy history of infecting human populations. Mainly, this disease spread to epidemic proportions during the 14th century in Europe and led to the death of over one third of the continent's population [101, 102]. Currently, with the help of antibiotics, the plague has become manageable and can be cured within days of drug administration. Only 1-5 cases per year occur within the U.S. and are usually the result of contact with infected rodents (WHO, CDC). However, this gram negative bacillus is highly infectious, and has the potential to be engineered into a powerful, antibiotic resistant weapon [103].

There have been many reports of the use of *Y. pestis* as a bio warfare agent [104, 105]. There is a significant concern that a possible bioterrorism attack with plague might employ a natural or bio-engineered drug-resistant strain. Natural resistance of *Y. pestis* to antibiotics is rare; however, in 1995, a plague isolate from Madagascar contained a multidrug-resistant transferable plasmid [106]. It has also been reported that during the Soviet biological weapons program, scientists developed a *Y. pestis* strain resistant to 16 different types of antibiotics [107]. The plague has been labeled as a Category A Bioterrorism Agent by the Centers for Disease Control because it is highly communicable and has an extremely high mortality rate [107]. This risk and potential misuse has initiated research to generate improved vaccines to prevent plague [105]. Currently, there is formalin-killed whole cell preparation *Y. pestis* organisms suspended in saline solution available as vaccine for military personnel and researchers at high risk. The limitation of this vaccine is that it doesn't provide protection against pneumonic plague it present with

reactions such as fever, headache, malaise, lymphadeno-pathy, erythema and induration at the injection site and is not recommended for the general public [108, 109].

The LcrV protein is a protective antigen and virulence factor of epidemic strains of *Y. pestis*. LcrV was discovered more than 50 years ago and is believed to be responsible for an array of immune modulatory effects on the host [42, 110]. LcrV is an adhesion molecule located on the tip of a needle-like type 3 secretion system (T3SS). T3SS are used by Gram negative bacteria to inject effector proteins into the host. LcrV regulates the injection of Yops (Yersinia outer proteins) that trigger cell death and inhibition of bacterial phagocytosis [47, 111].

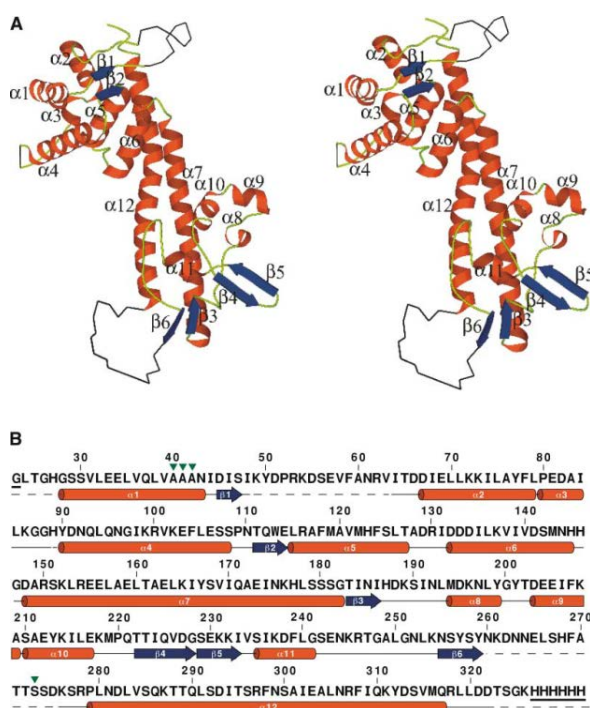


Figure 1.8. Structure of *Y. pestis* LcrV. A) Ribbon diagram of of LcrV, with helices and strands colored red and blue. B) LcrV amino acid sequence in single letter code. Figure reprinted with permission [112].

LcrV is a dumbbell-like molecule with two globular domains on either end separated by a coiled-coil motif that is uncommon in bacterial proteins (Figure 1.8). The

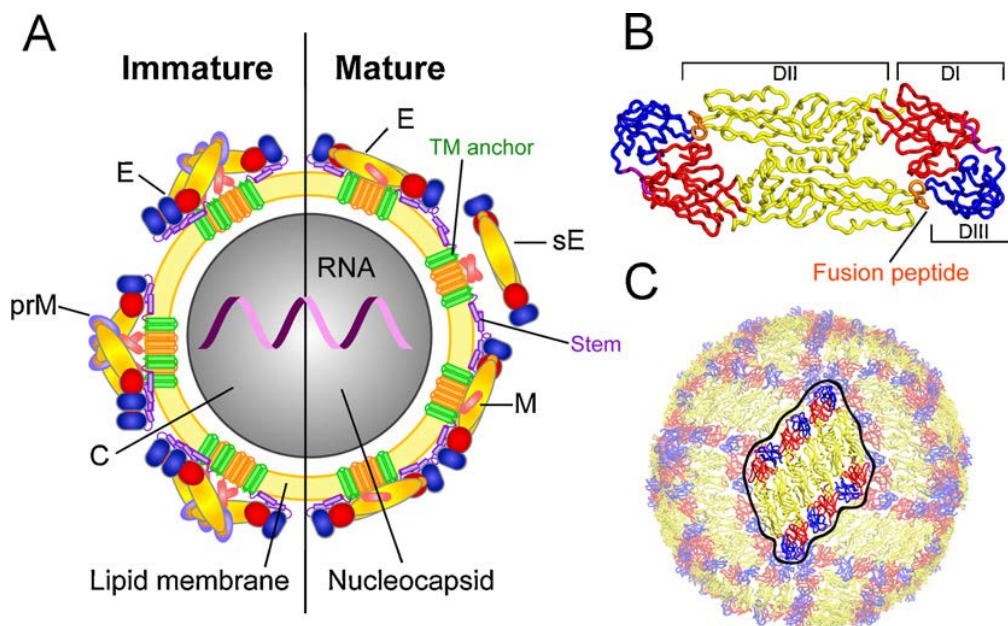
LcrV sequence is highly conserved between the epidemic strains of *Y. pestis* and is also found in pathogenic *Y. enterocolitica* [47, 112]. Research indicates that subunit vaccines with LcrV polypeptide can confer protection against bubonic and pneumonic plague in mice, rats, guinea pigs, rabbits, and African Green monkeys [113]. It is also reported that LcrV antibodies are successful in blocking *Y. pestis* type III translocation of Yop effectors into host immune cells [114, 115].

West Nile Virus and Domain III of the Envelope Protein

West Nile virus (WNV) belongs to the *Flaviviridae* family that is composed of single-stranded RNA viruses [116]. It was originally isolated in the West Nile district of Uganda in 1937 and from there it has spread to other parts of world including Africa, Asia and the Middle East. WNV was first reported in New York in 1999 and has since spread across the U.S. with major epidemics in both 2006 and 2012 [117, 118]. WNV is now endemic in the U.S. with disease occurring most often during summer, depending on latitude and seasonal temperatures [119]. Environmental factors, such as global warming, urbanization, and the availability of competent mosquito vectors, contribute to the annual number of cases. In 2012, there was a striking upsurge in WNV transmission in the U.S. resulting in the highest mortality rate recorded in this country, with 2873 cases of neuroinvasive disease and 286 deaths [119, 120]. Evidence suggests that the U.S. can forecast periodic outbreaks of WNV fever and neurologic disease in the coming years that may yield different clinical manifestations and transmission dynamics [121].

The majority of humans infected with WNV are asymptomatic or exhibit mild febrile illness or self-limiting symptoms, but approximately 1% of patients develop neuroinvasive disease that can lead to permanent disability or death [122, 123].

Neurological symptoms are most common and severe in aged patients of above 50 years with certain medical conditions, implying that host immune status plays an important role in the event of the disease outcome [124-126]. Cell culture infection studies indicate that cells of myeloid origin, including tissue macrophages, and immature dendritic cells have distinct susceptibility to WNV infection in the skin at the site of injection [127-129]. Interferon-dependent innate immune responses and the induction of neutralizing anti-WNV IgM early in the immune response weakens viremia as well as spread of infection [129, 130]. Studies show that a protective immune response must include humoral immunity for viral clearance, and neutralizing IgG and IgM antibodies against WNV surface envelope (E) and premembrane (prM) proteins are key [131, 132]. The WNV E protein acts as a site of viral recognition and binding, and antibodies to E can inhibit viral fusion and cellular uptake [133, 134]. Domain III is an immunoglobulin (Ig) like domain of the WNV E protein capable of producing the most effective neutralizing antibodies [133-136]. Purified DIII has been shown to stimulate protective responses in mice and monkeys, but vaccines have yet to advance to clinical trials [137]. There is much demand for the development of safe and effective vaccine candidates against WNV due to limited antiviral treatment options, and the vulnerability of human elderly and young populations [138].



Copyright © 2011 Elsevier Ltd

Figure 1.9. A) Schematic representation model of a flavivirus particle. Illustrating different components of the West Nile Virus B) Ribbon diagram Envelope protein E composed of three distinct domains (DI, DII, and DIII). C) Organization of E protein dimers at the surface of mature virions. Figure reprinted with permission [139].

The goal of this research was to develop and characterize a novel vaccine adjuvant, based on the non-toxic shiga toxin B subunit, to improve the strength and quality of immune responses to diverse vaccine antigen candidates. As described above, research has indicated that Ctx and the CTB subunit are strong mucosal vaccine adjuvants, but direct immune responses largely toward a Th2 humoral mechanism [65]. The structural similarity of Stx and Ctx, ability to target cells of the immune response, and pattern of retrograde trafficking indicate that Stx and the STB subunit will also prove to have significant adjuvant activity.

CHAPTER II. MATERIALS AND METHODS

2.1. Bacterial Strains, Vectors, and Construction of Plasmids

2.1.1. Bacterial Strains

E. coli TE1 is a $\Delta endA$ derivative of TX1 [F':Tn10 $proA^+B^+ lacI^q\Delta(lacZ)M15, glnV44 \Delta(hsdM-mcrB)5 \Delta(lac-proAB)thi$] [15]. This strain was used for the cloning of recombinant plasmids as well as expression of proteins. *E. coli* Top10 (Life Technologies, Grand Island, NY), Nova Blue (EMD Millipore, Billerica, MA), and Origami (EMD Milipore) bacterial cells were also used for cloning the vector plasmids. All the bacterial cells were cultured using Luria-Bertani (LB) agar plates or broth at 37°C supplemented with the appropriate antibiotics for selection including chloramphenicol (35 µg/ml), ampicillin (100µg/ml), and/or kanamycin (50 µg/ml). A clinical isolate of *Y. enterocolitica* (Idaho Department of Health and Welfare, Boise, ID) and the *Y. pestis* vaccine strain (KIM5) were used to isolate *lcrV* from genomic plasmid DNA. Both Stx genes (*stxA1* and *stxB*) were amplified from *E.coli* 0157:H7. WNV NY99 strain mRNA was isolated from infected mosquitoes and was the kind gift of Dr. Chris Ball (Idaho Bureau of Labs). Viral cDNA was synthesized using an Invitrogen Super Script cDNA Synthesis kit.

2.1.2. Plasmids and Their Construction

Plasmids were constructed using the primers and enzymes detailed in Tables 2.1 and 2.2. All prepared plasmids below were transformed into *E.coli* TE1, purified by plasmid Maxi prep (Qiagen, Valencia, CA) and sequenced for confirmation (SeqWright, Houston, TX).

pLGV002: *lcrV* from *Y. pestis* into pSW004 (made by Sara Wilson). *lcr V* was amplified using primers 060 and 036pr and cloned with SmaI and ApaI enzymes (Table 2.1).

pLGV003: *lcrV* from *Y. pestis* using primers 065 and 059pr (Table 2.1) cloned into pLGV001 using BamHI and KpnI enzymes.

pLGV004: Domain III (DIII) from WNV. DIII was amplified using primers 074pr and 075pr (Table 2.1) and cloned into pLGV001 using BamHI and XhoI enzymes.

pLGV005: DIII from WNV DIII was amplified using primers 081pr and 075pr (Table 2.1) and cloned into pSW004 using XhaI and XhoI enzymes.

pLGV006: DIII from WNV DIII was amplified using primers 082pr and 075pr (Table 2.1) and cloned into pSW004 using XbaI and XhoI enzymes.

pLGV007: *stx A₂B* from pSW004 was amplified using primers 083pr and 084pr (Table 2.2) and cloned into pBAD18CM (ATCC, Manassas, VA) using NheI and HindIII enzymes.

pLGV009: *stxA₂B* from pSW004 was amplified using primers 061 pri, 063 pri (Table 2.2) and cloned into BAD18CM(ATCC) using NheI and SphI enzymes.

pLGV010: WNV DIII was amplified using primers WNDIII pri & 115 pri (Table 2.2) and cloned into pJY013 (Jenny Yan) using primers SphI and XhoI enzymes.

Table 2.1. Primers, enzymes, and plasmids for shiga toxin A₂B expression

Name of the vector	Primers used	Restriction enzymes used
pLGV002	060 5'CAACCTCCCGGGGCATCACCATCACCATCACATTAGAGCCTACGAACAA 3' 036 5' GTTCGTAGGGCCCGTGGCAAAGTGAGATAATTC 3'	Sma I & Apa I
pLGV003	065 5' GCAACCTGGATCCATTAGAGCCTACGAACAA 3' 059 5' GTTCGTAGGTACCGTGGCAAAGTGAGATAATTC 3'	Bam HI & Kpn I
pLGV004	074 5' GTACTCCGGATCCCAGTTGAAGGGAACAACC 3' 075 5' GCTACTGCTCGAGGTTGTAAAGGCTTTGCC 3'	BamH I & Xho I
pLGV005	081 5' GTACTCCTCTAGACAGTTGAAGGGAACAACC 3' 075 5' GCTACTGCTCGAGGTTGTAAAGGCTTTGCC 3'	Xha I & Xho I
pLGV006	082 5' GTACTCCTCTAGACATCACCATCACCATCACCAGTTGAAGGGAACAACC 3' 075 5' GCTACTGCTCGAGGTTGTAAAGGCTTTGCC 3'	Xba I & Xho I
pLGV010	WNDIII 5' GACTGGGCATGCATTGCAGTTGAAGGG 3' 115 5' GTTCTGCTCGAGGTTGTAAAGGCTTTGCC 3'	Sph I & XhoI

Table 2.2. Primers, enzymes, and plasmids for shiga toxin B protein expression.

Name of the plasmid	Primers used	Restriction enzymes used
pLGV001	050 5' AAAATAATTATTTTTAGAGTGCTAAC 3' 051 5' ACGAAAAATAACTTCGCTGAATCC 3'	HindIII & ApaI
pLGV007	083 5' GGTCGTGCTAGCCGTATGGTGCTCAAGGAGTATTG 3' 084 5' GCACGTAAGCTTTTCAGTGATGGTGATGGTGATGACGAAAAATAACTTCGCTG 3'	Nhe I & Hind III
pLGV009	061 5' GCATGGGCTAGCGAACTATTAGCAGTTGAGGG 3' 063 5' GACTGCGCATGCGCCTGCTATTTTCACTGAGC 3'	Nhe I & Sph I

2.2 Protein Expression and Purification

To express recombinant proteins, bacterial cell cultures with plasmids pLGV002, pLGV003, pLGV004, pLGV005, pLGV006, pLGV010, pSW005 (Sara Wilson) or pLGV001, pLGV007, pLGV009 were grown to an optical density of 600 nm (OD₆₀₀) of 0.9 O.D and induced for 15 h or overnight with 0.2% L-arabinose or 1M IPTG. Proteins from vector constructs pLGV002 (6XHis-LcrV-STA₂/B), pLGV005 (DIII-STA₂/B), pLGV006 (6XHis-DIII-STA₂/B), pLGV007 (STA₂/B-6XHis), pLGV009 (STB) and pLGV010 (DIII-STA₂/B) were induced with 0.2% L-arabinose as pBAD is the upstream promoter on the plasmid. The arabinose binds to the repressor protein on the plasmid and leads to the transcription of mRNA to occur. Proteins from vector constructs pLGV001 (STB-6XHis), pLGV003 (LcrV-STA₂/B-6XHis), pLGV004 (DIII-STA₂/B-6XHis) and pLGV008 (STA₂/B) were induced with 1M IPTG as pLac is the upstream promoter of the plasmid. Induced cells were allowed to grow overnight and extracted by centrifugation. Periplasmic extracts and the cytoplasmic extracts (supernatant) were collected by centrifugation. The pellet was also collected and analyzed for protein expression.

Bacterial cell extractions of plasmids pLGV001 (STB-6XHis), pLGV002 (6XHis-LcrV-STA₂/B), pLGV003 (LcrV-STA₂/B-6XHis), pLGV004 (DIII-STA₂/B-6XHis), pLGV006 (6XHis-DIII-STA₂/B), pLGV007(STA₂/B-6XHis) were added to Talon nickel resin (Clontech, Mountain View, CA) and agitated for 20 minutes. The resin was then administered to 5 ml columns (Pierce) and washed with 1ml of 20mM Tris-Cl, 50mM NaCl, pH 8.0, washed again with 1ml 20mM Tri-Cl, 100mM NaCl, pH 8.0, washed again with 1ml 20mM Tri-Cl, 100mM NaCl, + 5mM imidazole, pH 8.0, and eluted with 20mM Tris, 100mM NaCl, 100 mM imidazole, pH 8.0.

Bacterial cell extractions of plasmids pLGV005 (DIII-STA2/STB), pLGV008 (STA2/STB), pLGV009 (STB), pLGV010 (DIII-STA2/STB) were added to 50% immobilized D-galactose gel (Pierce, Rockford, IL) and agitated at 4 degree C for 2 h. The Agarose was pelleted, resuspended in 1X PBS and added to a 5 ml column. Column beds were washed twice with 2 ml PBS, and eluted with 2 ml 1 M D-galactose.

2.3. Electrophoresis and Blotting

2.3.1. Agarose Gel Electrophoresis

Amplification of gene regions after PCR or restriction digested samples were examined using agarose gel electrophoresis on either a 0.9% gel or 2% gel depending on the size range of target fragments. Agarose was dissolved in 1X TAE buffer by heating in microwave shortly. 10 ul of ethidium bromide (EtBr) was added to the agarose gel to visualize fragments using UV transillumination. Samples and a 1kB DNA ladder (Fermentas, ThermoFisher) were added along with loading dye and allowed to run for 30-40 mins at 100V before observation.

2.3.2. SDS-PAGE

Bacterial samples for protein expression were boiled for 2 minutes in loading dye (0.25M Tris-HCl, pH 6.8, 15% SDS, 50% glycerol, 25% β -mercaptoethanol, 0.01% bromophenol blue) and separated by 12% sodium dodecyl sulfate-polyacrylamide gel electrophoresis (SDS-PAGE) through the buffer system of Laemmli [140]. Coomassie brilliant blue was used to stain and visualize the samples for protein bands.

2.3.3. Western Blot Analysis

Proteins from SDS gels were transferred to nitrocellulose membranes. The membranes were incubated in one of the following antibodies diluted in Western blot blocking buffer (1-PBS with 0.05% Tween-20 and 5% skim milk): rabbit anti-LcrV polyclonal antibody 1:4000 dilution (a-LcrV, kindly supplied by S.Little and J. Adamovicz, USAMRIID, Ft. Detrick, MD), and or anti-His6 (1:2,500; Abcam, Cambridge, MA), followed by horseradish peroxidase (HRP)-conjugated anti-rabbit IgG (1:5,000; Promega, Madison, WI) and developed with Immobilon Western HRP Substrate (Millipore, Billerica, MA).

2.4. Cell Culture Methods and Assays

2.4.1. Internalization of Toxins and Toxin Subunits in Cell Culture

Vero epithelial (ATC2.C, Manassas, VA) and C57BL/6 murine dendritic (DC2.4; kindly provided by K. L. Rock, Dana-Farber Cancer Institute, Boston, MA) cells were cultured to sub confluence on uncoated coverslips at 37°C with 5% CO₂ [141]. Protein toxin internalization was evaluated by confocal microscopy. Vero cells were cultivated in Dulbecco's modified Eagle's medium (DMEM) with 4 mM L-glutamine, 4,500 mg/liter glucose, 10% bovine growth serum (BGS), 100 IU/ml penicillin, and 100 g/ml streptomycin (DMEM + 10). DC2.4 cells were cultivated in RPMI 1640 medium with 2 mM L-glutamine, 10% BGS, 10 mM HEPES, 55 M 2-mercaptoethanol, nonessential amino acids, and penicillin-streptomycin (Pen-Strep). The cells were then washed in DMEM or RPMI without serum and incubated at 4°C for 5 mins to slow down the internalization process. The cover slips with adherent cells were exposed to 40 µl of 10

$\mu\text{g/ml}$ RFP-ST Chimera or $40\ \mu\text{l}$ of $10\ \mu\text{g/ml}$ FITC-OVA along with either $40\ \mu\text{l}$ of $50\ \mu\text{g/ml}$ of CTB or PTB or STB in phosphate-buffered saline (PBS) at 4°C for 15 min to allow protein binding to the plasma membrane. Some of these cell cultures were shifted to 37°C for 1 hr in order to yield for the internalization of proteins. Treated cells on cover slips were then washed in PBS and coverslips were mounted using hard-set medium with 4',6'-diamidino-2-phenylindole (DAPI; Vector Laboratories, Burlingame, CA) and visualized using a Zeiss LSM 510 META laser scanning confocal microscope running LSM 510 META software.

2.4.2. Cellular Proliferation Assay

Mouse macrophages (J774, ATCC) were grown by adding 5×10^5 cells in Dulbecco's modified Eagle medium (DMEM high glucose) supplemented with pen/strep and 10% fetal bovine serum in a 96 well plate. Some of the cells were activated with 20ng/ml of $\text{INF-}\gamma$ (Reprokine, Ltd in Rehovot, Israel) overnight. The cells were incubated for 24 hrs at 37°C and 5% CO_2 . with either $10\ \mu\text{l}$ of $5\ \mu\text{g/ml}$ of CT, $10\ \mu\text{g/ml}$ of CT, $5\ \mu\text{g/ml}$ of CTB, $10\ \mu\text{g/ml}$ of CTB, $5\ \mu\text{g/ml}$ of PTB, $10\ \mu\text{g/ml}$ of PTB, $5\ \mu\text{g/ml}$ of DIII, $10\ \mu\text{g/ml}$ of DIII, mock. The metabolic indicator Alamar Blue (Accumed International, Westlake, OH) was used to assay cellular proliferation. Fluorescence was measured on a BioTek Synergy HT plate reader using $560\ \text{nm}$ excitation, $590\ \text{nm}$ emission and gain 35 (BioTek, Winooski, VT). The stimulation index was determined as the ratio of mean fluorescence from stimulated to non-stimulated cells or PBS-treated cells.

2.4.3. Cytokine Assays

Cytokine levels were detected using ELISA. Levels of interleukin-12 (IL-12) and TNF alpha (TNF- α) produced by mouse macrophages (J774, ATCC) and mouse dendritic cells (DC2.4) activated with toxin and toxin subunits were determined by ELISA according to manufacturer's instructions (eBiosciences, San Diego, CA). Cells at 1×10^5 per well were cultivated in Dulbecco's modified Eagle medium (DMEM high glucose) supplemented with pen/strep and 10% fetal bovine serum in 96 well Maxi sorp plates (Nunc, ThermoFisher) and grown in 5% CO₂ and 37°C to subconfluence. Cells were then incubated O/N with 10 μ l of 20 ng/ml of INF- γ (Reprokine, Ltd in Rehovot, Israel) for 2 hrs followed by the addition of either 10 μ l of 5 μ g/ml CT, 5 μ g/ml of CTB, 5 μ g/ml of PTB, 5 μ g/ml of STB, or Mock/BKG. Supernatants were removed, centrifuged and frozen prior to analysis by ELISA. The assay sensitivity for IL-12 and TNF- α was 4 to 500 pg/ml and 15 to 2,000 pg/ml, respectively. A multi-analyte ELISArray cytokine assay (Qiagen, Valencia, CA) was performed according to manufacturer's instructions using DC 2.4 cell culture supernatants that had been incubated with 2 μ g/ml of CTB, 2 μ g/ml STB or PBS alone for 24 h.

2.4.4. B3Z Antigen Presentation Assay

C57Bl/6 murine dendritic cells (DC2.4, kindly supplied by Kenneth L. Rock, DFCI, Boston, MA, USA) were maintained in RPMI 1640 medium with L-glutamine supplemented with 10% BGS, 10 mM HEPES, 55 μ M 2-mercaptoethanol, 1X non-essential amino acid and pen/strep at 37 °C and 5% CO₂. The cells were incubated for 6 hrs with either 100 μ g/ml SIINFEKEL antigen (OVA peptide 257-264) Or 100 μ g/ml SIINFEKEL with 1 μ g/ml of CT , SIINFEKEL with 2 μ g/ml of CT, SIINFEKEL with 3

$\mu\text{g/ml}$ of CT, SIINFEKEL with $1\mu\text{g/ml}$ of LTB, $2\ \mu\text{l}$ of SIINFEKEL with $2\ \mu\text{g/ml}$ of LTB, SIINFEKEL with $0.01\ \mu\text{g/ml}$ of CT, SIINFEKEL with $1\ \mu\text{g/ml}$ of PTB, SIINFEKEL with $2\ \mu\text{g/ml}$ of PTB to allow proper antigen processing and presentation. DC2.4 cells were washed with 1 X PBS and $100\ \mu\text{l}$ of 5×10^4 cells/well B3Z cells were added. The plate containing cells was centrifuged at 800-900 rpm to initiate the contact between the cells and incubated for 16-20 hrs for T cell activation. The cells were treated with CPRG buffer and incubated for 4 h before the absorbance was measured at 595 nm in using a BioTek Synergy HT plate reader. B3Z cells were grown in B3Z media (RPMI 1640 with 1.5g NaHCO_3 , 2ml Na-Pyr , $10\text{ml glucose (}4.5\ \text{g/L)}$, 2.603g HEPES , $50\ \text{mL heat-inactivated FBS}$, 5mL P/S , 5.1mL L-Glutamine , $50\mu\text{M 2-mercaptoethanol}$, $5\text{mL NEAA (non-essential amino acids)}$ [142, 143].

2.4.5. Antigen Uptake Assay

Mouse macrophages (J774, ATCC) were cultivated at approximately 5×10^5 cells/well in DMEM high glucose supplemented with pen/strep and 10% fetal bovine serum in a 96 well plate. Some of the cells were activated with $20\ \text{ng/ml}$ of INF-gamma overnight. The cells were incubated for 2 hrs at 37°C and 5% CO_2 with either $10\ \mu\text{l}$ of $5\ \mu\text{g/ml}$ of CT and $10\ \mu\text{l}$ of $10\ \mu\text{g/ml}$ of FITC-OVA, $10\ \mu\text{g/ml}$ of CT and $10\ \mu\text{g/ml}$ of FITC-OVA, $50\ \mu\text{g/ml}$ of CTB and $10\ \mu\text{g/ml}$ of FITC-OVA, $100\ \mu\text{g/ml}$ of CTB and $10\ \mu\text{g/ml}$ of FITC-OVA, $50\ \mu\text{g/ml}$ of PTB and $10\ \mu\text{g/ml}$ of FITC-OVA, $100\ \mu\text{g/ml}$ of PTB and $10\ \mu\text{g/ml}$ of FITC-OVA, $50\ \mu\text{g/ml}$ of DIII and $10\ \mu\text{g/ml}$ of FITC-OVA, $100\ \mu\text{g/ml}$ of DIII and $10\ \mu\text{g/ml}$ of FITC-OVA, mock (endotoxin free control). The cells were washed with 1XPBS and measured the fluorescence at 494 nm and 518 nm emission in a plate

reader. The uptake index was calculated as the ratio of mean fluorescence from stimulated to non-stimulated cells or PBS-treated cells.

CHAPTER III. RESULTS

The objective of this research was to develop and characterize a novel vaccine adjuvant, based on the non-toxic shiga toxin B subunit, to improve the strength and quality of immune responses to diverse vaccine antigen candidates. As described above, research has indicated that Ctx and the CTB subunit are strong mucosal vaccine adjuvants, but direct immune responses largely toward a Th2 humoral mechanism [65]. The structural similarity of Stx and Ctx, and the ability ability to target cells of the immune response and pattern of retrograde trafficking, indicate that Stx and the STB subunit will also prove to have significant adjuvant activity.

Previous work has shown that A₂/B chimeras of Ctx are promising vaccine candidates in that they are 1) non-toxic, 2) retain overall holotoxin structure and stability, 3) retain the native pentameric toxin binding subunit, and 4) maintain a non-covalent association of toxin to antigen [144, 145]. Thus, initial work focused on the construction, purification, and characterization of novel StxA₂/B chimeras as vaccine candidates. Secondary work focused on the purification and *in vitro* characterization of the immunostimulatory activity of the STB subunit alone in comparison to other AB5 toxins.

Construction of Plasmids for A₂/B Chimeric Protein Expression

A number of plasmids had previously been constructed in our laboratory for shiga toxin I StxA₂/B chimera expression. Table 3.1 shows plasmids pSW004, pSW005, and pSW006. These plasmids were constructed by PCR amplification of the *stxA₂* and *stxB*

genes from *E.coli* O157:H7 and cloning behind the pBAD promoter (work performed by Sara Wilson 2008-2009). The *Y.pestis lcrV* gene was cloned into pSW004 to construct pSW006 for expression of an LcrV-StxA₂/B chimera. pSW006 was transformed into *E.coli* TE1 and expression was induced with 20% L-arabinose. As shown in Figure 3.1, LcrV-StxA₂/B was expressed and *E.coli* periplasmic protein preparations were analyzed by SDS-PAGE (Figure 3.1B). The protein preparations have indicated a potential LcrV-StxA₂ protein band and potential StxB band, along with other bacterial proteins, at 39.7 kDa and approximately 10kDa, respectively. Expression of the LcrV-StxA₂ peptide into the periplasm was confirmed through immunoblot analysis (Fig 3.1C) using α -LcrV antibodies. The LcrV-StxA₂/B chimera from this plasmid could not be studied further as there was little success in terms of purification away from other bacterial proteins. Thus, as shown in Table 3.1, we constructed new plasmids for StxA₂/B chimera expression containing 6X histidine tags on both the N terminus of the operon (pLGV002) and C terminus of the operon (pLGV003) to facilitate chimera purification using nickel chromatography.

Table 3.1 Plasmids for A₂/B chimeric proteins

pLGV002	HIS- <i>lcrV</i> into pSW004 plasmid to express His-LcrV-StxA ₂ /B
pLGV003	<i>lcrV</i> into pLGV001- to express LcrV-StxA ₂ /B-HIS chimera
pLGV004	WNV DIII into pLGV001 - to express WNVDIII-StxA ₂ /B-HIS
pLGV005	WNV DIII into pSW004 to express WNVDIII-StxA ₂ /B (no HIS)
pLGV006	WNV DIII into pSW004 to express HIS-DIII-StxA ₂ /B
pLGV010	WNV DIII into pJY013 to express DIII-StxA ₂ /B chimera
pSW004 (Wilson)	<i>stxA₂/B</i> into arabinose-inducible vector for chimera expression
pJKT36	Red fluorescent protein into pARLDR19 to make RFP-CtxA ₂ /B
pSW005 (Wilson)	Red fluorescent protein into pSW004 to make RFP-StxA ₂ /B
pSW006 (Wilson)	<i>lcrV</i> into pSW004 to express LcrV-StxA ₂ /B chimera

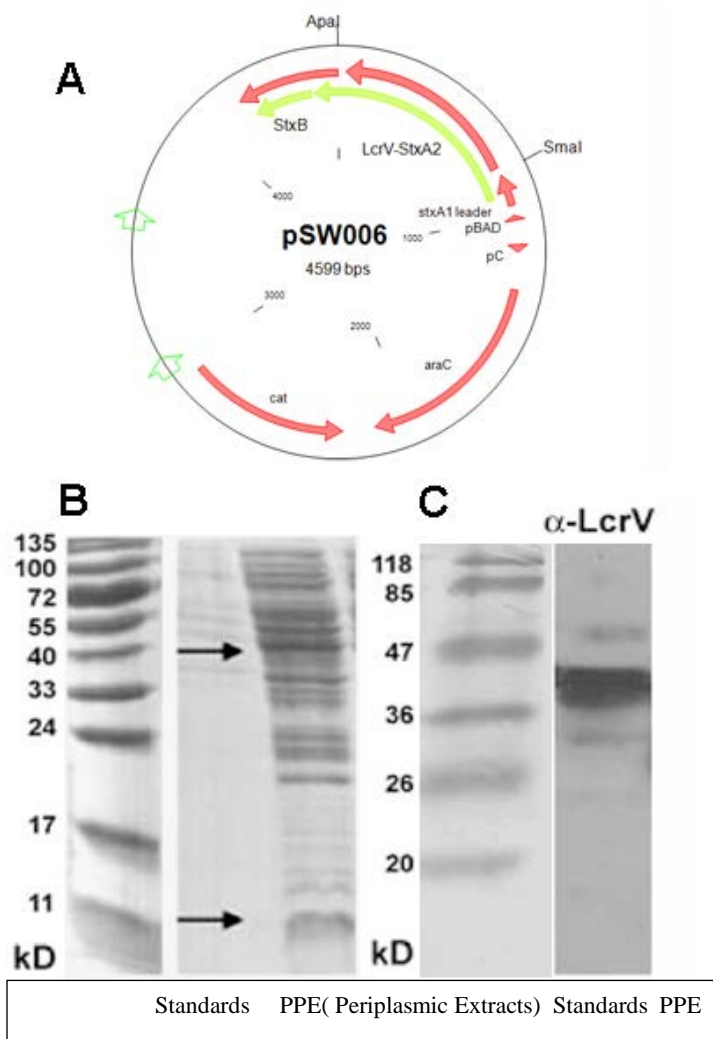


Figure 3.1. A) Schematic representation of pSW006. B) SDS gel of the *E.coli* periplasm showing LcrV –Stx A₂ at approximately 40 kDa and STB below 11 kDa. C. Western blot showing LcrV-StxA₂ using primary LcrV antibodies.

The plasmid pLGV002 was constructed such that the 6X histidine tag is present on the N terminus of the LcrV antigen. As shown in Figure 3.2, *lcrV* was amplified from both *Y.pestis* and *Y. enterocolitica* and cloned into pSW004 to make HIS-LcrV-StxA₂/B (Figure 3.2 A-C). pLGV002 was constructed and confirmed using colony PCR (Figure 3.2D) and sequenced for confirmation. To determine expression of HIS-LcrV-StxA₂/B, *E.coli* TE1 was transformed and induced for expression. Periplasmic protein preparations

were separated in 12% SDS-PAGE and stained with either Coomassie brilliant blue or transferred to nitrocellulose for Western blot analysis (Figure 3.3 A and B). The HIS-LcrV-StxA₂ peptide was purified in the nickel column elutions and found to be the expected size of 39.7 kDa. No copurification of the STB subunit was detected in elutions, indicating that the A₂/B chimera was not associating and folded properly in the periplasm. Protein preparations were analyzed by immunoblot using α -LcrV antibodies and did not reveal protein bands as expected.

The plasmid pLGV003 was constructed to express a chimeric LcrV-StxA₂/B molecule with the 6X histidine on the C-terminus of STB (Figure 3.4 A and B). The *lcrV* gene was amplified from *Y. pestis* for pLGV003. The constructed plasmid was transformed into *E.coli* TE1 and verified by colony PCR where it shows the presence of cloned *lcrV* insert of 835 bps (Figure 3.4 C). pLGV003 was induced and purified from the periplasm of *E.coli*. Proteins of approximately 39 kDa (LcrV-StxA₂) and 13 kDa (STB) were found in column wash and flow-through (Figure 3.4D). While pLGV003 appeared to express the predicted A₂ and B peptide subunits, the inability to bind and elute from the nickel column indicated inaccessibility of the histidine tag in the expressed StxA₂/B chimeric protein.

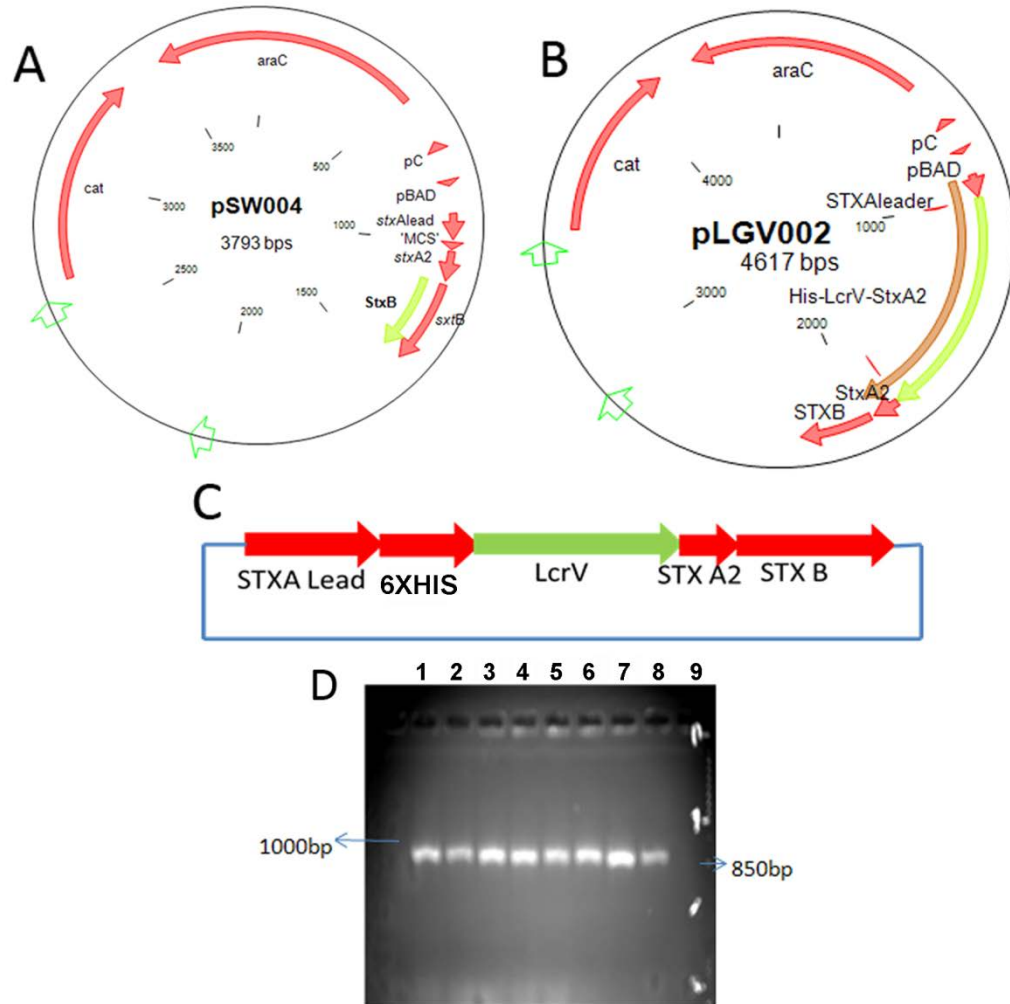


Figure 3.2. A) Schematic representation of pSW004. B and C) Schematic representation of pLGV002 and the multiple cloning site, to express HIS-LcrV-StxA₂/B. D) Colony PCR of pLGV002. Insert was found at the expected size of 854 bps.

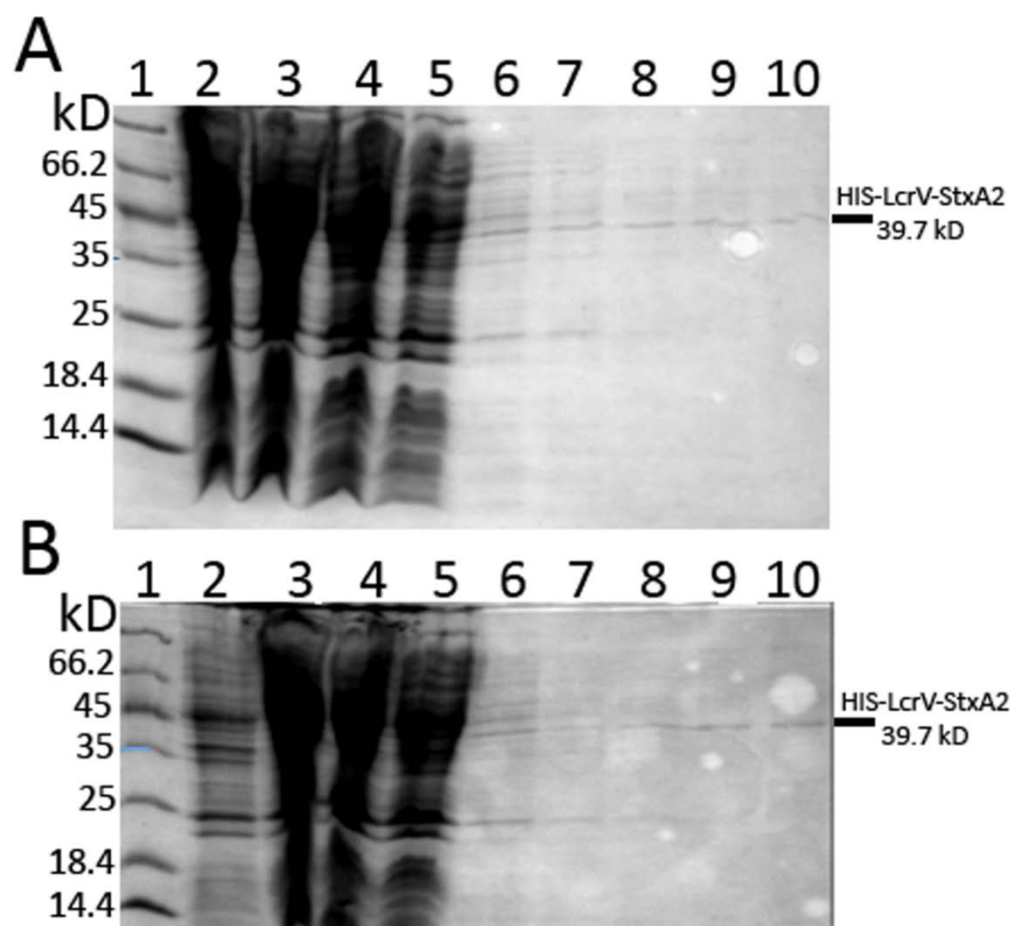


Figure 3.3. A) pLGV002 (*Yersinia pestis*) SDS-PAGE of *E. coli* periplasm. Protein band at approximately 39.7 kDa in protein preparations of periplasm and pellets. 1. protein ladder; 2. Cell pellet; 3. Culture PPE; 4. Column flow through; 5. wash 1; 6. wash 2; 7. wash 3; 8. Elution 1; 9. elution 2; 10. elution 3; B) pLGV002 (*Yersinia enterocolitica*) SDS gel of *E. coli* periplasm. Protein band showing approximately at 39.7 kDa in protein preparations of periplasm and pellets 1. Protein ladder; 2. Cell pellet; 3. culture supernatant; 4. Column flow through; 5. wash 1; 6. wash 2; 7. wash 3; 8. Elution 1; 9. Elution 2; 10. elution 3.

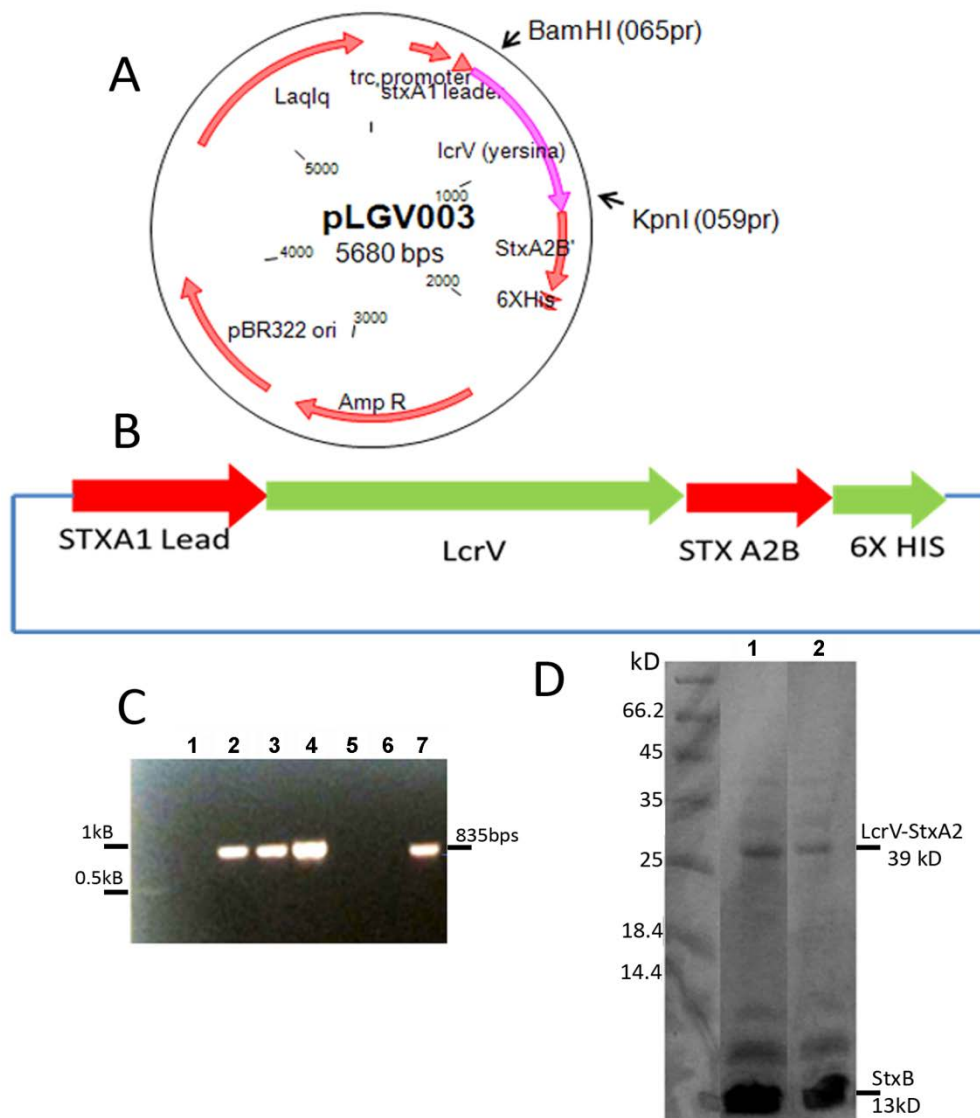


Figure 3.4. A and B) Schematic representation of pLGV003, the expression vector for LcrV-STX-His chimera. C) Colony PCR of pLGV003 Insert found at the expected size: 834bps. D) pLGV003 SDS gel of *E. coli* periplasm band showing approximately at 39kDa and 13kDa in protein preparations of periplasm and pellets 1-Ladder; 2. FT-PPE; 3. Wash 1 -PPE.

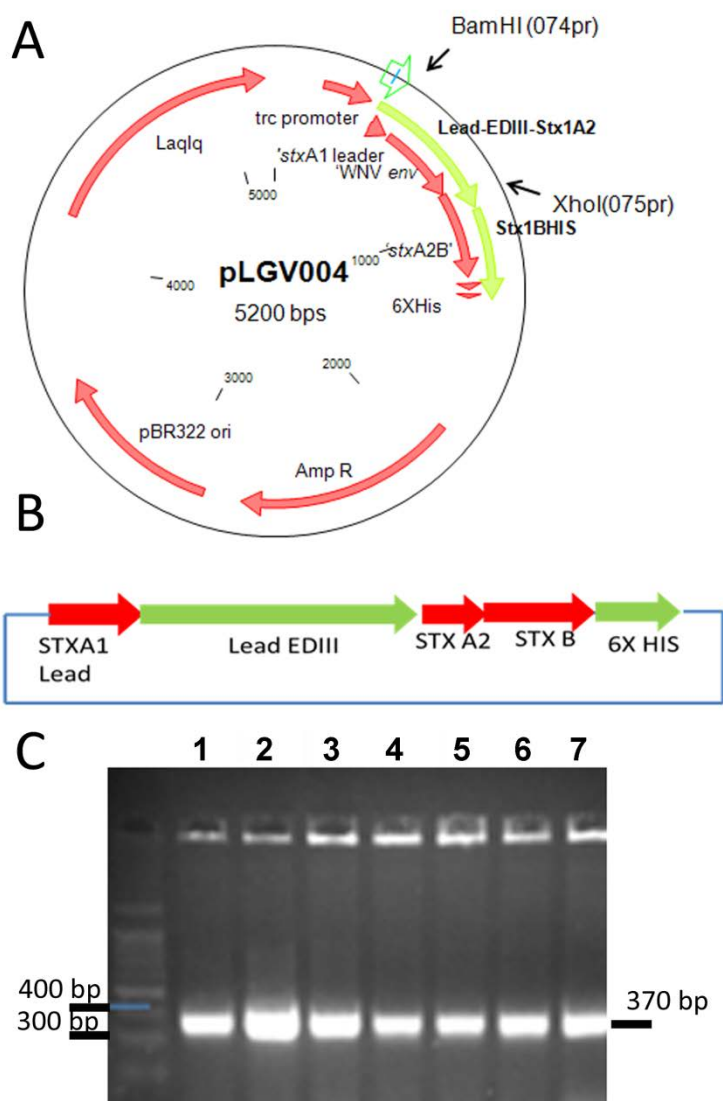


Figure 3.5. A and B) Schematic representation of pLGV004, the expression vector for WNVDIII-StxA₂/B-HIS chimera. C) Colony PCR of pLGV004. Insert found at expected size: 370bps. Lanes: 1 kb ladder; 1. Colony 1; 2. Colony 2; 3. Colony 3; 4. Colony 4; 5. Colony 5; 6. Colony 6; and 7. negative control.

The plasmid pLGV004 was constructed to express a WNVDIII-StxA₂/B-HIS chimera as shown in Figure 3.5 (A and B). The constructed vector plasmid was successfully transformed into bacterial cells and verified by colony PCR (Figure 3.5 C) where it shows the presence of the expected cloned DIII insert of 370bps. Expression

from this plasmid in *E.coli* and purification from the periplasm resulted in a similar outcome to that of pLGV003, with no binding and elution from the nickel column (data not shown). These results supported the notion that the 6X histidine tag is unavailable for binding when present on the C-terminus of STB.

The plasmid pLGV005 was constructed to express a WNVDIII-StxA₂/B chimera without an affinity tag (Figure 3.6, A and B). The constructed plasmid was transformed into *E.coli* TE1 and verified by colony PCR (Figure 3.6 C) where it shows the presence of the cloned DIII insert of the expected 370 bps. *E.coli* TE1 was transformed with pLGV005, induced, and proteins from the periplasm were analyzed by SDS-PAGE. Low expression of the DIII-StxA₂ of approximately 19.6 kDa and STB subunit of 9.7 kDa was noted (data not shown) however, attempts to purify the DIII-StxA₂/B chimera away from additional *E.coli* periplasmic proteins using D-galactose-agarose, fetuin-agarose and anion exchange chromatography were unsuccessful.

The plasmid pLGV006 was constructed to express a HIS-WNVDIII-StxA₂/B chimera (Figure 3.7 A and B). The constructed plasmid was transformed into *E.coli* TE1 and verified by colony PCR (Figure 3.7C) where it shows the presence of the cloned DIII insert of the expected 388 bp. TE1 cells were induced and found to express the His-DIII-StxA₂ fusion of approximately 20 kDa and the STB of 9.7 kDa as shown (Figure 3.7, D and E). Western blot using anti-6X histidine antibodies showed the HIS-DIII-StxA₂ fusion present largely within the insoluble pellet fraction of bacterial cells. The results indicate that there was aggregation of the HIS-DIII-StxA₂ fusion and no folding with STB to form an A₂/B chimera.

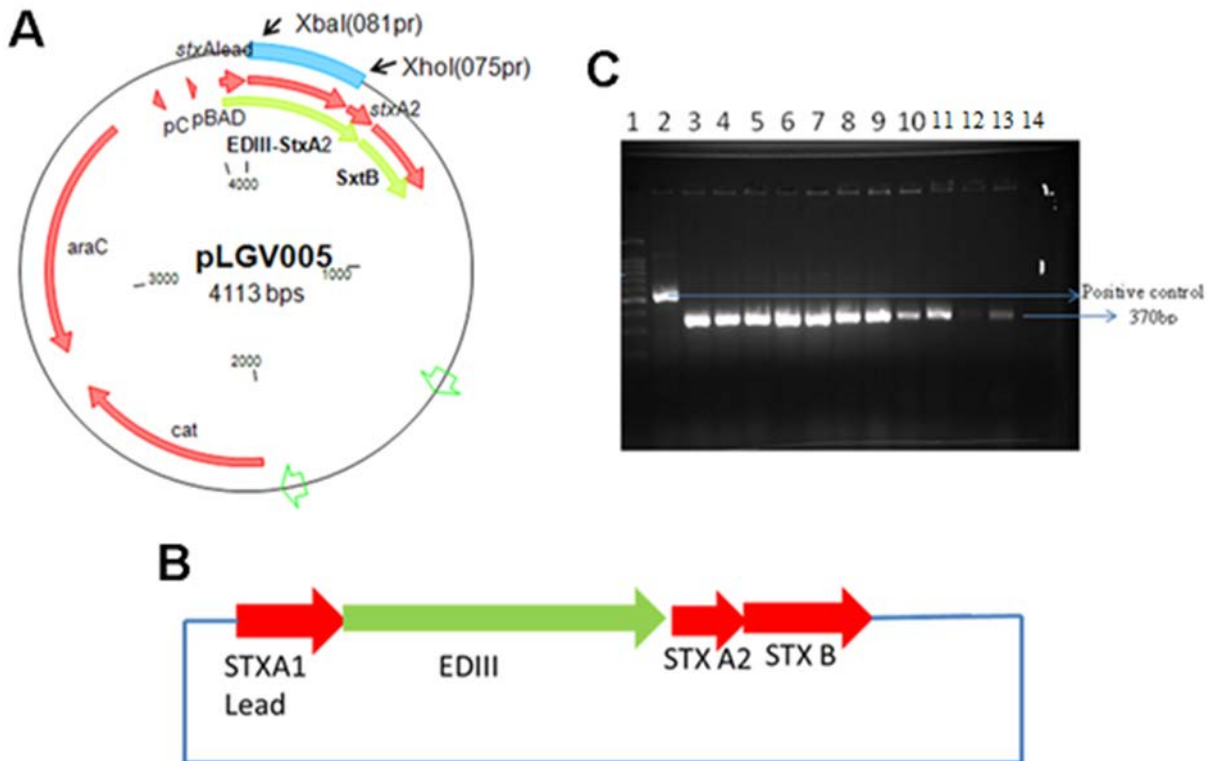


Figure 3.6. A and B) Schematic representation of pLGV005, the expression vector for WNVDIII-StxA₂/B chimera . C. Colony PCR of pLGV005 showing insert at expected size of 370bps. Lanes 1.1 kB DNA ladder; 2. Positive control; 3. Colony1; 4. Colony 2; 5. Colony 3; 6. Colony 4; 7. Colony 5; 8. Colony 6; 9. Colony 7; 10. Colony 8; 11.Colony 9; 12. Colony 10; 13. Colony 11; 14. negative control.

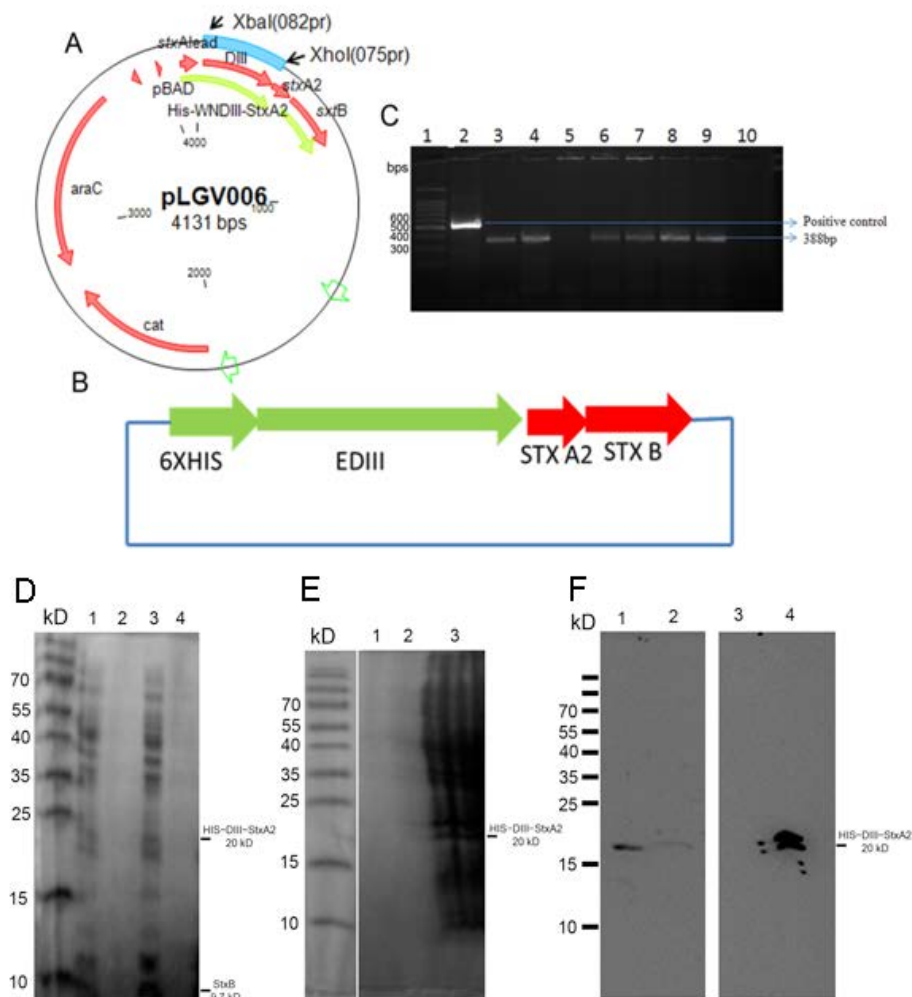


Figure 3.7. A and B) Schematic representation of pLGV006, the expression vector for HIS-DIII-StxA₂/B chimera. C) Colony PCR of pLGV006 showing insert at expected size of 388bps. Lanes: 1. 1 kB DNA ladder; 2. positive control; 3. colony 1; 4. colony 2; 5. colony 3; 6. colony 4; 7. colony 5; 8. colony 6; 9. colony 7; 10. negative control. D) SDS-PAGE of periplasmic and supernatant proteins from *E.coli* TE1 + pLGV006 purified on Ni column. Lanes: 1. flow through of periplasmic extracts (PPE); 2. Flow through of supernatant; 3. first wash of PPE (protein band visible at 20 kD for His-DIII-StxA₂ and at 9.7kDa for STB); 4. first wash of supernatant; E) SDS-PAGE of *E.coli* TE1 + pLGV006 elutions and pellet fraction; Lanes: 1. elution 1 of supernatant; 2. elute 2 of supernatant; 3. insoluble pellet fraction (protein band of HIS-LcrV-StxA₂ shown at 20kDa); F) Western blot of *E.coli* TE1 + pLGV006 protein preparations using anti-HIS antibodies; Lanes: 1. flow through of periplasmic extracts (PPE); 2. first wash of PPE; 3. blank; 4. insoluble pellet fraction.

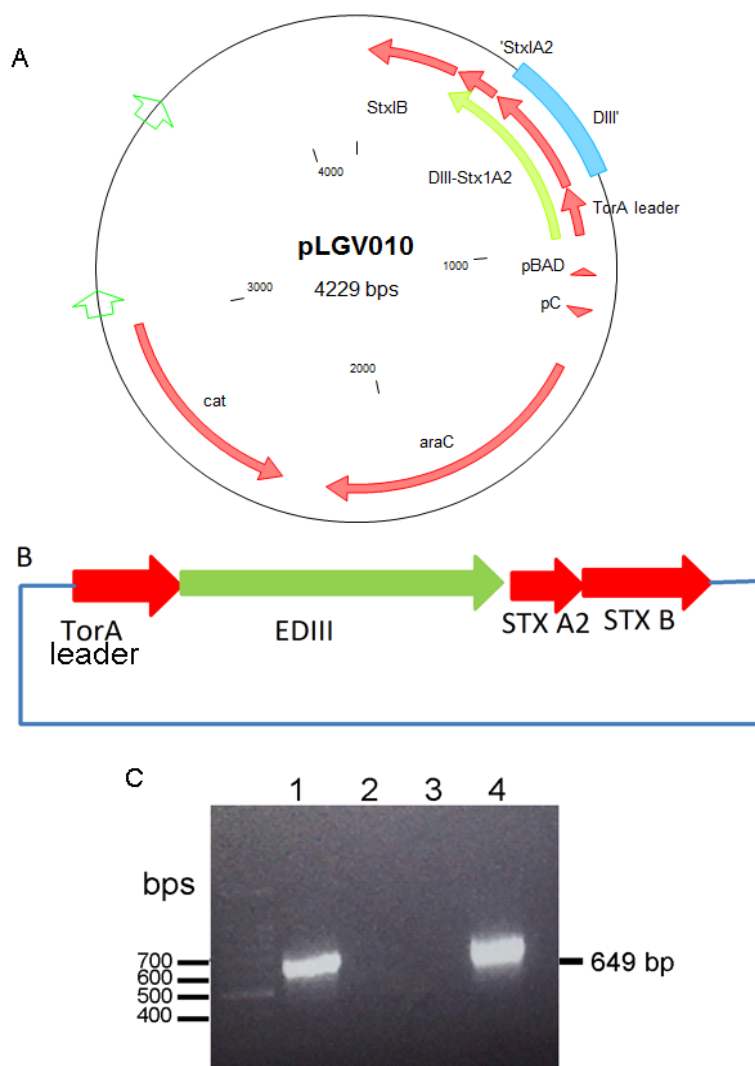


Figure 3.8. A and B) Schematic representation of pLGV0010, the expression plasmid for DIII-StxA₂/B chimera with TorA as the leader sequence for toxin secretion. C) Colony PCR of pLGV010 showing insert at the expected size of 649bps. Lanes: 1. colony 14; 2. colony 15; 3. colony 16; 4. colony 17.

Due to low expression from plasmid pLGV005, and the inability to affinity purify StxA₂/B chimeras using histidine tags, pLGV010 (Figure 3.8, A and B) was constructed to express a WNVDIII-StxA₂/B chimera that is secreted to the periplasm using the efficient TorA secretion signal. The TorA leader sequence has been used for the successful expression of DIII- cholera toxin chimera as well as other Ctx chimeras [144, 146] .pLGV010 was transformed into *E.coli* TE1 and verified by colony PCR (Figure

3.8C) to show the presence of cloned DIII insert of 649bps. *E.coli* TE1 was induced for expression, however, studies to date have indicated limited protein expression (data not shown) and, similar to pLGV005, no current effective mechanism to purify chimera away from contaminating periplasmic proteins.

Construction of Plasmids and Purification of Shiga Toxin A₂/B or STB

Concurrently with attempts to construct and purify StxA₂/B chimeric molecules, plasmids were developed to express the STB or the StxA₂/B subunits alone. These molecules could then be combined, or mixed, *in vitro* with antigens of interest (LcrV and WNVDIII) to characterize adjuvanticity and compared to that of CTB or LTIB. pLGV001 was originally constructed as a vector for cloning antigens for StxA₂/B chimera expression and was used to make the pLGV003 and pLGV004 plasmids (Table 3.1) for LcrV and WNVDIII chimera expression, purified respectively. However, this vector was also used alone to express StxA₂/B and purified using nickel affinity. pLGV001 (Table 3.2, Figure 3.9) was constructed from TOPO vector by inserting *stxA₂B* with 6X Histidine tag on the C terminus. The constructed vector was transformed into *E.coli* TE1 and verified by colony PCR (Figure 3.9 C) where it shows the presence of the cloned *stxA₂B* insert of 493 bp. Cells were induced to express StxA₂/B-HIS of approximately 13kDa as shown (Figure 3.9D).

Table 3.2 Plasmids for Shiga toxin A₂/B or STB expression

Name of the plasmid	Genes and purpose of the plasmid
pLGV001	<i>stxA₂/B</i> to express StxA ₂ /B-HIS for Ni purification
pLGV007	<i>stxB</i> into pBAD to express STB-HIS for Ni purification
pLGV009	<i>stxB</i> into pBAD-KN to express STB

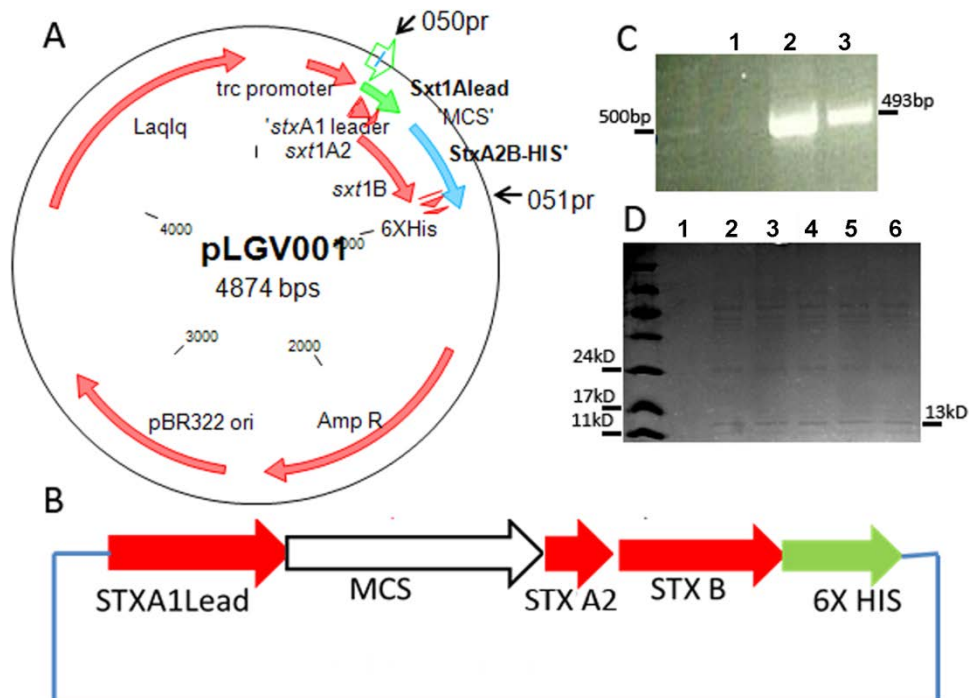


Figure 3.9. A and B) Schematic representation of pLGV001, the expression vector for DIII-StxA₂/B-HIS chimera construct and plasmid for the purification of StxA₂/B-HIS alone. C) Colony PCR of pLGV001 showing insert at expected size of 493bps. Lanes: 1. colony 1; 2. colony 2; 3. colony 3; D) SDS PAGE of protein preparations Lanes: 1. blank; 2. PPE of colony 2; 3. flowthrough of PPE of colony 2; 4. PPE of colony 3; 5. flow through of PPE of colony 3; 6. wash 1 of PPE of colony 2.

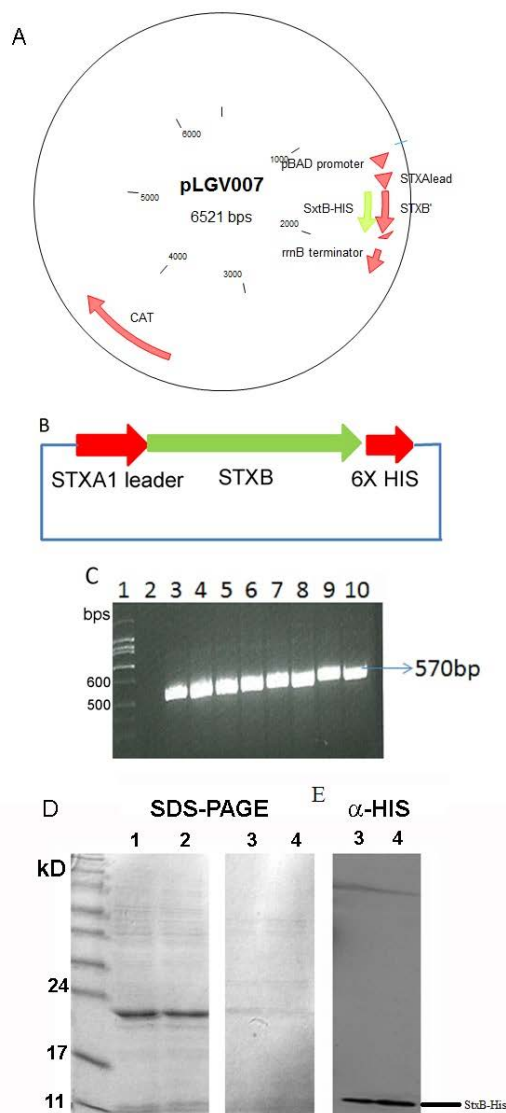


Figure 3.10. A and B) Schematic representation of pLGV007, the expression vector for STB-HIS C) Colony PCR of pLGV007 showing insert at the expected size of 570bps. Lanes: 1.1kB DNA ladder; 2. colony 1; 3. colony 2; 4. colony 3; 5. colony 4; 6. colony 5; 7. colony 6; 8. colony 7; 9. colony 8; 10. colony 9. D) SDS-PAGE of protein preparations from *E. coli* TE1 purified on Ni column. Lanes: 1.Flowthrough of PPE; 2. Wash 1; 3. Wash 2; 3. Wash 3; 4. wash 4 of PPE. E) Western blot of *E.coli* TE1 + pLGV007 protein preparations using anti-HIS antibodies with PPE.

The plasmid pLGV007 (Figure 3.10, A and B) was constructed to express STB-HIS for purification using nickel chromatography. The constructed plasmid was transformed into *E.coli* TE1 and verified by colony PCR (Figure 3.10 C) showing the presence of the cloned *stxB* insert of 570 bp. *E.coli* + pLGV007 was induced to express

STB-HIS and periplasmic extracts were purified using columns of nickel. Results revealed a low level of expression and purification of STB as compared to the chloramphenicol acetyl-transferase (CAT, approximately 20 kD) from this plasmid (Figure 3.10 D). Western blotting using anti-HIS antibodies revealed STB of approximately 13kDa (Figure 3.10 E).

The plasmid pLGV009 (Figure 3.11, A and B) was constructed to express STB without a histidine tag and using a plasmid with a distinct antibiotic selection marker (Kan^r). The plasmid was transformed into *E.coli* TE1 and verified by colony PCR (Figure 3.11 C) where it shows the presence of the cloned *stxB* insert of 349bp. Cells were induced and the periplasmic extract were purified by filtration. Extracts were found to over-express STB of the appropriate size (9.7kDa) as shown (Figure 3.11 D).

Subunit proteins were purified to compare and analyze their adjuvant activities. STB was expressed from plasmid pLGV009 and concentrated from the periplasm. Periplasmic preparations were filtered through a 30 kDa filter and the residual sample remaining on top of the filter found to contain monomeric STB (as shown in Figure 3.11 D). Pentameric STB is expected to be 48.5 kDa and thus the periplasm was then subjected to filtration through a 50 kDa concentrator/filter to remove larger contaminants. The filtrate from the 50 kDa concentrator was analyzed by SDS-PAGE (Figure 3.13 B). The final STB protein preparation was excised from SDS-PAGE and subjected to liquid chromatography–mass spectrometry (LC–MS). The results from the LC-MS confirmed the expected protein sample to be the Shiga toxin B subunit with a good 60.92% of coverage (Figure 3.12A). CTB was induced and expressed from plasmid pARLDR19 and was purified using D-galactose affinity chromatography from periplasmic extracts.

Elution samples were analyzed by SDS-PAGE and the results indicate the presence of CTB at an expected size of 11 kDa (Figure 3.12 C). Pertussis toxin was purchased from List Biological Laboratories INC, CA and was analyzed on SDS-PAGE to reveal subunits S2 and S3 at the expected sizes of 23 and 22 kDa, respectively (Fig 3.12 D). The B subunit of *E.coli* heat-labile toxin (LTB) was induced and expressed from plasmid pJKT68 and purified with D-galactose affinity chromatography from the periplasm of *E.coli* TE1. Elution samples were analyzed by SDS-PAGE and the results indicated the presence of LTB at the expected size of 11 kDa similar to CTB (Fig 3.12 E).

***In vitro* Adjuvant Characterization Assays**

The plasmid for the expression of red-fluorescent protein STA₂/B chimeras was made previously in our laboratory (pSW005, Table 3.1). To characterize the ability of this chimeric molecule to deliver antigens to cells, *in vitro* assays were performed. *E.coli* TE1 cells containing pSW005 were induced for expression and the periplasmic extract was isolated. To determine if the RFP-STA₂/B (Red fluorescent protein) chimera was equally effective at binding and transporting of RFP into tissue culture cells, the extracts containing RFP-StxA₂/B were incubated on green monkey kidney cells (Vero) and internalization was detected using confocal microscopy. Figure 3.12 shows the incubation of an RFP-CTA₂/B chimera (A) and the RFP-StxA₂/B chimera (B) on Vero cells at 4°C for 15 minutes to observe the surface binding of the chimera on to the cells. Internalization is observed at 37°C after 50-60 mins. These results suggested that the RFP-StxA₂/B chimera is internalized through a retrograde pathway to a perinuclear domain of the cell similar to Ctx [144].

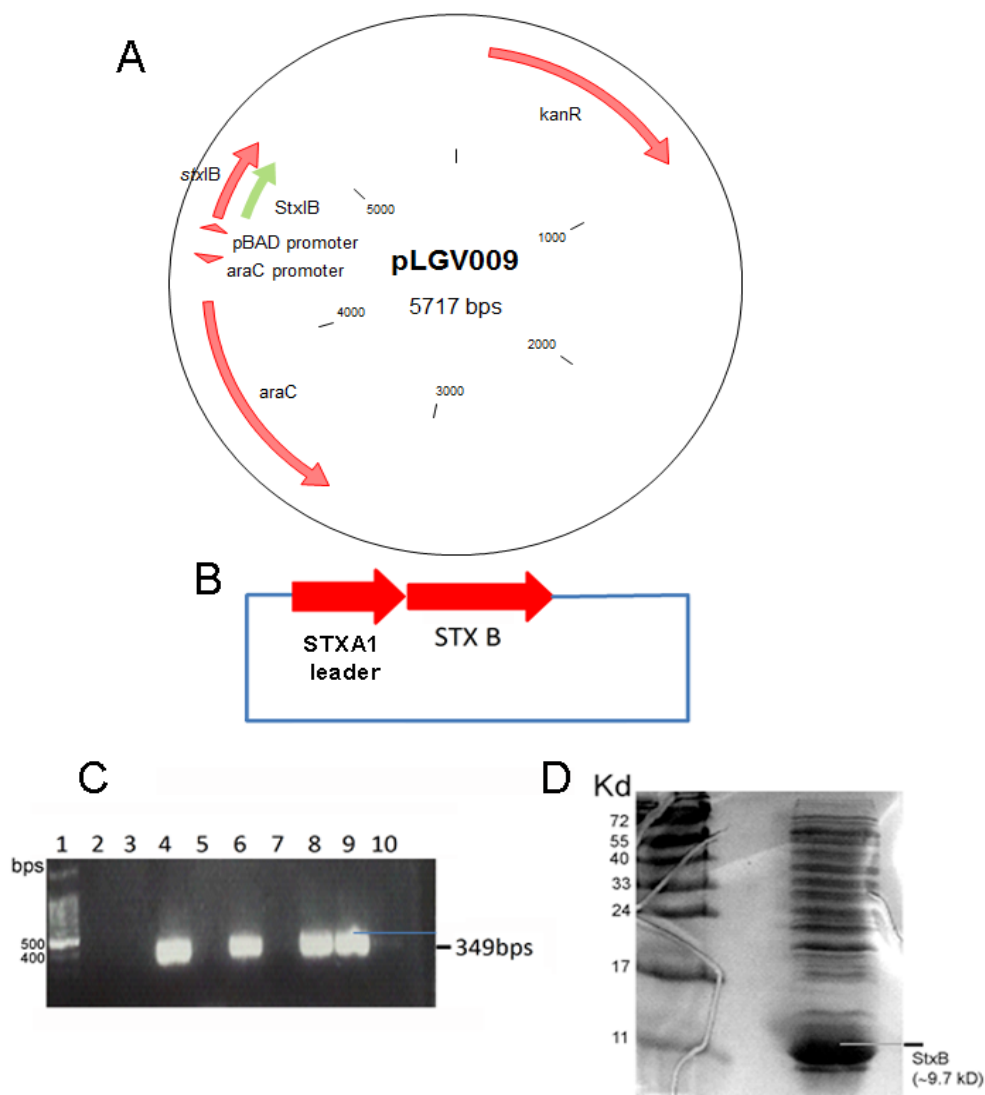


Figure 3.11. A and B) Schematic representation of pLGV009, the expression vector for STB C) Colony PCR of pLGV009 showing insert at the expected size of 349 bps. Lanes: 1.1 kB DNA ladder; 2. colony 13; 3. colony 14; 4. colony 15; 5. colony 16; 6. colony 17; 7. colony 18; 8. colony 19; 9. colony 20; 10. negative control; D) SDS-PAGE of periplasmic protein preparations from *E.coli* TE1 + pLGV009 after concentration with 30K filter.

A

Sequence Coverage of Top Protein

Protein name: Shiga toxin subunit B OS-Shigella dysenteriae serotype 1 (strain Sd197) GN-stxB PE-3 SV-1 - [STXB_SHIDS]

Coverage (%): 62.92

1 11 21 21 41 51 61 71 81

1 MKTLLIAR LFFFMALA TPCVYKVE YV **ENDDYEVYKQKALF ENYKQKAL LAGLSTQYV EDKNAQNG MFKKVEK**

A2	Sequence	# PSMs	# Proteins	# Protein Groups	Protein Group Accessions	Modifications	ΔCn
High	WNLGSLLSADITG MIVYK	1	1	1	10326V0		0.0000
High	ILSDTELTASDIR	1	1	1	1P64E5		0.0000
High	ALEKLGAKLR	2	1	1	1059G7		0.0000
High	AADVTGADISAVT R	1	14	1	1A3G9F1		0.0000
High	VGDKEFTNR	2	1	1	10326V0		0.0000
High	YNAHYGGGFSEV FR	1	1	1	10326V0	CA(Determinant y)	0.0000
High	YDODFTYK	6	1	1	10326V0		0.0000
High	WNLGSLLSADITG MIVYK	2	1	1	10326V0	M18(Cysteine)	0.0000
High	WVGGLNK	6	26	1	1ATZL5		0.0000
High	YNTLDLK	1	2	1	1025V97		0.0000
High	EYTSQYR	2	1	1	1P7E5		0.0000
High	LDLSSVDTLAK	1	1	1	1P22E		0.0000
High	WDEYELGGSA	2	1	1	101AVAS	M1(Cysteine)	0.0000

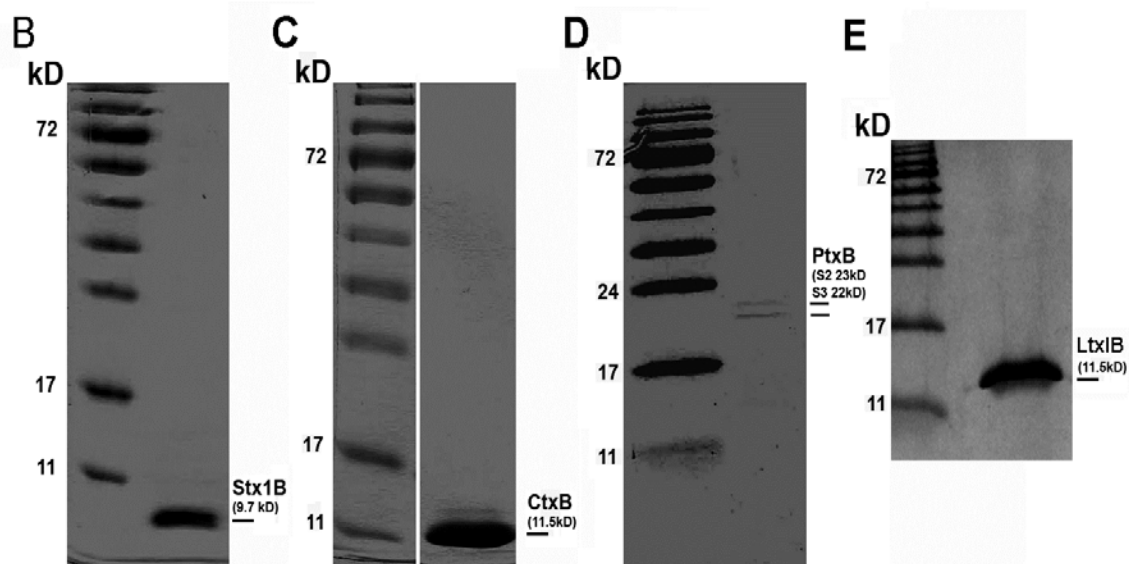


Figure 3.12. LC-MS of purified STB and SDS-PAGE of purified toxin B subunit proteins. A) LC-MS results from STB purification showing 60.92 % of coverage; B) SDS-PAGE of STB from pLGV009; C) SDS-PAGE of CTXB subunit from pARLDR19; D) SDS-PAGE of PTXB; E) SDS-PAGE of Heat labile toxin B subunit from pJKT68

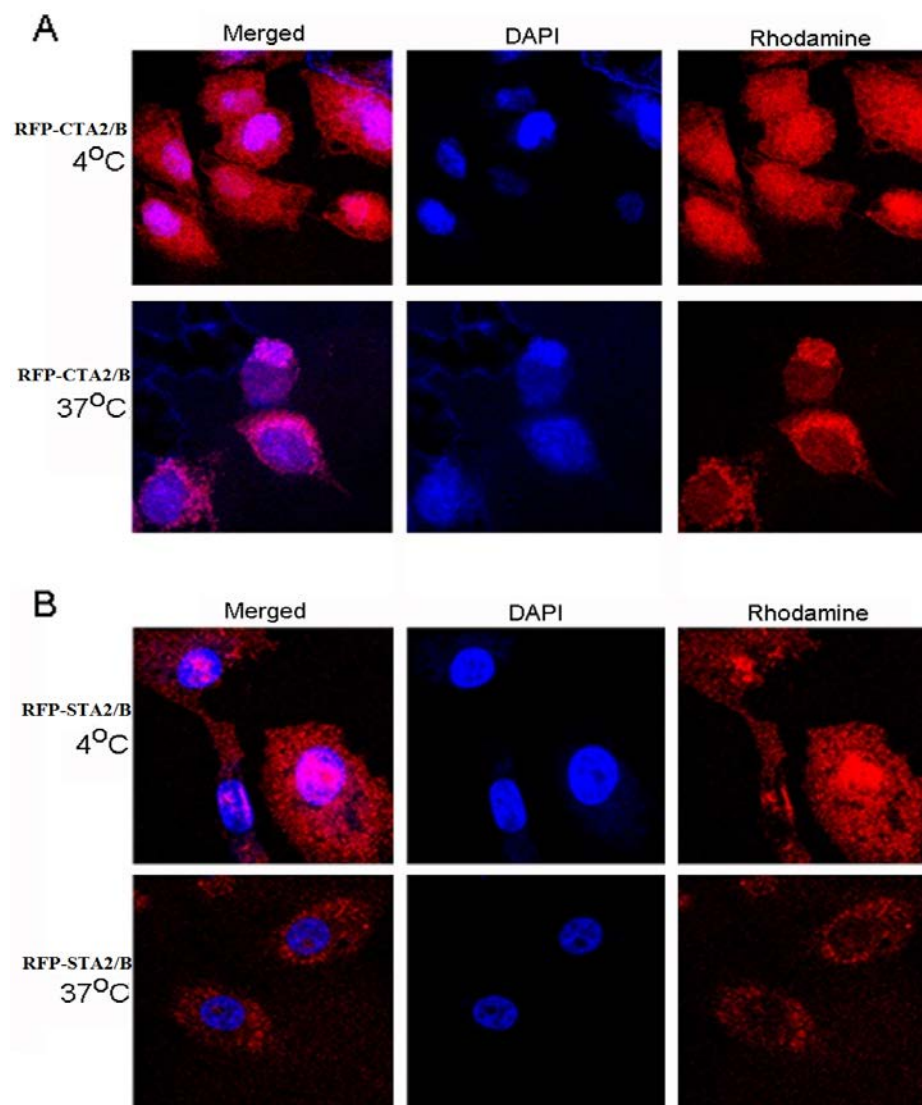


Figure 3.13. Binding and internalization of the A) RFP-CTA₂/B. B) RFP-StxA₂/B chimera on Vero cells at 4°C and at 37°C showing internalization. DAPI is labelling the nucleus of the cells as blue and red color indicates the Rhodamine fluorescence. Movement of Red fluorescence towards perinuclear space indicates the internalization.

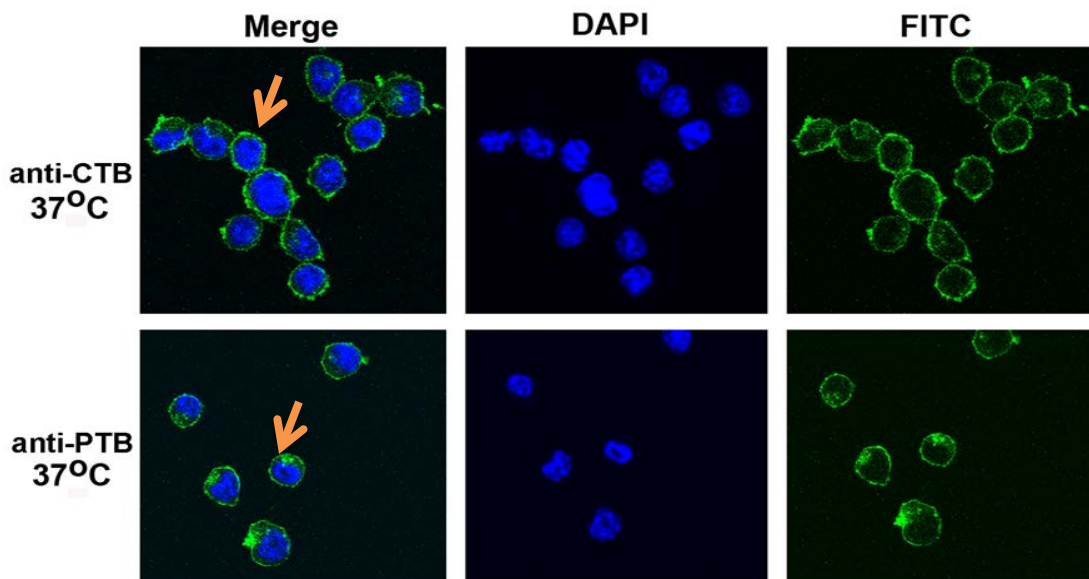


Figure 3.14. Confocal microscopy of CTB and PTB after incubation on dendritic cells (DC2.4) at 37°C for 1 hour using anti-CTB and anti-PTB primary antibodies and FITC labeled secondary antibodies. Results have indicated that antibody staining is showing good Internalization of B subunits of CT and PT. Movement of Green fluorescence towards perinuclear space indicates internalization (indicated by arrow). Blue color center indicated the Nucleus of the cells stained by DAPI.

To better understand the application of toxin B subunits alone as antigen-delivery vehicles, studies were completed to characterize the binding and internalization of toxin B subunits *in vitro*. The results shown in Figure 3.14 was conducted to compare the binding and internalization pattern of CTB to PTB on mouse dendritic DC2.4 cells using anti - CTB and anti-PTB staining after incubation at 37°C for 1 hour. These results suggest significant internalization of PTB into DC2.4 cells that is superior to CTB under these conditions. We were unable to compare STB in this assay as no affective anti-STB antibodies were available.

To extend the above study and compare the ability of toxin B subunits to promote the internalization of mixed antigen, we conducted a comparative study using CTB, PTB and STB as adjuvant with FITC-OVA as an antigen on mouse dendritic DC2.4 cells at

37°C (Figure 3.15). The result of this *in vitro* study are preliminary, but indicate that nontoxic STB promotes stronger binding and internalization of FITC-OVA to DC2.4 cells compared to PTB and CTB. We also attempted to quantify the uptake through use of an antigen uptake assay and thus far the results obtained have shown that the WNV DIII antigen alone may promote antigen uptake (data not shown).

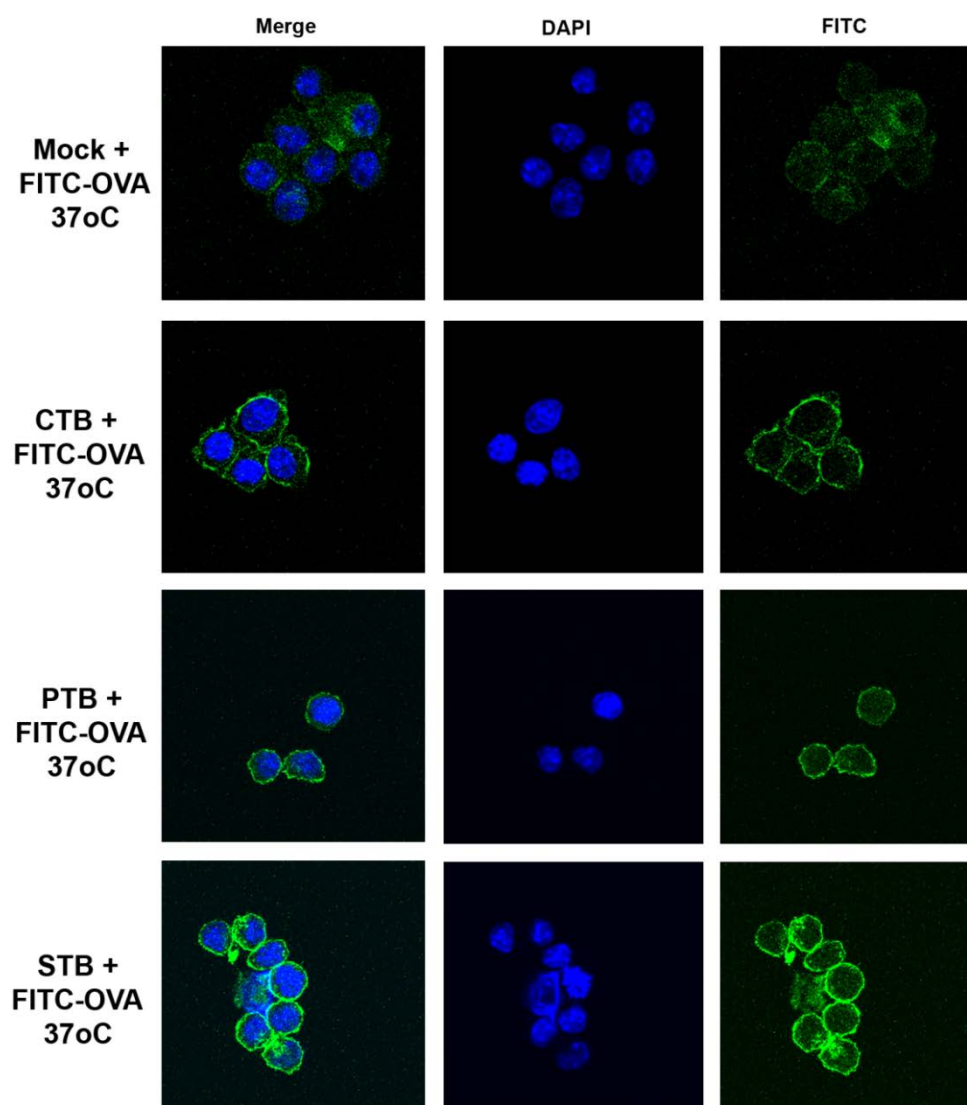


Figure 3.15. Confocal microscopy of FITC-OVA mixed with toxin B subunit proteins or mock extract and incubated on DC2.4 cells for 1 hour at 37°C. Blue-nucleus of the cells labelled by DAPI staining. Movement of green fluorescence towards perinuclear space indicates internalization.

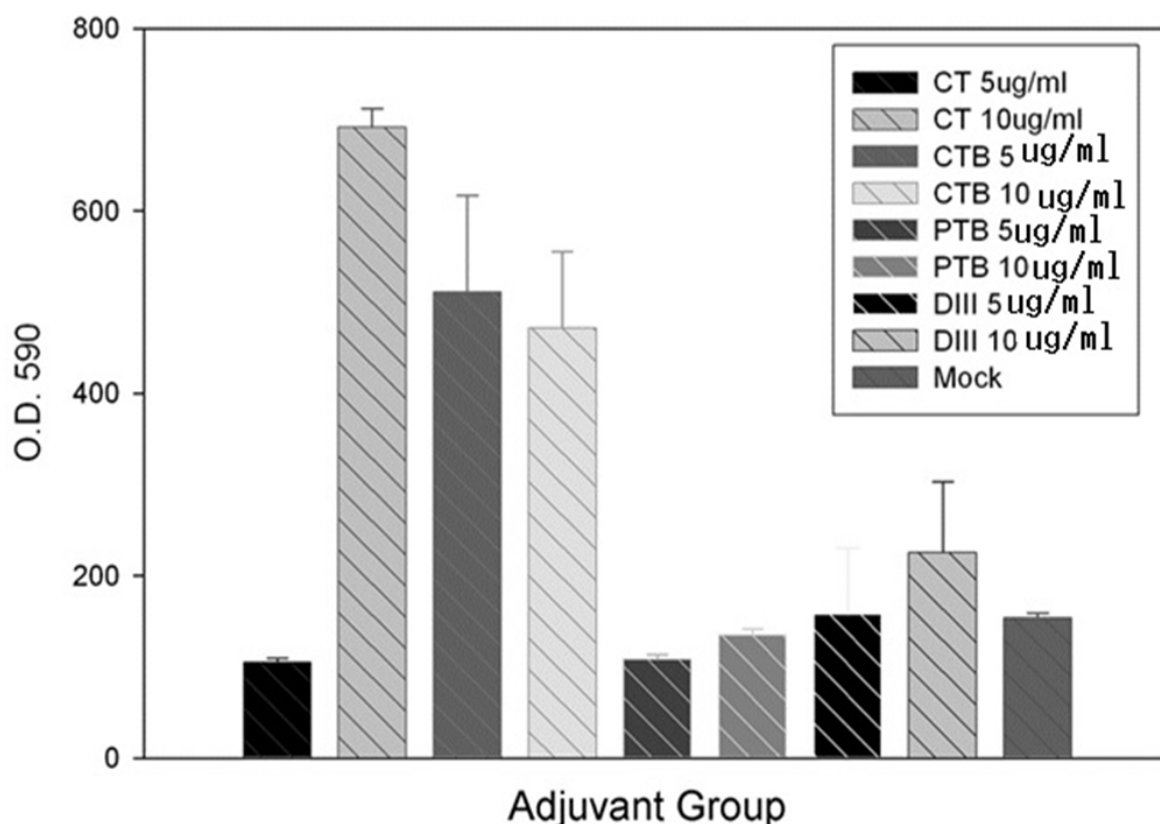


Figure 3.16. Metabolic activity as shown by Alamar blue on J774 macrophage cells with different adjuvants at different concentrations. Cholera toxin (CT) at 5 $\mu\text{g/ml}$, CT at 10 $\mu\text{g/ml}$, cholera toxin B subunit (CTB) at 5 $\mu\text{g/ml}$, CTB at 10 $\mu\text{g/ml}$, Pertussis toxin B subunit (PTB) at 5 $\mu\text{g/ml}$, PTB at 10 $\mu\text{g/ml}$, Envelope Domain III of West Nile Virus (DIII) at 5 $\mu\text{g/ml}$, and DIII at 10 $\mu\text{g/ml}$. Mock is the periplasmic extracts without testing protein. Error bars indicate STD error of assay performed in triplicate.

Cell proliferation assays monitor actively dividing cells, expressed either as the actual number of active cells or the ratio of proliferating to non-proliferating cells in culture. The results from Figure (3.16) show that Ctx at 10 $\mu\text{g/ml}$ showed highest proliferation followed by CTB subunit at 5 $\mu\text{g/ml}$ and 10 $\mu\text{g/ml}$. There is a decrease in the level of cell proliferation with PTB subunit at 5 $\mu\text{g/ml}$ compared to PTB at 10 $\mu\text{g/ml}$. DIII from West Nile Virus has shown similar effect of lower proliferation at 5 $\mu\text{g/ml}$

compared to 10 $\mu\text{g/ml}$ in a concentration dependent manner. This experiment was performed to assess the cellular proliferation ability of the non-toxic derivatives of bacterial enterotoxins CT, CTB, PTB, and DIII at different concentration. The higher proliferation capacity of the macrophages cells (J774's) indicates the better adjuvant property of the protein.

B3Z is a LacZ-inducible CD8⁺ T cell hybridoma expressing TCR specific for OVA257–264 (SIINFEKL), presented on the murine H2Kb MHC class I molecule. After incubation of antigen presenting cells with adjuvants plus SIINFEKL, cells are washed, and β -galactosidase activity is detected in live cells by using fluorescein di-b-D-galactopyranoside and propidium iodide according to the manufacturer's protocol (Figure 3.17, Invitrogen). Results from a primary study (Figure 3.17 A) show increased B3Z activation with increasing concentrations of native CT as well as the purified LTB subunit. LTB shows greater activation at higher concentrations and also greater activation than native CT. This result was unexpected, however, the possible rationale may due to the effect of lipopolysaccharide (LPS) content of the purified LTB. The second experiment was a comparative study between native CT and the B subunits of *Pertussis* (PTB). Results indicate that PTB at higher concentrations of 2 $\mu\text{g/ml}$ promotes better antigen presentation to the B3Z T cell line than native Ctx at 1 $\mu\text{g/ml}$.

We analyzed cells for their cytokine expression and stimulation upon reacting with the proteins through ELISA as it is important to show T cell activation and the immune response [147]. Results of TNF- α analysis (Figure 3.19A) indicate that the mock has the highest stimulation possibly due to LPS followed by STB, PTB, and CTB. In comparison, CT has the lowest stimulation, Research shows that the pro-inflammatory

cytokines like TNF- α are suppressed by Ctx [69, 148]. Comparative analysis of IL-12 (Figure 3.19B) indicates that PTB was able to stimulate IL-12 next to mock/ PBS. CT, CTB, and STB show a clear suppression of IL-12 in agreement with the evidence from literature stated above, that CT is shown to suppress cytokine IL-12 [149].

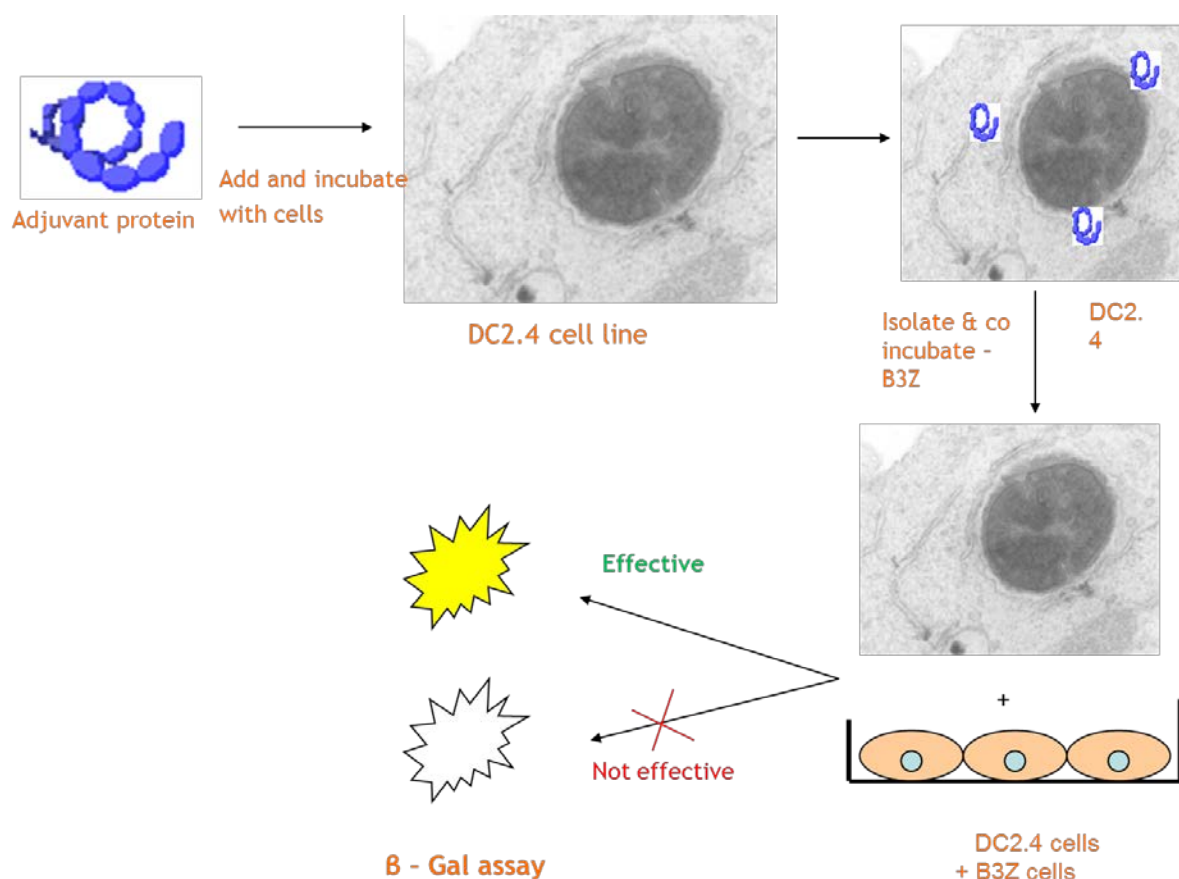


Figure 3.17. Schematic representation of the *in vitro* antigen presentation assay using the B3Z cell line. Adjuvant proteins and antigens are applied and incubated on DC2.4 cells followed by co-incubation of cells with B3Z cells and measurement of B3Z T cell stimulation through β -galactosidase activity.

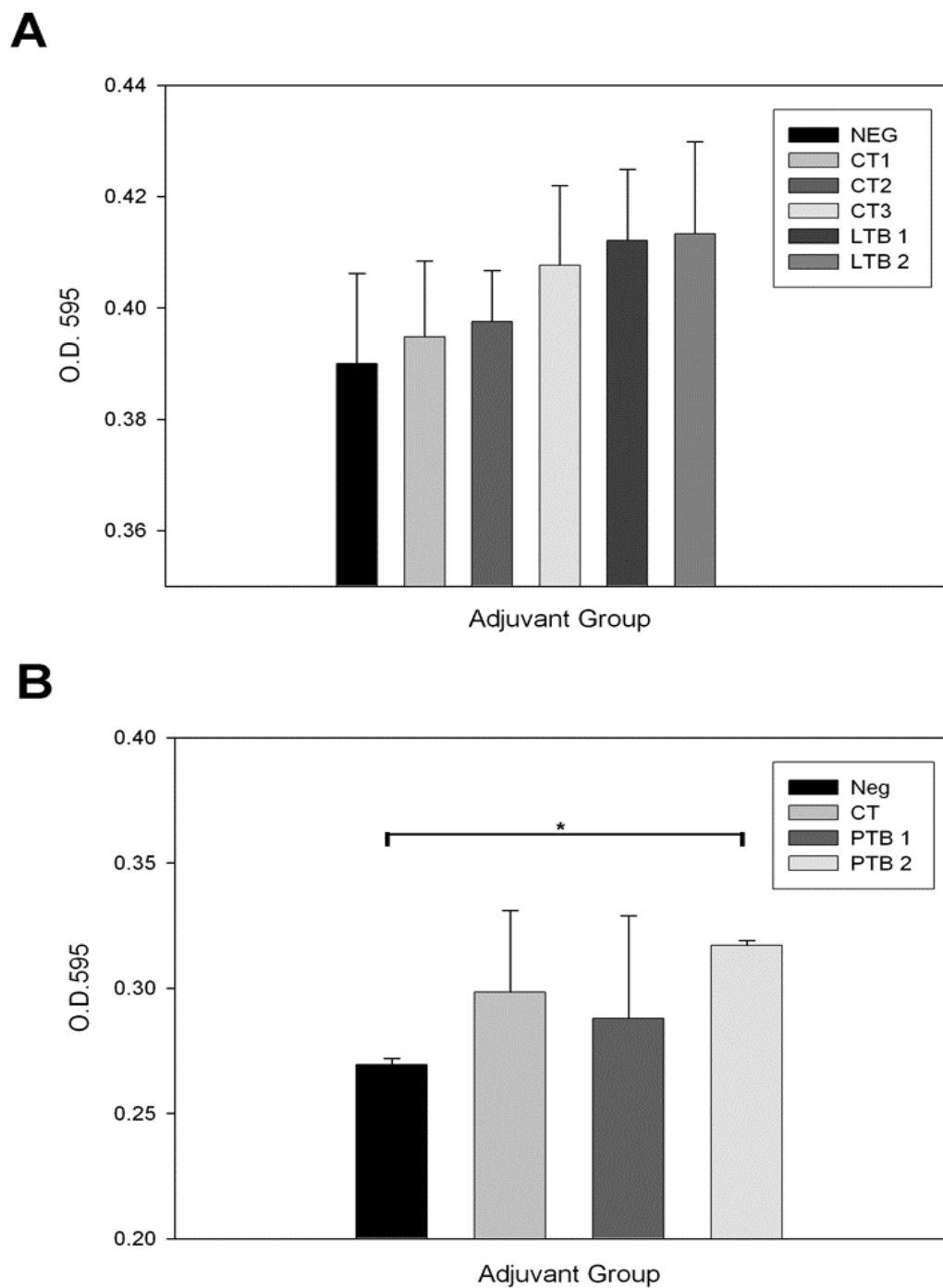


Figure 3.18. A) *In vitro* B3Z stimulation assay. Measurement of beta-galactosidase activity using adjuvants Cholera toxin (CT) and Heat labile toxin B subunit (LTB); CT1 (1 $\mu\text{g/ml}$); CT2 (2 $\mu\text{g/ml}$); CT3 (3 $\mu\text{g/ml}$); and LTB1 (1 $\mu\text{g/ml}$) and LTB2 (2 $\mu\text{g/ml}$). B) Comparative study of adjuvant activity between CT and PTB; CT (0.01 $\mu\text{g/ml}$); PTB1 (1 $\mu\text{g/ml}$) and PTB2 (2 $\mu\text{g/ml}$). Analyzed using student's t-test compared with the control value and based on two independent samples ($P < 0.05$).

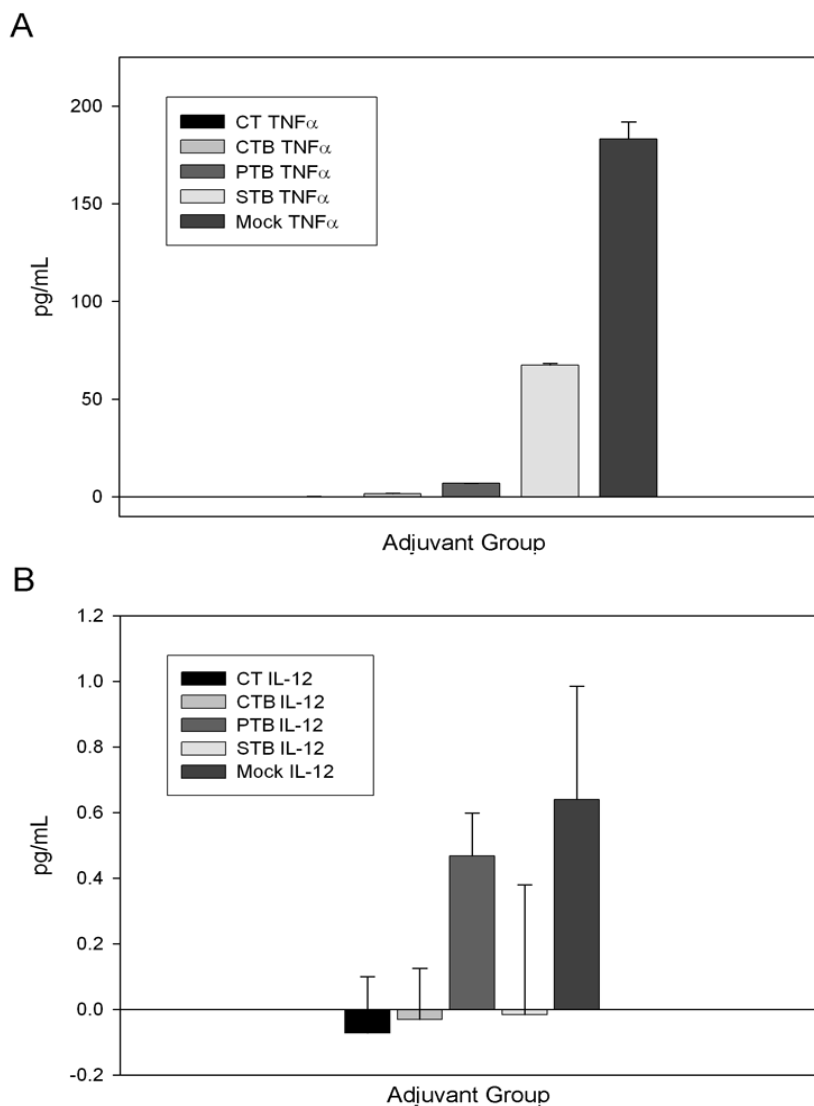


Figure 3.19. Cytokine production on C57Bl/6 murine dendritic cells line (DC2.4) stimulated with different purified adjuvant proteins. DC2.4 cells were incubated for 24 hours with media containing the indicated concentrations of proteins. A) Comparison between CT, CTB, PTB, and STB at different concentrations for the stimulation of TNF- α . CT (5 μ g/ml) CTB (5 μ g/ml), PTB (5 μ g/ml), STB (5 μ g/ml). B) Comparison of IL-12 stimulation by CT, CTB, PTB, and STB a different concentrations. CT (5 μ g/ml), CTB (5 μ g/ml), PTB (5 μ g/ml), STB (5 μ g/ml). The values were determined by ELISA and the data shown are determinations from two independent experiments.

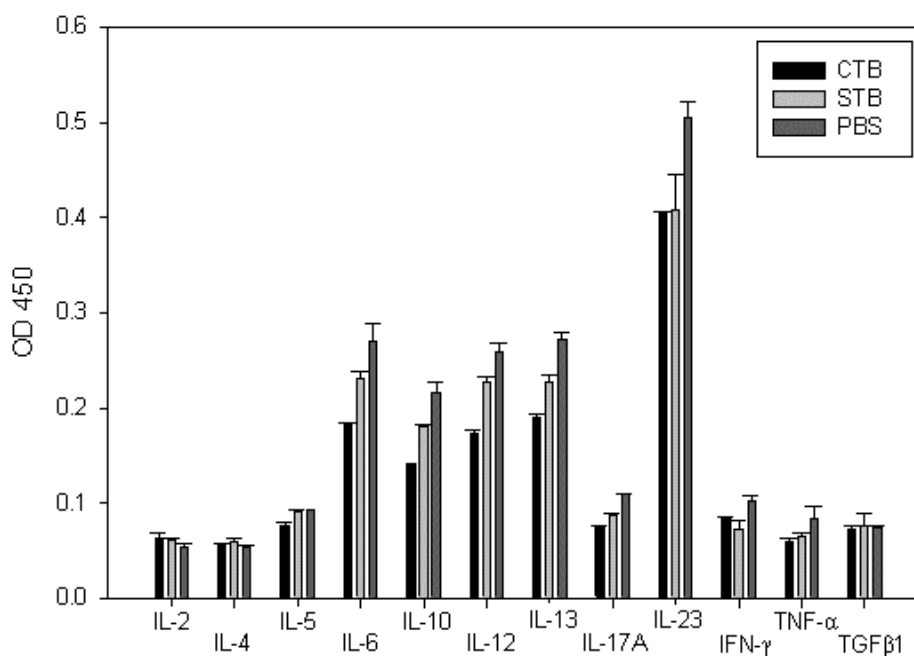


Figure 3.20. Multi-analyte cytokine analysis on C57Bl/6 murine dendritic cells line (DC2.4) stimulated with adjuvant proteins CTB and STB at 2 ug/ml concentration. DC2.4 cells were incubated with media containing the indicated concentrations of proteins for 24 hours prior to collection of supernatant. Standard error is based on results of two independent samples.

Broad analysis of many cytokines was completed using a multi-analyte cytokine assay. Although cytokine concentrations could not be determined in this assay, Figure 3.20 supports results from Figure 3.19 indicating that both CTB and STB inhibited TNF- α expression when compared to Mock or PBS. IL-12 expression was also inhibited and supports the results from earlier assays (Figure 3.19). Overall results suggest that CTB and STB were inhibiting the expression of most of the cytokines, including; IL-6 (Th2), IL-10 (Th2), IL-12 (Th1), IL-13 (Th-2), IL-17A (Th17), IL-23 (Th17), INF- γ (Th1), and TNF α (Th1) at the concentration of 2 μ g/ml. However, STB, similarly to CTB, may be promoting the stimulation of Th-2 type and anti-inflammatory cytokines like IL-2 (Th1), IL-4 (Th2), IL-5 (Th2) and TGF- β (Th2/Th17).

CHAPTER IV. DISCUSSION AND CONCLUSIONS

The objective of the current thesis was to develop and characterize novel vaccine adjuvants that are based on non-toxic bacterial toxin derivatives. The goal of vaccination is to generate a strong and specific immune response to the administered antigen to induce long-term protection against infection. As vaccine development progresses more towards the use of killed or purified subunit vaccines as opposed to live attenuated vaccines for safety reasons, effective immune induction often requires the addition of an adjuvant [150]. In addition, the development of vaccines that can be administered through non-invasive routes, such as intranasal, sublingual, transdermal, or subdermal is highly desirable and requires the use of novel adjuvants. Lastly, there is an ever-increasing need to develop vaccines for bioterror, antibiotic resistant and new emerging pathogens. Over the last 200 years, the use of vaccines has proven to be one of the most successful medical interventions in the reduction of disease caused by infectious agents[151].

Adjuvants are defined as substances that can elevate and enhance the potency and endurance of the desired immune response when co-administered or coupled with antigens in vaccines, but have little to no toxicity and immune properties of their own [152-154]. The word adjuvant comes from the Latin word *adjuvare*, which means to help, aid or to enhance[150, 155]. The inclusion of adjuvants in vaccines helps in the augmentation and sustainability of the antigen-specific response and to efficiently regulate the appropriate immune responses [153, 155]. Adjuvants can be used for

different purposes, including: 1) to enhance the immunogenicity of highly purified or recombinant antigens, 2) to reduce the dosage or quantity of antigen or the number of immunizations needed for establishing protective immunity, 3) to improve the efficacy of vaccines in pregnant women, newborns, the elderly or immuno-compromised persons, or 4) as an antigen delivery systems for the uptake of antigens by the mucosa [150].

Bacterial components constitute an important source of vaccine adjuvants because of their immunostimulatory capacity[72]. Constituents of Gram negative bacteria like cell wall peptidoglycan or lipopolysaccharide (LPS) boost the immune response to co-administered antigens through the activation of Toll like receptors which transfer threat signals leading to the activation of immune defense systems[156]. Various bacterial species that have been used as a source of adjuvants include: *Mycobacterium* species, *Corynebacterium parvum*, *Bordetella pertussis* and *Neisseria meningitides*. However these live whole or killed cells can induce strong inflammatory responses and are not safe for human use due to their toxic nature[157].

Shiga toxin 1 (Stx1), secreted by *Shigella dysenteriae* and *Escherichia coli* EHEC, has considerable structural similarity to cholera toxin (Ctx), but distinct immunostimulatory characteristics. Ctx has long been recognized as an excellent vaccine adjuvant, or immunomodulator, with the ability to stimulate specific immune responses to co-administered antigens (vaccine antigens) delivered through the oral or nasal route [158]. High specific receptor-binding affinity and stability appear to be the basis for these unique immunomodulatory properties. However, the toxicity of Ctx is a limiting factor for use as an adjuvant in human vaccines. Chimeric A₂B molecules, as well as other non-toxic derivatives, of Ctx have shown much promise as novel mucosal vaccine candidates

[5, 49]. A₂B chimeras of Ctx retain the capacity to introduce antigens into host cells and modulate the immune response, and toxic domains are replaced with a vaccine antigen of interest. We hypothesized that, due to significant structural homology, Stx1 can also act as a vaccine adjuvant, but with distinct receptor binding specificities that may more directly target immune cells and produce a different response.

The goal of this research was to construct plasmids to express and purify Stx1A₂B chimeric molecules, and the STB subunit alone, and to characterize these molecules *in vitro* as novel vaccines and vaccine adjuvants. Previous work has shown the successful construction of plasmids and purification of Ctx A₂/B chimeric proteins [15, 144-146, 159]. CtxA₂/B chimeras are easily purified on commercially available D-galactose agarose affinity resins. The availability of D-galabiose affinity resin and structural similarity of Ctx and Stx1 supported our hypothesis that Stx1A₂/B chimeras could be purified for characterization as novel vaccines [160]. The work presented in the first part of this thesis shows the successful construction of recombinant plasmids with Stx1 A₂/B containing the vaccine antigens LcrV from *Yersinia pestis* and the Envelope protein Domain III (DIII) from West Nile virus. These plasmids were confirmed through colony PCR (Table 3.1 and Figures 3.1D, 3.2C, 3.3C, 3.4C, 3.5C, 3.6C, 3.7C, 3.8C, and 3.10C) and nucleotide sequencing (data not shown). Near the start of this work, D-galabiose resin became unavailable as the commercial vendors stopped supply, limiting our options for StxA₂/B chimera purification. Thus, some of the constructed plasmids incorporated a 6X histidine (HIS-tag) to promote purification using nickel chromatography. The plasmids were constructed with the HIS-tag on either the C-

terminus of the STB subunit (3.7A and B, 3.2A and B, 3.3 A and B, 3.8A and B) or on the N-terminus of the A₂ fusion peptide (3.1A and B, 3.5A and B).

Previous studies using the LcrV antigen from *Yersinia pestis* revealed successful incorporation into a CtxA₂/B chimera and co-purification of LcrV-CtxA₂/B peptide with the CTB subunits on D-galactose [15]. However, many factors influence the expression of proteins including the alignment of the amino acids, folding of protein chains, and culturing conditions. The chimeric proteins from pLGV002 (His-LcrV-STA₂B) and pLGV003 (LcrV-STA₂B-His) were expressed and purified using nickel column chromatography. Figure 3.2 illustrates the presence of the His-LcrV-STA₂ fusion, but the STB subunit was not co-purified. Similarly, for the proteins expressed from pLGV003, the HIS-STB peptide was purified as shown in Figure 3.4, but there was no co-purification of the LcrV-StxA₂ peptide. These results indicate that the StxA₂ domain and the STB subunit were not able to fold properly into holotoxin within the periplasm of *E.coli*. The reason for this ineffective folding may be due to the differences in the non-covalent interactions between the A₂ and B regions between Ctx and Stx. The A₂ domain of Ctx is 46 amino acids long and produces more hydrogen bonds with CTB, whereas the A₂ domain of Stx gene is only about 12 bases apart from B subunit and has relatively weaker bonds with STB [161, 162]. Literature published indicated that A₂ part of Shiga toxin is an essential factor for holotoxin assembly and any disturbance to A₂ domain during molecular cloning process could cause a negative effect on holotoxin formation [163].

Purification of StxA₂/B chimeric molecules containing the DIII antigen from West Nile virus was also of limited success. These plasmids included pLGV004 (DIII-

STA₂/B-HIS), which resulted in limited expression despite performing experiments at different time intervals and temperatures, and pLGV006 (HIS –DIII-STA₂B), which resulted in protein aggregation and insolubility. We also designed chimeric DIII-StxA₂/B with no HIS (pLGV005) to attempt purification on other lectin affinity columns, such as D-galactose and fetuin-agarose. The results indicated that, unlike Ctx and Ptx, Stx had no binding capacity for these resins. A final strategy to express DIII-StxA₂/B molecules was based on previous success using a strong *E.coli* signal sequence (TorA) to direct the A₂ fusion to the *E.coli* periplasmic space (pLGV010, Figure 3.8) [146]. Expression studies thus far from pLGV010 have indicated limited protein expression even in the insoluble pellet fractions. Limited expression could be due to the absence of N terminus StxI leader sequence as studies show that N-terminus leader sequence of the StxI gene is essential for production and assembly of the subunits to yield an active recombinant holotoxin in *E.coli* [164]. Thus, while there was significant success creating a number of new plasmids for StxA₂/B chimeric vaccine expression, the current evidence indicates that Stx A₂/B chimeras do not fold with the same efficiency and stability that CtxA₂/B chimeras do, resulting in insoluble subunits that cannot be co-purified. StxA₂/B molecules are also not expressed as well in the *E. coli* periplasm. Toxic effects may result from over-expression of StxA₂/B that select for transformants that do not express to a high degree. Lastly, our inability to purify using Gb3 affinity chromatography was a severe limitation for the purification of StxA₂B chimeras. Alignment of STA subunit with that of CTA indicated that there is a lot of variability among these two toxins subunits and that may have contributed to the poor expression as well as folding of the recombinant proteins.

In addition to plasmids to produce StxA₂/B molecules, plasmids were constructed to over-express STB alone, with or without HIS tags to promote purification (Table 3.2 and 3.9, 3.10, 3.11). The hypothesis of this work was that the immunogenicity of purified STB and CTB could be compared *in vitro* and would be distinct. The plasmids pLGV001, pLGV007, and pLGV009 (Figures 3.9, 3.10 and 3.11) were used to over-express STB with or without a HIS tag. Plasmid pLGV007 (STB-HIS) did express STB, as confirmed by Western blot (Figure 3.10D and E) but we could not separate contaminant proteins by purification. Plasmid pLGV009 (STB) over-expressed STB to a high concentration and we were able to separate contaminant protein to a high purity by filtration. The identity of STB from this preparation was confirmed by LCMS (Figure 3.11D).

The final goal of this work was to characterize the antigen-uptake capacity and adjuvanticity of StxA₂/B chimeras and STB *in vitro*. The trafficking of antigens stimulated by SxtA₂/B and STB was analyzed using confocal microscopy and tissue culture of epithelial (Vero) or leukocyte (J774 macrophage and DC2.4 dendritic) origin. We showed the internalization of RFP-StxA₂/B Vero cells (Figures 3.13A and B). These results indicated that the RFP –StxA₂/B is able to bind to and internalize into Vero cells at 37°C, and deliver a large antigen (RFP) to a perinuclear domain within the host cell, in a similar manner to the RFP-CtxA₂/B construct. This antigen-delivery capacity is a highly desirable quality of effective adjuvants. The trafficking of the nontoxic B subunits of Ctx and Ptx was directly compared using anti-toxin antibodies on DC2.4 dendritic cells (Figure 3.14). These results indicated that PTB (Pertussis toxin B subunit) was as efficient, or more so, than CTB at trafficking and internalization into this cell type. In order to study the uptake and internalization properties of the B subunits into cells

further, Shiga toxin B subunit, Pertussis Toxin B subunit and Cholera Toxin B subunit were incubated along with the large FITC–OVA antigen on DC2.4 cells. These results showed good antigen binding that was stimulated with the addition of the toxin B subunits, and uptake that may be superior with STB over the other toxin subunits (Figure 3.15). We attempted to quantify the antigen uptake capacity using a microplate-based fluorescent antigen uptake assay, but results have thus far have not shown significant differences between toxin subunits (data not shown). Proliferation and activation of macrophages is also considered as an important quality of adjuvanticity and we tested the capacity for native CT, CTB, and PTB to activate the macrophage cell line (J774) using the Alamar blue metabolic dye. Results indicate that native CT has significant stimulation properties on these cells, followed by the CTB subunit and the DIII antigen alone (Figure 3.16). The WNV DIII antigen binds to $\alpha_v\beta_3$ integrins and may have adjuvant properties of its own as research shows that DIII may possibly be entering through cholesterol-rich rafts and dynamin as reported in [146, 165].

Further studies were conducted to characterize the ability of STB to deliver antigens to antigen presenting cells *in vitro* using a model antigen and sensitive T-cell line (B3Z cell line). Comparisons between STB and native Ctx, CTB, LTB, and PTB were analyzed. Although Ctx is known to be a good adjuvant, results indicated that LTB was better able to present the SIINFEKL antigen to B3Z T cells compared to Ctx (Figure 3.18A). This effect may be attributed to residual lipopolysaccharide (LPS) in the LTB protein sample preparations despite endotoxin removal from this preparation. LPS is a powerful adjuvant and may act at even very low concentrations [166]. Another comparative B3Z assay was performed between commercially prepared and endotoxin-

free native Ctx (CT). Results indicate that while PTB can stimulate antigen presentation at high concentrations, native Ctx is better at concentrations as much as 100-fold lower (Figure 3.18 B). While STB was not used in this assay due to concerns over purity and LPS contamination, the B3Z assay was found to be an effective method for the *in vitro* comparison of toxin adjuvants and will be used for future studies.

The ability of proteins STB, PTB, CTB, and CT to stimulate or inhibit cytokines *in vitro* was also characterized. Understanding of Cytokines production helps to determine the kind of immune responses that these proteins are capable of eliciting. As mentioned above, Ctx has been shown to inhibit TNF- α on macrophages *in vitro* and we observed a similar pattern on dendritic cells (Figure 3.19) [69]. Less is known about the cytokines affected by Stx, however, it has been reported that TNF- α plays an important role in HUS (Hemolytic Uremic Syndrome) progression by increasing the Stx receptor Gb3 in human cerebral endothelial cell and sensitizing the cells to the toxic enzymatic activity [167, 168]. In our assay, STB was found to inhibit TNF- α production, but to a lesser degree than CT or CTB (Figure 3.19A). These results are in contrast to a recent study indicating that STB and a mutated Stx (substituted amino acids in A subunit) from *E.coli* to possess adjuvant activity for primary dendritic cells through the stimulation of TNF- α [169]. Differences in protein preparation, including the host for protein expression, purification techniques, and possible impurities, such as LPS, as well as the nature of the dendritic cells (i.e.primary versus immortalized), might explain the differences in outcome between this study and our study. While Ohmura et al. (2005) did not specifically analyze IL-12 expression, our results also indicate that IL-12 has not been stimulated by STB and may be inhibited (Figure 3.19B). A recent study on Ptx and its B

subunit shows that Ptx can induce dendritic cells production of interleukin (IL)-6, TNF- α , IL-12, and interferon-inducible protein, and PTB was capable of stimulating the production of interferon-inducible protein [88]. Our results indicated that PTB may also inhibit TNF- α production, but has little effect when compared to mock expression on IL-12 production from DC2.4 cells (Figure 3.19). A multi analyte cytokine assay using endotoxin-free preparations of CTB and STB indicates that both CTB and STB may inhibit the induction of Th1-type, such as IFN- γ and TNF- α , and promote the induction of Th-2 type and anti-inflammatory cytokines like IL-4, IL-5, and TGF- β . However, overall cytokine levels were very low in all of our assays, indicating that the immortalized DC2.4 cells were largely inactive and immature.

Future studies to support this work will need to include the isolation and implementation of primary bone marrow derived or peripheral monocytes for the analysis of cytokine activation or inhibition, as well as antigen-uptake. Alternatively, improved methods for the activation of immortalized cells can be implemented [170]. In addition, *in vitro* characterization studies could be enhanced by the addition of Gb3 to the cells *in vitro* to identify improvements in Stx immunostimulation. Protein expression and purification of STB and Stx chimeras can be improved through the construction of D-galabiose affinity columns, or Stx antibody-based affinity purification. In addition, making use of different affinity tags, expression vectors, *stx* sequences, and host organisms may improve protein expression and yield. Recently an endotoxin free strain of *E.coli* (Clean Coli, Lucigen, WI) has become available to ensure proteins are prepared in the absence of immune-stimulating LPS.

The development of novel adjuvants will improve the immunogenicity of purified vaccine antigens and is recognized as a top priority in vaccine research. Adjuvants have long been of great interest to vaccine development as they are commonly necessary to strengthen immune responses. Adjuvants are also key to the development of effective mucosal vaccines because they can compensate for the often poorly immunogenic nature of orally and nasally administered vaccine antigens. Much of the protection available at mucosal surfaces such as respiratory, gastrointestinal, and urogenital tracts is provided by the production of secretory IgA and antibodies, which are effectively produced only when the vaccine is administered by a mucosal route. In an effort to develop novel adjuvants, Stx or STB represent important candidates for further characterization due to their ability to target dendritic cells and to induce antigen-specific responses. Although many details of the molecular mechanisms behind the enhancement of immune responses by AB₅ toxin derivatives remain to be elucidated, the present study represents a novel attempt to design and characterize primary Stx derived adjuvants and compare the immunogenicity of non-toxic subunits of AB₅ bacterial toxins.

REFERENCES

- [1] M. Mohamadzadeh, *Microbial Toxins: Current Research and Future Trends. Expert Review of Anti-infective Therapy* 7 (2009) 695-696.
- [2] N. Ng, D. Littler, J. Le Nours, A.W. Paton, J.C. Paton, J. Rossjohn, T. Beddoe, Cloning, expression, purification and preliminary X-ray diffraction studies of a novel AB₅ toxin. *Acta Crystallographica Section F: Structural Biology and Crystallization Communications* 69 (2013) 0-0.
- [3] T. Beddoe, A.W. Paton, J. Le Nours, J. Rossjohn, J.C. Paton, Structure, biological functions and applications of the AB₅ toxins. *Trends in Biochemical Sciences* 35 (2010) 411-418.
- [4] E.A. Merritt, W. Hol, AB₅ toxins. *Current opinion in structural biology* 5 (1995) 165-171.
- [5] O. Odumosu, D. Nicholas, H. Yano, W. Langridge, AB Toxins: A Paradigm Switch from Deadly to Desirable. *Toxins* 2 (2010) 1612-1645.
- [6] H. Smits, A. Gloudemans, M. Van Nimwegen, M. Willart, T. Soullie, F. Muskens, E. de Jong, L. Boon, C. Pilette, F. Johansen, Cholera toxin B suppresses allergic inflammation through induction of secretory IgA. *Mucosal Immunology* 2 (2009) 331-339.
- [7] Z. Gong, Y. Jin, Y. Zhang, Suppression of diabetes in non-obese diabetic (NOD) mice by oral administration of a cholera toxin B subunit–insulin B chain fusion protein vaccine produced in silkworm. *Vaccine* 25 (2007) 1444-1451.
- [8] N. Engedal, T. Skotland, M.L. Torgersen, K. Sandvig, Shiga toxin and its use in targeted cancer therapy and imaging. *Microbial biotechnology* 4 (2011) 32-46.
- [9] M. Maak, U. Nitsche, L. Keller, P. Wolf, M. Sarr, M. Thiebaud, R. Rosenberg, R. Langer, J. Kleeff, H. Friess, Tumor-specific targeting of pancreatic cancer with Shiga toxin B-subunit. *Molecular Cancer Therapeutics* 10 (2011) 1918-1928.
- [10] O.N. Kovbasnjuk, M. Donowitz, Treatment of metastatic colon cancer with b-subunit of shiga toxin, Google Patents, 2011.
- [11] S.R. Waterman, P. Small, Acid-sensitive enteric pathogens are protected from killing under extremely acidic conditions of pH 2.5 when they are inoculated onto certain solid food sources. *Applied and Environmental Microbiology* 64 (1998) 3882-3886.
- [12] T.M. Fuchs, Molecular mechanisms of bacterial pathogenicity. *Naturwissenschaften* 85 (1998) 99-108.

- [13] K. Teter, M.G. Jobling, D. Sentz, R.K. Holmes, The cholera toxin A13 subdomain is essential for interaction with ADP-ribosylation factor 6 and full toxic activity but is not required for translocation from the endoplasmic reticulum to the cytosol. *Infection and immunity* 74 (2006) 2259-2267.
- [14] J. Clemens, S. Shin, D. Sur, G.B. Nair, J. Holmgren, New-generation vaccines against cholera. *Nature Reviews Gastroenterology and Hepatology* 8 (2011) 701-710.
- [15] J.K. Tinker, C.T. Davis, B.M. Arlian, Purification and characterization of *Yersinia enterocolitica* and *Yersinia pestis* LcrV–cholera toxin A₂/B chimeras. *Protein Expression and Purification* 74 (2010) 16-23.
- [16] W.I. Lencer, *Microbes and Microbial Toxins: Paradigms for Microbial-Mucosal Interactions*. V. Cholera: invasion of the intestinal epithelial barrier by a stably folded protein toxin. *AMERICAN JOURNAL OF PHYSIOLOGY* 280 (2001) G781-G786.
- [17] B. Mudrak, M.J. Kuehn, Heat-Labile Enterotoxin: Beyond G M1 Binding. *Toxins* 2 (2010) 1445-1470.
- [18] Å. Holmner, A. Mackenzie, M. Ökvist, L. Jansson, M. Lebens, S. Teneberg, U. Krengel, Crystal Structures Exploring the Origins of the Broader Specificity of *Escherichia coli* Heat-Labile Enterotoxin Compared to Cholera Toxin. *Journal of molecular biology* 406 (2011) 387-402.
- [19] S. Teneberg, T.R. Hirst, J. Ångström, K.-A. Karlsson, Comparison of the glycolipid-binding specificities of cholera toxin and porcine *Escherichia coli* heat-labile enterotoxin: identification of a receptor-active non-ganglioside glycolipid for the heat-labile toxin in infant rabbit small intestine. *Glycoconjugate journal* 11 (1994) 533-540.
- [20] I. Sospedra, C. De Simone, J.M. Soriano, J. Mañes, P. Ferranti, A. Ritieni, Characterization of Heat-Labile toxin-subunit B from *Escherichia coli* by liquid chromatography–electrospray ionization-mass spectrometry and matrix-assisted laser desorption/ionization time-of-flight mass spectrometry. *Food and Chemical Toxicology* 50 (2012) 3886-3891.
- [21] T.R. Branson, W.B. Turnbull, Bacterial toxin inhibitors based on multivalent scaffolds. *Chemical Society Reviews* 42 (2013) 4613-4622.
- [22] J.L. Mellies, F. Navarro-Garcia, I. Okeke, J. Frederickson, J.P. Nataro, J.B. Kaper, espC pathogenicity island of enteropathogenic *Escherichia coli* encodes an enterotoxin. *Infection and immunity* 69 (2001) 315-324.
- [23] N.A. Daniels, Enterotoxigenic *Escherichia coli*: traveler's diarrhea comes home. *Clinical Infectious Diseases* 42 (2006) 335-336.
- [24] S. Isidean, M. Riddle, S. Savarino, C. Porter, A systematic review of ETEC epidemiology focusing on colonization factor and toxin expression. *Vaccine* 29 (2011) 6167-6178.
- [25] R.B. Sack, S.L. Gorbach, J.G. Banwell, B. Jacobs, B. Chatterjee, R.C. Mitra, Enterotoxigenic *Escherichia coli* isolated from patients with severe cholera-like disease. *Journal of infectious diseases* 123 (1971) 378-385.

- [26] F. Qadri, A.-M. Svennerholm, A. Faruque, R.B. Sack, Enterotoxigenic *Escherichia coli* in developing countries: epidemiology, microbiology, clinical features, treatment, and prevention. *Clinical microbiology reviews* 18 (2005) 465-483.
- [27] C. Wennerås, V. Erling, Prevalence of enterotoxigenic *Escherichia coli*-associated diarrhoea and carrier state in the developing world. *Journal of Health, Population and Nutrition (JHPN)* 22 (2011) 370-382.
- [28] B. Nagy, P.Z. Fekete, Enterotoxigenic *Escherichia coli* in veterinary medicine. *International Journal of Medical Microbiology* 295 (2005) 443-454.
- [29] X. Hagnerelle, C. Plisson, O. Lambert, S. Marco, J. Louis Rigaud, L. Johannes, D. Lévy, Two-dimensional structures of the Shiga toxin B-subunit and of a chimera bound to the glycolipid receptor Gb3. *Journal of Structural Biology* 139 (2002) 113-121.
- [30] A.F. Trofa, H. Ueno-Olsen, R. Oiwa, M. Yoshikawa, Dr. Kiyoshi Shiga: Discoverer of the Dysentery Bacillus. *Clinical Infectious Diseases* 29 (1999) 1303-1306.
- [31] M.J. Smith, L.D. Teel, H.M. Carvalho, A.R. Melton-Celsa, A.D. O'Brien, Development of a hybrid Shiga holotoxoid vaccine to elicit heterologous protection against Shiga toxins types 1 and 2. *Vaccine* 24 (2006) 4122-4129.
- [32] K. Sandvig, J. Bergan, A.-B. Dyve, T. Skotland, M.L. Torgersen, Endocytosis and retrograde transport of Shiga toxin. *Toxicon* 56 (2010) 1181-1185.
- [33] J.P. Nataro, J.B. Kaper, Diarrheagenic *Escherichia coli*. *Clinical Microbiology Reviews* 11 (1998) 142-201.
- [34] M.A. Karmali, The Medical Significance of Shiga Toxin-Producing *Escherichia coli* Infections: An Overview, in: D. Philpott, F. Ebel (Eds.) *E coli: Shiga Toxin Methods and Protocols*, Humana Press, Totowa, N.J., 2003, pp. 1-7.
- [35] J.C. Paton, A.W. Paton, Shiga toxin 'goes retro' in human primary kidney cells. *Kidney international* 70 (2006) 2049-2051.
- [36] I. Majoul, T. Schmidt, M. Pomasanova, E. Boutkevich, Y. Kozlov, H.-D. Söling, Differential expression of receptors for Shiga and Cholera toxin is regulated by the cell cycle. *Journal of Cell Science* 115 (2002) 817-826.
- [37] D. Johansson, E. Kosovac, J. Moharer, I. Ljuslinder, T. Brännström, A. Johansson, P. Behnam-Motlagh, Expression of verotoxin-1 receptor Gb3 in breast cancer tissue and verotoxin-1 signal transduction to apoptosis. *BMC Cancer* 9 (2009) 1-9.
- [38] V.L. Tesh, Induction of apoptosis by Shiga toxins. *Future microbiology* 5 (2010) 431-453.
- [39] J.C. Paton, A.W. Paton, Pathogenesis and diagnosis of Shiga toxin-producing *Escherichia coli* infections. *Clinical microbiology reviews* 11 (1998) 450-479.
- [40] M. Nasso, G. Fedele, F. Spensieri, R. Palazzo, P. Costantino, R. Rappuoli, C.M. Ausiello, Genetically Detoxified Pertussis Toxin Induces Th1/Th17 Immune Response through MAPKs and IL-10-Dependent Mechanisms. *The Journal of Immunology* 183 (2009) 1892-1899.

- [41] M. Tamura, K. Nogimori, S. Murai, M. Yajima, K. Ito, T. Katada, M. Ui, S. Ishii, Subunit structure of islet-activating protein, pertussis toxin, in conformity with the A-B model. *Biochemistry* 21 (1982) 5516-5522.
- [42] R.W. DePaolo, F. Tang, I. Kim, M. Han, N. Levin, N. Ciletti, A. Lin, D. Anderson, O. Schneewind, B. Jabri, Toll-Like Receptor 6 Drives Differentiation of Tolerogenic Dendritic Cells and Contributes to LcrV-Mediated Plague Pathogenesis. *Cell Host & Microbe* 4 (2008) 350-361.
- [43] C. Locht, J.M. Keith, Pertussis Toxin Gene: Nucleotide Sequence and Genetic Organization. *Science* 232 (1986) 1258-1264.
- [44] W.J. Black, J.J. Munoz, M.G. Peacock, P.A. Schad, J.L. Cowell, J.J. Burchall, M. Lim, A. Kent, L. Steinman, S. Falkow, ADP-Ribosyltransferase Activity of Pertussis Toxin and Immunomodulation by *Bordetella pertussis*. *Science* 240 (1988) 656-659.
- [45] H.R. Kaslow, D.L. Burns, Pertussis toxin and target eukaryotic cells: binding, entry, and activation. *The FASEB Journal* 6 (1992) 2684-2690.
- [46] R.D. Plaut, N.H. Carbonetti, Retrograde transport of pertussis toxin in the mammalian cell. *Cellular Microbiology* 10 (2008) 1130-1139.
- [47] A.P. Anisimov, S.V. Dentovskaya, E.A. Panfertsev, T.y.E. Svetoch, P.K. Kopylov, B.W. Segelke, A. Zemla, M.V. Telepnev, V.L. Motin, Amino acid and structural variability of *Yersinia pestis* LcrV protein. *Infection, Genetics and Evolution* 10 (2010) 137-145.
- [48] M.H. Samore, G.R. Siber, Pertussis toxin enhanced IgG1 and IgE responses to primary tetanus immunization are mediated by interleukin-4 and persist during secondary responses to tetanus alone. *Vaccine* 14 (1996) 290-297.
- [49] M. Pizza, M.M. Giuliani, M.R. Fontana, E. Monaci, G. Douce, G. Dougan, K.H.G. Mills, R. Rappuoli, G. Del Giudice, Mucosal vaccines: non toxic derivatives of LT and CT as mucosal adjuvants. *Vaccine* 19 (2001) 2534-2541.
- [50] M.T. De Magistris, Mucosal delivery of vaccine antigens and its advantages in pediatrics. *Advanced Drug Delivery Reviews* 58 (2006) 52-67.
- [51] M. Singh, M. Ugozzoli, J. Kazzaz, J. Chesko, E. Soenawan, D. Mannucci, F. Titta, M. Contorni, G. Volpini, G.D. Guidice, D.T. O'Hagan, A preliminary evaluation of alternative adjuvants to alum using a range of established and new generation vaccine antigens. *Vaccine* 24 (2006) 1680-1686.
- [52] M.L. Mbow, E. De Gregorio, N.M. Valiante, R. Rappuoli, New adjuvants for human vaccines. *Current opinion in immunology* 22 (2010) 411-416.
- [53] R.L. Coffman, A. Sher, R.A. Seder, Vaccine adjuvants: putting innate immunity to work. *Immunity* 33 (2010) 492-503.
- [54] D. Lomada, R. Gambhira, P.N. Nehete, F.A. Guhad, A.K. Chopra, J.W. Peterson, K.J. Sastry, A two-codon mutant of cholera toxin lacking ADP-ribosylating activity functions as an effective adjuvant for eliciting mucosal and systemic cellular immune responses to peptide antigens. *Vaccine* 23 (2004) 555-565.

- [55] M.L. Francis, J. Ryan, M.G. Jobling, R.K. Holmes, J. Moss, J.J. Mond, Cyclic AMP-independent effects of cholera toxin on B cell activation. II. Binding of ganglioside GM1 induces B cell activation. *The Journal of Immunology* 148 (1992) 1999-2005.
- [56] H.-Y. Wu, M.W. Russell, Induction of mucosal and systemic immune responses by intranasal immunization using recombinant cholera toxin B subunit as an adjuvant. *Vaccine* 16 (1998) 286-292.
- [57] L. Wassen, M. Jertborn, Kinetics of Local and Systemic Immune Responses after Vaginal Immunization with Recombinant Cholera Toxin B Subunit in Humans. *Clinical and Diagnostic Laboratory Immunology* 12 (2005) 447-452.
- [58] E.C. Lavelle, A. Jarnicki, E. McNeela, M.E. Armstrong, S.C. Higgins, O. Leavy, K.H.G. Mills, Effects of cholera toxin on innate and adaptive immunity and its application as an immunomodulatory agent. *Journal of Leukocyte Biology* 75 (2004) 756-763.
- [59] A. George-Chandy, K. Eriksson, M. Lebens, I. Nordström, E. Schön, J. Holmgren, Cholera Toxin B Subunit as a Carrier Molecule Promotes Antigen Presentation and Increases CD40 and CD86 Expression on Antigen-Presenting Cells. *Infection and Immunity* 69 (2001) 5716-5725.
- [60] C.M. Gockel, M.W. Russell, Induction and recall of immune memory by mucosal immunization with a non-toxic recombinant enterotoxin-based chimeric protein. *Immunology* 116 (2005) 477-486.
- [61] B. Vingert, O. Adotevi, D. Patin, S. Jung, P. Shrikant, L. Freyburger, C. Eppolito, A. Sapozhnikov, M. Amessou, F. Quintin-Colonna, W.H. Fridman, L. Johannes, E. Tartour, The Shiga toxin B-subunit targets antigen *in vivo* to dendritic cells and elicits anti-tumor immunity. *European Journal of Immunology* 36 (2006) 1124-1135.
- [62] C.A. Lingwood, Shiga Toxin Receptor Glycolipid Binding, in: D. Philpott, F. Ebel (Eds.) *E coli: Shiga Toxin Methods and Protocols*, Humana Press, Totowa, N.J., 2003, pp. 165-186.
- [63] N.A. Williams, T.R. Hirst, T.O. Nashar, Immune modulation by the cholera-like enterotoxins: from adjuvant to therapeutic. *Immunology today* 20 (1999) 95-101.
- [64] A.B. Hartman, L.L. Van De Verg, M.M. Venkatesan, Native and mutant forms of cholera toxin and heat-labile enterotoxin effectively enhance protective efficacy of live attenuated and heat-killed *Shigella* vaccines. *Infection and immunity* 67 (1999) 5841-5847.
- [65] J. Holmgren, A.M. Harandi, C. Czerkinsky, Mucosal adjuvants and anti-infection and anti-immunopathology vaccines based on cholera toxin, cholera toxin B subunit and CpG DNA. *Expert Review of Vaccines* 2 (2003) 205-217.
- [66] M. Soriani, L. Bailey, T.R. Hirst, Contribution of the ADP-ribosylating and receptor-binding properties of cholera-like enterotoxins in modulating cytokine secretion by human intestinal epithelial cells. *Microbiology* 148 (2002) 667-676.
- [67] V. Lampropoulou, E. Calderon-Gomez, T. Roch, P. Neves, P. Shen, U. Stervbo, P. Boudinot, S.M. Anderton, S. Fillatreau, Suppressive functions of activated B cells in

autoimmune diseases reveal the dual roles of Toll-like receptors in immunity. *Immunological reviews* 233 (2010) 146-161.

[68] J.-B. Sun, C. Czerkinsky, J. Holmgren, B lymphocytes treated in vitro with antigen coupled to cholera toxin B subunit induce antigen-specific Foxp3⁺ regulatory T cells and protect against experimental autoimmune encephalomyelitis. *The Journal of Immunology* 188 (2012) 1686-1697.

[69] M.O. Domingos, R.G. Andrade, K.C. Barbaro, M.M. Borges, D.J. Lewis, R.R.C. New, Influence of the A and B subunits of cholera toxin (CT) and *Escherichia coli* toxin (LT) on TNF- α release from macrophages. *Toxicon* 53 (2009) 570-577.

[70] M.I. Block, H.R. Alexander, J.A. Norton, Cholera toxin pretreatment protects against tumor necrosis factor lethality without compromising tumor response to therapy. *Archives of Surgery* 127 (1992) 1330-1334.

[71] A.K. Gloudemans, M. Plantinga, M. Guilliams, M.A. Willart, A. Ozir-Fazalalikhani, A. Van Der Ham, L. Boon, N.L. Harris, H. Hammad, H.C. Hoogsteden, The mucosal adjuvant cholera toxin B instructs non-mucosal dendritic cells to promote IgA production via retinoic acid and TGF- β . *PloS one* 8 (2013) e59822.

[72] W. Langridge, B. Dénes, I. Fodor, Cholera toxin B subunit modulation of mucosal vaccines for infectious and autoimmune diseases. *Current opinion in investigational drugs* (London, England: 2000) 11 (2010) 919-928.

[73] R.J. Salmond, J.A. Luross, N.A. Williams, Immune modulation by the cholera-like enterotoxins. *Expert Reviews in Molecular Medicine* 4 (2002) 1-16.

[74] G. Hajishengallis, S. Arce, C. Gockel, T. Connell, M. Russell, Immunomodulation with enterotoxins for the generation of secretory immunity or tolerance: applications for oral infections. *Journal of dental research* 84 (2005) 1104-1116.

[75] V.P. Da Hora, F.R. Conceição, O.A. Dellagostin, D.L. Doolan, Non-toxic derivatives of LT as potent adjuvants. *Vaccine* 29 (2011) 1538-1544.

[76] N.G. Anosova, S. Chabot, V. Shreedhar, J.A. Borawski, B.L. Dickinson, M.R. Neutra, Cholera toxin, *E. coli* heat-labile toxin, and non-toxic derivatives induce dendritic cell migration into the follicle-associated epithelium of Peyer's patches. *Mucosal Immunol* 1 (2008) 59-67.

[77] D.J.M. Lewis, H. Zhiming, S. Barnett, I. Kromann, R. Giemza, E. Galiza, M. Woodrow, B. Thierry-Carstensen, P. Andersen, D. Novicki, G. Del Giudice, R. Rappuoli, Transient Facial Nerve Paralysis (Bell's Palsy) following Intranasal Delivery of a Genetically Detoxified Mutant of *Escherichia coli* Heat Labile Toxin. *PLoS ONE* 4 (2009) 1-5.

[78] M. Mutsch, W. Zhou, P. Rhodes, M. Bopp, R.T. Chen, T. Linder, C. Spyr, R. Steffen, Use of the inactivated intranasal influenza vaccine and the risk of Bell's palsy in Switzerland. *New England journal of medicine* 350 (2004) 896-903.

[79] Y. Hagiwara, T. Iwasaki, H. Asanuma, Y. Sato, T. Sata, C. Aizawa, T. Kurata, S.-i. Tamura, Effects of intranasal administration of cholera toxin (or< i> *Escherichia*

coli heat-labile enterotoxin) B subunits supplemented with a trace amount of the holotoxin on the brain. *Vaccine* 19 (2001) 1652-1660.

[80] A.M. Eriksson, K.M. Schön, N.Y. Lycke, The cholera toxin-derived CTA1-DD vaccine adjuvant administered intranasally does not cause inflammation or accumulate in the nervous tissues. *The Journal of Immunology* 173 (2004) 3310-3319.

[81] M.E. Armstrong, E.C. Lavelle, C.E. Loscher, M.A. Lynch, K.H. Mills, Proinflammatory responses in the murine brain after intranasal delivery of cholera toxin: implications for the use of AB toxins as adjuvants in intranasal vaccines. *Journal of Infectious Diseases* 192 (2005) 1628-1633.

[82] M. Ohmura-Hoshino, M. Yamamoto, Y. Yuki, Y. Takeda, H. Kiyono, Non-toxic Stx derivatives from *Escherichia coli* possess adjuvant activity for mucosal immunity. *Vaccine* 22 (2004) 3751-3761.

[83] C.M. Denking, M.D. Denking, T.G. Forsthuber, Pertussis toxin-induced cytokine differentiation and clonal expansion of T cells is mediated predominantly via costimulation. *Cellular immunology* 246 (2007) 46-54.

[84] M. Ryan, L. McCarthy, R. Rappuoli, B.P. Mahon, K. Mills, Pertussis toxin potentiates Th1 and Th2 responses to co-injected antigen: adjuvant action is associated with enhanced regulatory cytokine production and expression of the co-stimulatory molecules B7-1, B7-2 and CD28. *International immunology* 10 (1998) 651-662.

[85] C. MMWR, Pertussis Vaccination: Use of Acellular Pertussis Vaccines Among Infants and Young Children. March 28, 1997/Vol. 46/No, RR-7.

[86] C. Andreasen, D.A. Powell, N.H. Carbonetti, Pertussis toxin stimulates IL-17 production in response to *Bordetella pertussis* infection in mice. *PLoS One* 4 (2009) e7079.

[87] C. Murphey, S. Chang, X. Zhang, B. Arulanandam, T.G. Forsthuber, Induction of polyclonal CD8+ T cell activation and effector function by Pertussis toxin. *Cellular immunology* 267 (2011) 50-55.

[88] Z.Y. Wang, D. Yang, Q. Chen, C.A. Leifer, D.M. Segal, S.B. Su, R.R. Caspi, Z.O. Howard, J.J. Oppenheim, Induction of dendritic cell maturation by pertussis toxin and its B subunit differentially initiate Toll-like receptor 4-dependent signal transduction pathways. *Experimental hematology* 34 (2006) 1115-1124.

[89] X. Chen, R.T. Winkler-Pickett, N.H. Carbonetti, J.R. Ortaldo, J.J. Oppenheim, O. Howard, Pertussis toxin as an adjuvant suppresses the number and function of CD4+ CD25+ T regulatory cells. *European journal of immunology* 36 (2006) 671-680.

[90] N.-W. Choi, M.K. Estes, W.H.R. Langridge, Oral immunization with a shiga toxin B subunit:rotavirus NSP4₉₀ fusion protein protects mice against gastroenteritis. *Vaccine* 23 (2005) 5168-5176.

[91] N. Haicheur, F. Benchetrit, M. Amessou, C. Leclerc, T. Falguières, C. Fayolle, E. Bismuth, W.H. Fridman, L. Johannes, E. Tartour, The B subunit of Shiga toxin coupled to full-size antigenic protein elicits humoral and cell-mediated immune responses

associated with a T_H1-dominant polarization. *International Immunology* 15 (2003) 1161-1171.

[92] R.-S. Lee, E. Tartour, P. Van der Bruggen, V. Vantomme, I. Joyeux, B. Goud, W.H. Fridman, L. Johannes, Major histocompatibility complex class I presentation of exogenous soluble tumor antigen fused to the B-fragment of Shiga toxin. *European Journal of Immunology* 28 (1998) 2726-2737.

[93] N. Haicheur, E. Bismuth, S. Bosset, O. Adotevi, G. Warnier, V. Lacabanne, A. Regnault, C. Desaynard, S. Amigorena, P. Ricciardi-Castagnoli, B. Goud, W.H. Fridman, L. Johannes, E. Tartour, The B Subunit of Shiga Toxin Fused to a Tumor Antigen Elicits CTL and Targets Dendritic Cells to Allow MHC Class I-Restricted Presentation of Peptides Derived from Exogenous Antigens. *The Journal of Immunology* 165 (2000) 3301-3308.

[94] J. Bockemühl, 100 years after the discovery of the plague-causing agent--importance and veneration of Alexandre Yersin in Vietnam today]. *Immunität und Infektion* 22 (1994) 72.

[95] K.J. Ryan, C.G. Ray, *Medical microbiology*. Appleton & Lange, Norwalk, Connecticut (1994).

[96] E.J. Bottone, *Yersinia enterocolitica*: overview and epidemiologic correlates. *Microbes and Infection* 1 (1999) 323-333.

[97] R.D. Perry, J.D. Fetherston, *Yersinia pestis*--etiologic agent of plague. *Clinical microbiology reviews* 10 (1997) 35-66.

[98] R.W. Titball, E.D. Williamson, Vaccination against bubonic and pneumonic plague. *Vaccine* 19 (2001) 4175-4184.

[99] D. Josko, *Yersinia pestis*: still a plague in the 21st century. *Clinical laboratory science: journal of the American Society for Medical Technology* 17 (2004) 25.

[100] G. Campbell, D. Dennis, Plague and other *Yersinia* infections. *HARRISONS PRINCIPLES OF INTERNAL MEDICINE* 1 (2001) 993-1000.

[101] M.J. Echenberg, *Pestis Redux: The Initial Years of the Third Bubonic Plague Pandemic, 1894-1901*. *Journal of World History* 13 (2002) 429-449.

[102] N.M. Ampel, *Plagues—what's past is present: thoughts on the origin and history of new infectious diseases*. *Review of Infectious Diseases* 13 (1991) 658-665.

[103] W. Mwengee, T. Butler, S. Mgema, G. Mhina, Y. Almasi, C. Bradley, J.B. Formanik, C.G. Rochester, Treatment of plague with gentamicin or doxycycline in a randomized clinical trial in Tanzania. *Clinical infectious diseases* 42 (2006) 614-621.

[104] T.V. Inglesby, D.T. Dennis, D.A. Henderson, J.G. Bartlett, M.S. Ascher, E. Eitzen, A.D. Fine, A.M. Friedlander, J. Hauer, J.F. Koerner, Plague as a biological weapon. *JAMA: the journal of the American Medical Association* 283 (2000) 2281-2290.

[105] S. Riedel, *Plague: From Natural Disease to Bioterrorism*. *Proceedings (Baylor University Medical Center)* 18 (2005) 116-124.

- [106] M. Galimand, A. Guiyoule, G. Gerbaud, B. Rasoamanana, S. Chanteau, E. Carniel, P. Courvalin, Multidrug resistance in *Yersinia pestis* mediated by a transferable plasmid. *New England Journal of Medicine* 337 (1997) 677-681.
- [107] S. Riedel, Biological warfare and bioterrorism: a historical review. *Proceedings (Baylor University Medical Center)* 17 (2004) 400.
- [108] S.T. Smiley, Current challenges in the development of vaccines for pneumonic plague. (2008).
- [109] K. Meyer, D.C. Cavanaugh, P.J. Bartelloni, J.D. Marshall, Plague immunization. I. Past and present trends. *Journal of Infectious Diseases* 129 (1974) S13-S18.
- [110] V.M. Abramov, V.S. Khlebnikov, A.M. Vasiliev, I.V. Kosarev, R.N. Vasilenko, N.L. Kulikova, A.V. Khodyakova, V.I. Evstigneev, V.N. Uversky, V.L. Motin, G.B. Smirnov, R.R. Brubaker, Attachment of LcrV from *Yersinia pestis* at Dual Binding Sites to Human TLR-2 and Human IFN- γ Receptor. *Journal of Proteome Research* 6 (2007) 2222-2231.
- [111] M.H. Hamad, M.L. Nilles, Roles of YopN, LcrG and LcrV in Controlling Yops Secretion by *Yersinia pestis*, in: R.D. Perry, J.D. Fetherston (Eds.) *The Genus Yersinia - From Genomics to Function*, Springer, New York, 2007, pp. 225-234.
- [112] U. Derewenda, A. Mateja, Y. Devedjiev, K.M. Routzahn, A.G. Evdokimov, Z.S. Derewenda, D.S. Waugh, The Structure of *Yersinia pestis* V-Antigen, an Essential Virulence Factor and Mediator of Immunity against Plague. *Structure* 12 (2004) 301-306.
- [113] L.E. Quenee, N.A. Ciletti, D. Elli, T.M. Hermanas, O. Schneewind, Prevention of pneumonic plague in mice, rats, guinea pigs and non-human primates with clinical grade rV10, rV10-2 or F1-V vaccines. *Vaccine* 29 (2011) 6572-6583.
- [114] N.C. Miller, L.E. Quenee, D. Elli, N.A. Ciletti, O. Schneewind, Polymorphisms in the *lcrV* Gene of *Yersinia enterocolitica* and Their Effect on Plague Protective Immunity. *Infection and Immunity* 80 (2012) 1572-1582.
- [115] K.G. Ligtenberg, N.C. Miller, A. Mitchell, G.V. Plano, O. Schneewind, LcrV Mutants That Abolish *Yersinia* Type III Injectisome Function. *Journal of Bacteriology* 195 (2013) 777-787.
- [116] G. Valiakos, L.V. Athanasiou, A. Touloudi, V. Papatsiros, V. Spyrou, L. Petrovska, C. Billinis, West Nile Virus: Basic Principles, Replication Mechanism, Immune Response and Important Genetic Determinants of Virulence, in: G. Rosas-Acosta (Ed.) *Viral Replication*, InTech, Rijeka, Croatia, 2013, pp. 43-68.
- [117] R. Lanciotti, J. Roehrig, V. Deubel, J. Smith, M. Parker, K. Steele, B. Crise, K. Volpe, M. Crabtree, J. Scherret, Origin of the West Nile virus responsible for an outbreak of encephalitis in the northeastern United States. *Science* 286 (1999) 2333-2337.
- [118] K.C. Smithburn, Hughes, TP, Burke AW, Paul KC A neutropic virus isolated from the blood of a native of Uganda. *Am J Trop Med* 20 (1940) 471-492

- [119] D.W. Beasley, A.D. Barrett, R.B. Tesh, Resurgence of West Nile neurologic disease in the United States in 2012: What happened? What needs to be done? Antiviral research (2013).
- [120] C.f.D.C.a. Prevention, West Nile virus and other arboviral diseases-United States, 2012. MMWR Morbidity and mortality weekly report 62 (2013) 513.
- [121] E.B. Hayes, N. Komar, R.S. Nasci, S.P. Montgomery, D.R. O'Leary, G.L. Campbell, Epidemiology and transmission dynamics of West Nile virus disease. Emerging infectious diseases 11 (2005) 1167.
- [122] J.J. Sejvar, M.B. Haddad, B.C. Tierney, G.L. Campbell, A.A. Marfin, J.A. Van Gerpen, A. Fleischauer, A.A. Leis, D.S. Stokic, L.R. Petersen, Neurologic manifestations and outcome of West Nile virus infection. JAMA: the journal of the American Medical Association 290 (2003) 511-515.
- [123] L.R. Petersen, A.A. Marfin, West Nile virus: a primer for the clinician. Annals of Internal Medicine 137 (2002) 173-179.
- [124] E.B. Hayes, J.J. Sejvar, S.R. Zaki, R.S. Lanciotti, A.V. Bode, G.L. Campbell, Virology, pathology, and clinical manifestations of West Nile virus disease. Emerging infectious diseases 11 (2005) 1174.
- [125] N.P. Lindsey, J.E. Staples, J.A. Lehman, M. Fischer, Medical risk factors for severe West Nile virus disease, United States, 2008–2010. The American journal of tropical medicine and hygiene 87 (2012) 179-184.
- [126] N.P. Lindsey, J.J. Sejvar, A.V. Bode, W.J. Pape, G.L. Campbell, Delayed mortality in a cohort of persons hospitalized with West Nile virus disease in Colorado in 2003. Vector-Borne and Zoonotic Diseases 12 (2012) 230-235.
- [127] M.C. Silva, A. Guerrero-Plata, F.D. Gilfoy, R.P. Garofalo, P.W. Mason, Differential activation of human monocyte-derived and plasmacytoid dendritic cells by West Nile virus generated in different host cells. Journal of virology 81 (2007) 13640-13648.
- [128] M.S. Diamond, B. Shrestha, A. Marri, D. Mahan, M. Engle, B cells and antibody play critical roles in the immediate defense of disseminated infection by West Nile encephalitis virus. Journal of virology 77 (2003) 2578-2586.
- [129] M.S. Diamond, B. Shrestha, E. Mehlhop, E. Sitati, M. Engle, Innate and adaptive immune responses determine protection against disseminated infection by West Nile encephalitis virus. Viral immunology 16 (2003) 259-278.
- [130] M.S. Diamond, E.M. Sitati, L.D. Friend, S. Higgs, B. Shrestha, M. Engle, A critical role for induced IgM in the protection against West Nile virus infection. The Journal of experimental medicine 198 (2003) 1853-1862.
- [131] M.S. Diamond, T.C. Pierson, D.H. Fremont, The structural immunology of antibody protection against West Nile virus. Immunological reviews 225 (2008) 212-225.
- [132] B. Shrestha, T. Ng, H.-J. Chu, M. Noll, M.S. Diamond, The relative contribution of antibody and CD8⁺ T cells to vaccine immunity against West Nile encephalitis virus. Vaccine 26 (2008) 2020-2033.

- [133] J. Chu, R. Rajamanonmani, J. Li, R. Bhuvanakantham, J. Lescar, M.-L. Ng, Inhibition of West Nile virus entry by using a recombinant domain III from the envelope glycoprotein. *Journal of General Virology* 86 (2005) 405-412.
- [134] M.D. Sanchez, T.C. Pierson, D. McAllister, S.L. Hanna, B.A. Puffer, L.E. Valentine, M.M. Murtadha, J.A. Hoxie, R.W. Doms, Characterization of neutralizing antibodies to West Nile virus. *Virology* 336 (2005) 70-82.
- [135] L.C.M. Tan, A.J.S. Chua, L.S.L. Goh, S.M. Pua, Y.K. Cheong, M.L. Ng, Rapid purification of recombinant dengue and West Nile virus envelope Domain III proteins by metal affinity membrane chromatography. *Protein Expression and Purification* 74 (2010) 129-137.
- [136] T. Oliphant, G.E. Nybakken, S.K. Austin, Q. Xu, J. Bramson, M. Loeb, M. Throsby, D.H. Fremont, T.C. Pierson, M.S. Diamond, Induction of epitope-specific neutralizing antibodies against West Nile virus. *Journal of virology* 81 (2007) 11828-11839.
- [137] J. Schmitz, J. Roehrig, A. Barrett, J. Hombach, Next generation dengue vaccines: a review of candidates in preclinical development. *Vaccine* 29 (2011) 7276-7284.
- [138] D.W. Beasley, Vaccines and immunotherapeutics for the prevention and treatment of infections with West Nile virus. *Future Oncology* 8 (2012) 943-960.
- [139] F.X. Heinz, K. Stiasny, Flaviviruses and flavivirus vaccines. *Vaccine* 30 (2012) 4301-4306.
- [140] U. Laemmli, Cleavage of structural proteins during the assembly of the head of bacteriophage T4 *Nature* 227: 680–685. Find this article online (1970).
- [141] Z. Shen, G. Reznikoff, G. Dranoff, K.L. Rock, Cloned dendritic cells can present exogenous antigens on both MHC class I and class II molecules. *The Journal of Immunology* 158 (1997) 2723-2730.
- [142] A.T. Reinicke, K.D. Omilusik, G. Basha, W.A. Jefferies, Dendritic cell cross-priming is essential for immune responses to *Listeria monocytogenes*. *PloS one* 4 (2009) e7210.
- [143] M.-J. Gubbels, B. Striepen, N. Shastri, M. Turkoz, E.A. Robey, Class I major histocompatibility complex presentation of antigens that escape from the parasitophorous vacuole of *Toxoplasma gondii*. *Infection and immunity* 73 (2005) 703-711.
- [144] J.K. Tinker, J.L. Erbe, R.K. Holmes, Characterization of fluorescent chimeras of cholera toxin and *Escherichia coli* heat-labile enterotoxins produced by use of the twin arginine translocation system. *Infection and immunity* 73 (2005) 3627-3635.
- [145] B.M. Arlian, J.K. Tinker, Mucosal immunization with a *Staphylococcus aureus* IsdA-cholera toxin A2/B chimera induces antigen-specific Th2-type responses in mice. *Clinical and Vaccine Immunology* 18 (2011) 1543-1551.
- [146] J.K. Tinker, J. Yan, R.J. Knippel, P. Panayiotou, K.A. Cornell, Immunogenicity of a West Nile Virus DIII-Cholera Toxin A2/B Chimera after Intranasal Delivery. *Toxins* 6 (2014) 1397-1418.

- [147] H. Li, S. Hong, J. Qian, Y. Zheng, J. Yang, Q. Yi, Cross talk between the bone and immune systems: osteoclasts function as antigen-presenting cells and activate CD4+ and CD8+ T cells. *Blood* 116 (2010) 210-217.
- [148] M. Martin, D.J. Metzger, S.M. Michalek, T.D. Connell, M.W. Russell, Distinct cytokine regulation by cholera toxin and type II heat-labile toxins involves differential regulation of CD40 ligand on CD4+ T cells. *Infection and immunity* 69 (2001) 4486-4492.
- [149] A. la Sala, J. He, L. Laricchia-Robbio, S. Gorini, A. Iwasaki, M. Braun, G.S. Yap, A. Sher, K. Ozato, B. Kelsall, Cholera toxin inhibits IL-12 production and CD8 α + dendritic cell differentiation by cAMP-mediated inhibition of IRF8 function. *The Journal of experimental medicine* 206 (2009) 1227-1235.
- [150] N. Petrovsky, J.C. Aguilar, Vaccine adjuvants: current state and future trends. *Immunology and cell biology* 82 (2004) 488-496.
- [151] J.H. Wilson-Welder, M.P. Torres, M.J. Kipper, S.K. Mallapragada, M.J. Wannemuehler, B. Narasimhan, Vaccine adjuvants: current challenges and future approaches. *Journal of pharmaceutical sciences* 98 (2009) 1278-1316.
- [152] M. Oloomi, S. Bouzari, Assessment of immune response of the B subunit of Shiga toxin fused to AAF adhesin of Enteroaggregative *Escherichia coli*. *Microbial pathogenesis* 50 (2011) 155-158.
- [153] S.G. Reed, S. Bertholet, R.N. Coler, M. Friede, New horizons in adjuvants for vaccine development. *Trends in immunology* 30 (2009) 23-32.
- [154] A. Wack, R. Rappuoli, Vaccinology at the beginning of the 21st century. *Current opinion in immunology* 17 (2005) 411-418.
- [155] F.R. Vogel, Immunologic adjuvants for modern vaccine formulations. *Annals of the New York Academy of Sciences* 754 (1995) 153-160.
- [156] L.A. O'Neill, N. Novak, H. Wagner, A.E. Parker, K. Triantafilou, Modulation of Toll-Like Receptor Signalling as a New Therapeutic Principle.
- [157] J. Aguilar, E. Rodriguez, Vaccine adjuvants revisited. *Vaccine* 25 (2007) 3752-3762.
- [158] J. Sánchez, J. Holmgren, Cholera toxin—a foe & a friend. *The Indian journal of medical research* 133 (2011) 153.
- [159] J.K. Tinker, J.L. Erbe, W.G. Hol, R.K. Holmes, Cholera holotoxin assembly requires a hydrophobic domain at the A-B5 interface: mutational analysis and development of an in vitro assembly system. *Infection and immunity* 71 (2003) 4093-4101.
- [160] M.T. Tarragó-Trani, B. Storrie, A method for the purification of Shiga-like toxin 1 subunit B using a commercially available galabiose-agarose resin. *Protein expression and purification* 38 (2004) 170-176.
- [161] H. Lockman, J.B. Kaper, Nucleotide sequence analysis of the A2 and B subunits of *Vibrio cholerae* enterotoxin. *Journal of Biological Chemistry* 258 (1983) 13722-13726.

- [162] M.P. Jackson, J.W. Newland, R.K. Holmes, A.D. O'Brien, Nucleotide sequence analysis of the structural genes for Shiga-like toxin I encoded by bacteriophage 933J from *Escherichia coli*. *Microbial pathogenesis* 2 (1987) 147-153.
- [163] P.R. Austin, P.E. Jablonski, G.A. Bohach, A.K. Dunker, C.J. Hovde, Evidence that the A2 fragment of Shiga-like toxin type I is required for holotoxin integrity. *Infection and immunity* 62 (1994) 1768-1775.
- [164] M. Oloomi, S. Bouzari, M. Arshadi, N-terminus leader sequence of Shiga toxin (Stx) 1 is essential for production of active recombinant protein in *E. coli*. *Protein and peptide letters* 13 (2006) 509-512.
- [165] T. Gianni, V. Gatta, G. Campadelli-Fiume, α V β 3-integrin routes herpes simplex virus to an entry pathway dependent on cholesterol-rich lipid rafts and dynamin2. *Proceedings of the National Academy of Sciences* 107 (2010) 22260-22265.
- [166] Z. Kaya, T. Tretter, J. Schlichting, F. Leuschner, M. Afanasyeva, H.A. Katus, N.R. Rose, Complement receptors regulate lipopolysaccharide-induced T-cell stimulation. *Immunology* 114 (2005) 493-498.
- [167] P.B. Eisenhauer, P. Chaturvedi, R.E. Fine, A.J. Ritchie, J.S. Pober, T.G. Cleary, D.S. Newburg, Tumor necrosis factor alpha increases human cerebral endothelial cell Gb3 and sensitivity to Shiga toxin. *Infection and immunity* 69 (2001) 1889-1894.
- [168] G.H. Foster, C.S. Armstrong, R. Sakiri, V.L. Tesh, Shiga toxin-induced tumor necrosis factor alpha expression: requirement for toxin enzymatic activity and monocyte protein kinase C and protein tyrosine kinases. *Infection and immunity* 68 (2000) 5183-5189.
- [169] M. Ohmura, M. Yamamoto, C. Tomiyama-Miyaji, Y. Yuki, Y. Takeda, H. Kiyono, Nontoxic Shiga toxin derivatives from *Escherichia coli* possess adjuvant activity for the augmentation of antigen-specific immune responses via dendritic cell activation. *Infection and immunity* 73 (2005) 4088-4097.
- [170] T. He, C. Tang, S. Xu, T. Moyana, J. Xiang, Interferon gamma stimulates cellular maturation of dendritic cell line DC2.4 leading to induction of efficient cytotoxic T cell responses and antitumor immunity. *Cell Mol Immunol* 4 (2007) 105-111.